



Steel Bridge Design Handbook

.....

**CHAPTER 13**

# Bracing System Theory and Design for I-Girders and Tub Girders

February 2022



.....  
**Smarter.  
Stronger.  
Steel.**

© AISC 2022

by

American Institute of Steel Construction

*All rights reserved. This book or any part thereof must not be reproduced in any form without the written permission of the publisher.  
The AISC and NSBA logos are registered trademarks of AISC.*

The information presented in this publication has been prepared following recognized principles of design and construction. While it is believed to be accurate, this information should not be used or relied upon for any specific application without competent professional examination and verification of its accuracy, suitability and applicability by a licensed engineer or architect. The publication of this information is not a representation or warranty on the part of the American Institute of Steel Construction, its officers, agents, employees or committee members, or of any other person named herein, that this information is suitable for any general or particular use, or of freedom from infringement of any patent or patents. All representations or warranties, express or implied, other than as stated above, are specifically disclaimed. Anyone making use of the information presented in this publication assumes all liability arising from such use.

Caution must be exercised when relying upon standards and guidelines developed by other bodies and incorporated by reference herein since such material may be modified or amended from time to time subsequent to the printing of this edition. The American Institute of Steel Construction bears no responsibility for such material other than to refer to it and incorporate it by reference at the time of the initial publication of this edition.

Printed in the United States of America

## Foreword

The Steel Bridge Design Handbook covers a full range of topics and design examples to provide bridge engineers with the information needed to make knowledgeable decisions regarding the selection, design, fabrication, and construction of steel bridges. The Handbook has a long history, dating back to the 1970s in various forms and publications. The more recent editions of the Handbook were developed and maintained by the Federal Highway Administration (FHWA) Office of Bridges and Structures as FHWA Report No. FHWA-IF-12-052 published in November 2012, and FHWA Report No. FHWA-HIF-16-002 published in December 2015. The previous development and maintenance of the Handbook by the FHWA, their consultants, and their technical reviewers is gratefully appreciated and acknowledged.

This current edition of the Handbook is maintained by the National Steel Bridge Alliance (NSBA), a division of the American Institute of Steel Construction (AISC). This Handbook, published in 2021, has been updated and revised to be consistent with the 9th edition of the AASHTO LRFD Bridge Design Specifications which was released in 2020. The updates and revisions to various chapters and design examples have been performed, as noted, by HDR, M.A. Grubb & Associates, Don White, Ph.D., and NSBA. Furthermore, the updates and revisions have been reviewed independently by Francesco Russo, Ph.D., P.E., Brandon Chavel, Ph.D., P.E., and NSBA.

The Handbook consists of 19 chapters and 6 design examples. The chapters and design examples of the Handbook are published separately for ease of use, and available for free download at the NSBA website, [www.aisc.org/nsba](http://www.aisc.org/nsba).

The users of the Steel Bridge Design Handbook are encouraged to submit ideas and suggestions for enhancements that can be implemented in future editions to the NSBA and AISC at [solutions@aisc.org](mailto:solutions@aisc.org).

## TECHNICAL REPORT DOCUMENTATION PAGE

<p><b>1. Title and Subtitle</b> Steel Bridge Design Handbook Chapter 13: Bracing System Theory and Design for I-Girders and Tub Girders</p>	<p><b>2. Report Date</b> February 2022</p>
<p><b>3. Original Author(s)</b> Todd Helwig, Ph.D. and Joseph Yura, Ph.D. (University of Texas at Austin)</p>	<p><b>4. Revision Author(s)</b> Michael Grubb, P.E. (M. A. Grubb and Associates, LLC)</p>
<p><b>5. Sponsoring Agency Name and Address</b> National Steel Bridge Alliance, a division of the American Institute of Steel Construction 130 E. Randolph, Suite 2000 Chicago, IL 60601</p>	<p><b>6. Revision Performing Organization Name and Address</b> HDR, Inc. 301 Grant Street, Suite 1700 Pittsburgh, PA 15219</p>
<p><b>7. Supplementary Notes</b> The previous edition of this Handbook was published as FHWA-HIF-16-002 and was developed to be current with the 7<sup>th</sup> edition of the AASHTO LRFD Bridge Design Specifications. This edition of the Handbook was updated to be current with the 9<sup>th</sup> edition of the AASHTO LRFD Bridge Design Specifications, released in 2020.</p>	
<p><b>8. Abstract</b> This volume discusses the design of bracing systems for the superstructures of straight and curved girder systems. I-girder and box shaped members are covered. Bracing for other types of bridges, such as truss, arch or towers is not specifically addressed; however much of the information included in this volume may be applicable. Bracing systems serve a number of important roles in both straight and horizontally curved bridges. The braces provide stability to the primary girders as well as improving the lateral or torsional stiffness and strength of the bridge system both during construction and in service. Depending on the geometry of the bridge, braces may be designated as either primary or secondary members.</p> <p>The Engineer needs to recognize the importance of the bracing systems and bracing member design for appropriate construction and in-service stages. This volume provides an overview of the design requirements for the braces so that engineers can properly size the members to provide adequate strength and stiffness.</p> <p>This volume provides: a) an overview of bracing utilized for I-girders, b) a discussion of the bracing systems for tub girders, and c) design requirements for the members and connections of bracing systems.</p>	
<p><b>9. Keywords</b> Steel Bridge, Bracing, Bracing System, Bracing Design, I-girder, Tub-girder, Curved Girder, Top Flange Lateral Bracing, Lean-on Bracing</p>	<p><b>10. AISC Publication No.</b> B913-22</p>

# Steel Bridge Design Handbook: Bracing System Theory and Design for I-Girders and Tub Girders

## Table of Contents

1.0	INTRODUCTION .....	1
1.1	Torsional Behavior of Open and Closed Girders.....	2
1.2	Lateral Torsional Buckling .....	5
1.3	Categories of Bracing .....	5
2.0	BRACING OF I-GIRDERS.....	7
2.1	General Requirements.....	8
2.1.1	Cross-Frame Spacing and Proportions.....	8
2.1.2	Top and Bottom Flange Lateral Systems.....	10
2.2	Cross-Frame Forces in Horizontally Curved Girders .....	11
2.3	Stability Bracing of I-Girders .....	12
2.3.1	Torsional Bracing Design Requirements, $\beta_T$ .....	14
2.3.2	Stiffness of Cross-Frame and Diaphragm Systems $\beta_b$ .....	16
2.3.3	Web Distortional Stiffness, $\beta_{sec}$ .....	18
2.3.4	In-Plane Stiffness of Girders, $\beta_g$ .....	21
2.3.5	Connection Stiffness, $\beta_{conn}$ .....	22
2.4	Effects of Support Skew .....	23
2.5	Lean-On and Staggered Bracing.....	27
2.5.1	Lean-On Bracing.....	27
2.5.2	Staggered Bracing.....	32
2.6	System Buckling of Interconnected Girders .....	32
2.7	Lateral Bracing Systems .....	36
2.8	Continuous Bracing .....	38
3.0	BRACING OF TUB GIRDER SYSTEMS.....	39
3.1	Top Flange Lateral Truss.....	40
3.1.1	Top Lateral Brace Forces.....	41

3.1.2	Selecting the Top Lateral Bracing Layout .....	45
3.1.3	Determining the Brace Forces .....	46
3.1.3.1	Torsion .....	47
3.1.3.2	Sloping Webs .....	48
3.1.3.3	Vertical Bending .....	49
3.1.4	Top Flange Truss Details .....	51
3.1.5	Controlling Global Lateral Buckling .....	52
3.2	Intermediate Internal Cross-Frames.....	55
3.2.1	Tub Girder Distortion .....	56
3.2.2	Internal Cross-Frame Details .....	59
3.3	End Diaphragms.....	59
3.3.1	Diaphragm Strength Design Requirements .....	61
3.3.2	Diaphragm Stiffness Design Requirements .....	62
3.4	Intermediate External Cross-Frames.....	64
3.4.1	Analysis Approaches for Intermediate External Diaphragms .....	65
3.4.2	Spacing of Intermediate External K-frames .....	66
3.4.3	Forces in Intermediate External K-frames .....	66
4.0	BRACING MEMBER DESIGN AND CONNECTION DETAILS .....	69
4.1	Design of Tees and Angles .....	69
4.1.1	Tension Members.....	69
4.1.2	Compression Members .....	69
4.1.2.1	Single angles .....	69
4.1.2.2	Tees and Double Angles .....	70
4.2	Fatigue Design of Cross-frame Members .....	71
4.3	Welded and Bolted Connection Details.....	71
5.0	SIMPLIFIED GEOMETRIC PROPERTIES FOR TUB GIRDERS.....	76
5.1	Shear Center, $e_y$ , for Open and Quasi-Closed Sections [61].....	76
5.2	Monosymmetry Coefficient, $\beta_x$ – Open section only [62].....	77
5.3	Warping Moment of Inertia, $C_w$ – Open section only [62].....	77
6.0	REFERENCES .....	78

## List of Figures

Figure 1	Warping Stiffness is Related to the Bending Stiffness of the Plate Elements.....	2
Figure 2	Shear Flow in Tub Girder Due to Saint-Venant Torsion .....	4
Figure 3	Categories of Bracing .....	6
Figure 4	Collapse of a Bridge over the Tennessee River due to Insufficient Bracing Provided During Steel Erection.....	7
Figure 5	Web Distortion .....	13
Figure 6	Restraining Forces .....	13
Figure 7	Bending Stresses in Singly Symmetric Section.....	16
Figure 8	Diaphragm Stiffness, $\beta_b$ .....	17
Figure 9	Stiffness Formulas for Twin Girder Cross-Frames [21].....	17
Figure 10	Web Stiffener Geometry.....	19
Figure 11	Diaphragm and Cross-Frame Geometry for Rolled Sections.....	19
Figure 12	Beam Load from Braces .....	22
Figure 13	Plan View of Bridge with Skewed Supports .....	23
Figure 14	Brace Orientations for Bridges with Skewed Supports.....	24
Figure 15	Bent Plate Connection Detail Frequently Used in Bridges with Skewed Supports ....	26
Figure 16	Half-Pipe Web Stiffener .....	26
Figure 17	Summation of $\Sigma P$ Concept for Sideway Frame Stability .....	27
Figure 18	Beams Linked Together at Compression Flange.....	27
Figure 19	Graph of $\Sigma P$ Concept for Beams .....	28
Figure 20	Lean-on Cross-Frame Bracing .....	29
Figure 21	Plan View of Bridge with Lean-On Cross-Frame Bracing .....	29
Figure 22	Lean-on Bracing Layout in Bridge with Large Numbers of Girders .....	30
Figure 23	Stiffness and Strength Requirements for Lean-On Cross-Frames .....	31
Figure 24	Staggered Cross-Frame Layout .....	32
Figure 25	System Buckling of a Twin Girder Widening, where the system has buckled out of plane nearly 10 inches during deck placement .....	33
Figure 26	Comparison of Individual Buckling Mode and System Buckling Mode .....	34
Figure 27	Plan View of Typical Lateral (Relative) Bracing System .....	37

Figure 28 Twin Tub Girder System .....	39
Figure 29 Types of Bracing Systems for Tub Girders .....	39
Figure 30 Geometric Layout and Equivalent Plate Thickness of Top Lateral Systems [40] .....	40
Figure 31 Top Lateral Truss Forces for Various Tub Girder Bracing Systems.....	44
Figure 32 Deformations of different box girder bracing systems.....	45
Figure 33 Diagonal Lateral Brace Forces Due to Torsion in a Tub Girder .....	47
Figure 34 Strut Forces from Torsion .....	48
Figure 35 Strut Forces from Top Flange Loads.....	48
Figure 36 Tub Girder Vertical Bending Stresses .....	49
Figure 37 Bending Induced Truss Forces .....	51
Figure 38 Strut eccentricity in a tub girder cross section.....	52
Figure 39 Effect of $t_{eq}$ on global buckling on a tub girder section using a X-type lateral bracing system .....	54
Figure 40 Effect of Partial End Panel Bracing on Girder Buckling Stress.....	55
Figure 41 Internal Intermediate Cross-Frame Layouts for Tub Girders.....	56
Figure 42 Sources of Torsion in a Tub Girder.....	56
Figure 43 Pure Torsional and Distortional Components in a Tub Girder.....	57
Figure 44 Sign Convention for Eccentricity .....	57
Figure 45 Approximate Distortional Forces in Intermediate Cross-Frames in a Tub Girder.....	58
Figure 46 Typical End Diaphragm Geometry .....	60
Figure 47 Non-continuous flanges illustrated by a 3D FEM of the end diaphragm of a twin box girder model .....	60
Figure 48 Girder end torsional demand that acts on diaphragms and the resulting shears.....	61
Figure 49 Idealized Rectangular Diaphragm Plate .....	62
Figure 50 Girder and Diaphragm Deformations.....	63
Figure 51 Relative Deformation between Adjacent Girders.....	64
Figure 52 K-frame Geometry.....	67
Figure 53 External K-Frame Forces .....	67
Figure 54 Eccentrically loaded WT section.....	71
Figure 55 Improper orientation and sizing of WT section used for top flange lateral bracing member .....	72

Figure 56 Strut offset below diagonal.....	73
Figure 57 Large gusset plates used so working lines of bracing members intersect .....	74
Figure 58 Shim plates can significantly increase the eccentricity of WT sections.....	74
Figure 59 Partial depth end diaphragm.....	75
Figure 60 Calculation of Shear Center for Open and Quasi-Closed Sections .....	76

## 1.0 INTRODUCTION

Bracing systems serve a number of important roles in both straight and horizontally curved bridges. The braces provide stability to the primary girders as well as improving the lateral or torsional stiffness and strength of the bridge system both during construction and in service. Depending on the geometry of the bridge, braces may be designated as either primary or secondary members. In the AASHTO LRFD Bridge Design Specifications (hereafter referred to as the *AASHTO LRFD BDS*) [1], the member designation as primary or secondary is typically assigned depending on whether or not the member or component transmits gravity loads through a necessary as-designed load path. For example, a first-order analysis on a straight bridge with little or no skew during construction will often result in little or no force in the cross-frame members, which are designated as secondary members in such bridges. However, in some situations during construction, the removal of one or more of these bracing members can potentially result in a partial or complete collapse of the structure due to instabilities that can develop as a result of the larger unbraced lengths that result from the removal of these members. In cases such as this, the engineer needs to recognize the importance of the brace and design the members accordingly despite their designation as secondary members. This volume provides an overview of the design requirements of the braces so that engineers can properly size the members to provide adequate strength and stiffness.

In general, this volume discusses the design of bracing systems for the superstructures of straight and curved girder systems. I-girder and box shaped members (e.g., tub girders) are covered throughout this volume. Bracing for other types of bridges, such as truss, arch or towers is not specifically addressed; however much of the information included in this volume may be applicable.

The volume has been divided into five primary sections. Following this introduction, an overview of bracing utilized for I-girders is covered. A discussion of the bracing systems for tub girders is then provided. The next section of this volume outlines the design requirements for the members and connections of bracing systems. The final section contains simplified solutions for the calculation of geometric properties for tub girders.

Regardless of whether the bracing systems are utilized in straight or horizontally curved girders, a clear understanding of the torsional behavior of both I-shaped and tub girder sections is important. The need for torsional stiffness in horizontally curved girders is relatively obvious since the girders are subjected to large torques due to the geometry of the bridge. However, understanding the necessity of adequate torsional stiffness in straight girders is also important since lateral-torsional buckling often controls the design of the girders during construction. In many sections, such as tub girders, the presence of bracing dramatically impacts the torsional stiffness of the section. Lateral instability of flexural members always involves torsion of the cross section. Therefore, the remainder of this introductory section is focused on the torsional stiffness of open and closed cross sections as well as a discussion of the buckling behavior of steel bridge systems.

## 1.1 Torsional Behavior of Open and Closed Girders

Torsional moments are resisted by the shear stresses on the girder cross section. The torsional resistance in thin-walled structures is usually categorized as either Saint-Venant torsional stiffness or warping torsional resistance. The Saint-Venant stiffness is often referred to as uniform torsion since the stiffness does not vary along the length and is also not sensitive to the support conditions of the section. St. Venant torsion results in a pure shear deformation in the plane of the plates that make up the member.

The warping torsional resistance, on the other hand, is often referred to as non-uniform torsion since the stiffness is associated with the bending deformation in the plane of the individual plates. The warping stiffness of a section is related to the member's resistance to warping deformation. Two I-shaped sections subjected to a torque at the ends are shown in plan in Figure 1 to illustrate warping deformation and also warping stiffness. Figure 1a shows that warping deformation consists of a twist of the flanges relative to each other about a vertical axis through the web. Warping deformation distorts the cross section such that it no longer is a plane section because the two flanges have distorted relative to each other. Twist about the longitudinal axis of the member in Figure 1a is prevented at one end, however the warping deformations are not restrained. Since the section is free to warp along the entire length, the flanges remain straight as they twist relative to each other and the member only possesses St. Venant torsional stiffness.

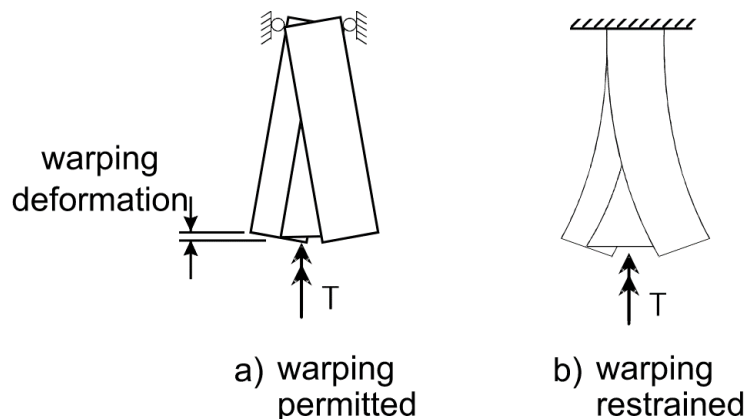


**Figure 1 Warping Stiffness is Related to the Bending Stiffness of the Plate Elements.**

The I-shaped section in Figure 1b has both twist and warping deformation prevented at one end. With warping restrained at just one location along the length, the member cannot twist without bending the flanges. Since the flanges must bend if the member twists, the section therefore has warping stiffness. The warping torsion produces nonuniform longitudinal stresses in the flanges of the member; these stresses are also sometimes called flange lateral bending stresses.

Many members do not have a physical restraint preventing warping as shown in Figure 1b, however the member still has warping stiffness if twist is prevented at a minimum of two points along the longitudinal axis. The twist restraint can come from sources such as cross-frames that prevent the section from rotating about the longitudinal axis, but otherwise do not specifically

restrain warping deformation of the section. Since the bending stiffness is very sensitive to the unsupported length, the warping stiffness is highly variable with the unbraced length.

In general, both Saint-Venant and warping torsional stiffness are developed when thin-walled members are twisted. The torsional moment resistance,  $T_T$ , of a section is a function of the uniform torsional ( $T_{UT}$ ) and warping torsional ( $T_w$ ) components as follows:

$$T_T = T_{UT} + T_w \quad (1)$$

The uniform torsional component can be expressed as follows:

$$T_{UT} = GJ \frac{d\phi}{dx} \quad (2)$$

where  $G$  is the shear modulus,  $J$  is the torsional constant,  $\phi$  is the rotation of the cross section, and  $x$  denotes the longitudinal axis of the member. The torsional constant of a thin-walled open section is given by the following expression:

$$J = \frac{1}{3} \sum_i b_i t_i^3 \quad (3)$$

where  $b_i$  and  $t_i$  are the respective width and thickness of the plate elements that make up the cross section of the girder. The torsional constant for single cell box or tub girders is given by

$$J = \frac{4A_0^2}{\sum_i b_i / t_i} \quad (4)$$

where  $A_0$  is the enclosed area of the cross section of the box girder, and the variables  $b_i$  and  $t_i$  in the summation are the respective width and thickness of the  $i$ th plate that make up the cross section. For example, in a box or tub girder with a cross section made up of four plates, the denominator in Equation 4 is calculated by simply summing the width-to-thickness ratios of the four plate elements.  $A_0$  is typically defined by the area enclosed from the mid-thickness of the plates that make up the cross section.

The warping torsional component can be expressed as follows:

$$T_w = EC_w \frac{d^3\phi}{dx^3} \quad (5)$$

where  $E$  is the modulus of elasticity, and  $C_w$  is the warping constant. For I-shaped sections bent in the plane of the web, the warping constant is given by the expression:

$$C_w = I_t h_o^2 \rho (1-\rho) \quad (6)$$

$$\rho = \frac{I_{yc}}{I_y} \quad (7)$$

where  $I_{yc}$  and  $I_y$  are the respective moments of inertia for the compression flange and the entire section about an axis through the web, and  $h_o$  is the spacing between flange centroids. For a doubly symmetric section, the value of  $\rho$  is 0.5 and Equation 6 reduces to the following expression:

$$C_w = \frac{I_y h_o^2}{4} \quad (8)$$

A rigorous theory for warping torsion was established by Vlasov [2]. The warping torsional stiffness often plays an important role in the total stiffness in girders with an open cross section such as I-shaped girders. For open sections with a relatively long length, the St. Venant stiffness dominates the total stiffness, while for shorter segments the warping torsional stiffness plays a much more significant component in the total stiffness. Closed box or tub girders are usually dominated by Saint-Venant torsion due to the closed cross section and the longitudinal normal stresses due to warping torsion are usually negligible [2]. The large Saint-Venant stiffness of a box or tub girder provides a torsional stiffness that may be 100~1000 times that of a comparable I-section.

The shear stress due to Saint-Venant torsion can be solved using Prandtl's membrane analogy [2]. For example, for girders with a single cell cross-section, a uniform shear flow,  $q$ , develops along the perimeter of the box and can be determined using the Bredt's equation:

$$q = \tau t = \frac{T_T}{2A_0} \quad (9)$$

in which  $t$  is the thickness of the plate, and  $\tau$  is the shear stress, which is essentially uniform through the thickness of the plates. The distribution of torsional shear stress is demonstrated for a tub girder in Figure 2.

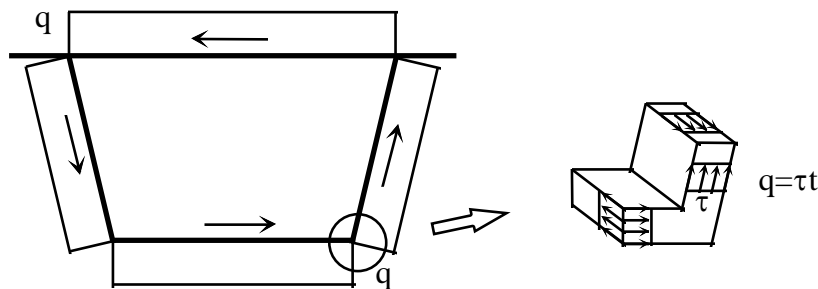


**Figure 2 Shear Flow in Tub Girder Due to Saint-Venant Torsion**

Although the torsional warping stresses in the box or tub girder are usually negligible, significant warping stresses due to the cross-sectional distortion of tub girders may develop, as discussed later in this volume. The large torsional stiffness of box or tub sections in bridges is the result of the closed cross section once the concrete deck cures. During construction of tub girders, the steel

girder is an open section and requires bracing to be designed by the engineer that will stiffen the tub girder. The bracing systems for tub girders are covered later in this volume.

## 1.2 Lateral Torsional Buckling

The overall stability of the girder system can be improved by either altering the geometry of the individual girders or by providing braces to reduce the unsupported length of the girders. Providing bracing is usually the more efficient solution and there are a variety of bracing systems that are provided as is discussed later in this volume. The elastic buckling solution for doubly-symmetric beams is given in the following solution derived by Timoshenko [3]:

$$M_{cr} = \frac{\pi}{L_b} \sqrt{EI_y GJ + \left( \frac{\pi E}{L_b} \right)^2 I_y C_w} \quad (10)$$

where,  $L_b$  is the unbraced length, and the other terms are as defined above. The first term under the radical in Eq. 10 relates to the St. Venant torsional stiffness, while the second term within the radical reflects the warping stiffness of the beam. Equation 10 was derived for the case of uniform moment loading. Most design specifications make use of solutions derived for uniform moment and then use a moment gradient modifier ( $C_b$ ) applied to the uniform moment solution to account for the benefits of variable moment. In the derivation of the buckling expression, Timoshenko assumed that the ends of the sections were restrained from twist. Although restraint against lateral translation of the section was stated in the original derivation, the assumed support condition was never applied or required to derive the expression. Therefore, effective bracing of beams can be achieved by restraining twist of the section, which is the primary means of bracing I-shaped members in bridges with the use of cross-frames or diaphragms. Twist of the section can also be restrained by preventing lateral translation of the compression flange of the section, which therefore introduces another means of bracing. Both lateral and torsional bracing requirements are discussed later in this volume.

Lateral torsional buckling of closed box girders is not typically a concern due to the extremely large torsional stiffness of the closed cross section. During construction of tub girders, a quasi-closed section is typically created by using bracing that simulates the stiffness of a top plate (known as top flange lateral bracing). Global buckling failures of tub girder sections have occurred during construction when proper top flange lateral bracing was not provided [4].

## 1.3 Categories of Bracing

Bracing systems that are used to increase the stability of structural systems can be divided into the four categories represented in Figure 3. This section introduces the basic bracing categories, which are covered in more detail in the remainder of this volume. Although the focus of this document is on bracing for the superstructure elements of steel bridges, the basic categories also apply to columns and frames, which is demonstrated in Figure 3. Diagonal bracing such as that depicted in Figure 3a fits into the category of relative bracing since the braces control the relative movement of two adjacent points at different lengths along the main members. The lateral trusses that are used to create quasi-closed tub girders and the bottom flange bracing on I-girder systems to

improve the lateral stiffness fit into the category of relative bracing. Another very common type of bracing in steel bridges are nodal systems such as those depicted in Figure 3b. Nodal braces control the deformation of a single point along the length of the member. Cross-frames or plate diaphragms that frame between adjacent girders fit into the category of nodal torsional bracing since the cross-frames restrain girder twist at a single location. The unbraced length of the girders is defined as the spacing between adjacent nodal braces. Figure 3c illustrates continuous bracing in which the bracing is connected along the entire length of the main members. One form of continuous bracing is the concrete deck that is often connected to the girder top flange through the welded shear studs. The slab provides both continuous lateral and torsional restraint to the girders. In typical bridge design, the lateral restraint provided by the concrete deck is taken into account; but the torsional restraint offered by the deck is ignored. Lean-on bracing concepts such as those depicted in Figure 3d are commonly used in framed structures where lightly loaded members can provide bracing to other heavily loaded members by providing struts to connect the main members. The heavier loaded members lean on the other members for stability. The lean-on concepts also work by providing bracing between one set of girders and then leaning several girders on a single brace.

Some bracing systems may fit into multiple categories; however, the bracing design is usually based upon selecting one design concept for a specific category. The design philosophies for the different categories are covered in more detail in the remainder of this volume. The bracing behavior for I-shaped girders is discussed first followed by the behavior for tub girders.

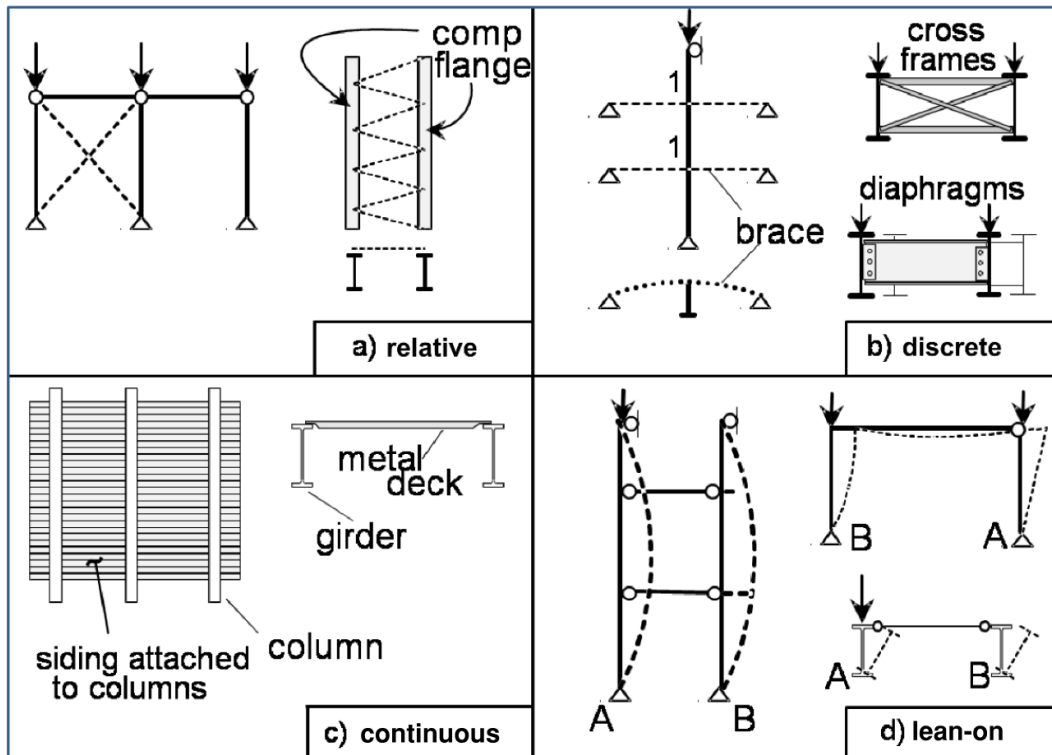


**Figure 3 Categories of Bracing**

## 2.0 BRACING OF I-GIRDERS

Bracing in steel bridges serves the dual purpose of providing overall stability of the girders as well as directly increasing the stiffness and strength of the system. Typically, bridge girders are braced by truss-type cross-frames or solid web diaphragms, while lateral bracing (bracing in a horizontal plane between adjacent girders) is typically used when it is necessary to resist larger lateral loads and limit lateral deflections during construction. In addition to resisting lateral and/or torsional loads, the cross-frame type bracing also aids in distributing gravity loads in the structure. Additionally, from a stability perspective, effective bracing must have sufficient stiffness and strength. Therefore, in subsequent discussions of stability bracing both stiffness and strength requirements are outlined.

Most reported failures of I-girder bridges occur during the construction stage prior to the hardening of the bridge deck. Except for lifting problems with curved girders, the majority of construction failures can be traced to bracing issues. The collapse of the partially erected State Highway 69 plate girder bridge over the Tennessee River on May 16, 1995 shown in Figure 4 illustrates the importance of properly designed bracing. In this case, the three 14 ft. deep plate girders with a main span of 525 ft had been successfully in place for a few days. There was a substantial bottom flange relative lateral bracing system (a lateral truss) to help resist wind and other lateral forces. There was no top flange relative lateral system provided because the bridge deck performs that function after the concrete hardens. Cross-frames with double angle members in a K-frame configuration between girders were specified to stabilize the top flange of the girders, with the highest flange stresses occurring during the planned deck pour. To facilitate erection of the third girder, during the successful lifting operation the contractor had only a few of the cross-frames in place to support just the dead weight of the girders. During the process of installing the missing cross-frames of the third erected girder, one of the previously erected cross-frames was removed because an angle member had sustained some damage. With the cross-frame removed, the unbraced length of the top flange was too large to support the dead weight of the steel and the girder buckled leading to a total collapse of the bridge as shown in Figure 4.



**Figure 4 Collapse of a Bridge over the Tennessee River due to Insufficient Bracing Provided During Steel Erection**

Bracing systems for I-girders may consist of combinations of cross-frames, solid diaphragms, as well as top and/or bottom flange lateral truss systems. In this volume, the term *cross-frame* will generally be used to also represent solid diaphragms since their functions are similar. For straight-girder bridges, the bracing system design is typically dominated by stability issues and differential deflection issues resulting from support skew. In horizontally curved-girder bridges, the effects of torsion and lateral flange bending generally control the bracing design.

This section discusses bracing on two levels: 1) Bracing needed to transfer loads within a bridge system, and 2) Bracing required to provide stability to the bridge system. In the following subsections, the design requirements and geometric arrangements for bracing systems affected by torsion, stability and skew are presented. Sections 2.1 and 2.2 provide general design requirements necessary to properly transfer the static and transient loads within a bridge system. Section 2.3 provides details for the computations associated with determining the stability requirements of a given bridge system. Also discussed within this section are the effects that support skew has on bracing systems, the use of lean-on and staggered bracing, system buckling of interconnected girders, lateral bracing systems, and continuous bracing systems.

The details and equations provided in Section 2.3 can be used to determine the stability bracing forces. These equations and methods are usually sufficient for typical I-girder bridges, including straight, curved, and skewed bridges. Using these equations, the stability bracing forces are additive to the bracing forces resulting from a first-order type of analysis (dead load, live load, etc.). For more complex bridges, or as alternative to using the equations discussed in Section 2.3, a large displacement analysis can be used to determine the bracing forces. In this type of analysis, the bracing forces will include the bracing forces required to transfer loads within the bridge system and the bracing forces required for stability. When a large displacement analysis is used, the effects of imperfections must be considered in order to achieve the desired analysis results. Furthermore, the equations provided in Section 2.3 will generally yield conservative bracing forces, as compared to those that result from a large displacement analysis.

## **2.1 General Requirements**

For I-girder bridge systems the most common bracing is a discrete torsional system consisting of cross-frames with a K- or X-configuration. Solid plate or channel diaphragms are also used. The braces are usually fabricated from angles or of solid diaphragms constructed with channel-type sections for ease in attachment to girder stiffeners. In some cases, top or bottom lateral truss bracing (a relative brace system) may be needed as temporary bracing during construction or permanent bracing to mainly resist wind loads. The requirements given below for cross-frames and lateral flange bracing are generally taken from the *AASHTO LRFD BDS* [1].

### **2.1.1 Cross-Frame Spacing and Proportions**

Cross-frames are necessary at all supports of straight and curved I-girder bridges to transfer lateral loads from the superstructure to the bearings, to provide no-twist boundary conditions for lateral buckling evaluation and transmit torsional overturning and uplift forces to the foundation. For straight girders, previous bridge specifications required that intermediate cross-frames be spaced

at no more than 25 feet. Since the first publication of the *AASHTO LRFD BDS* in 1994, this requirement has been replaced with the statement that the cross-frame spacing should be determined by a rational analysis [1]. The elimination of the specified maximum spacing for straight girders is intended to result in a reduction in the number of fatigue-prone attachments. However, various Owner-agencies may have their own requirements and preferred practices regarding cross-frame spacing that may supersede the *AASHTO LRFD BDS*.

To determine the spacing of intermediate cross-frames, at a minimum, a rational analysis should consider the following:

- The need for cross-frames during all stages of the assumed construction staging, as well as in the final condition.
- Lateral support to bottom flange for deck overhang construction brackets.
- Sufficient transfer of lateral wind loads from the bottom of the girder to the deck.
- Stability of the bottom flange for loads producing compression in the bottom flange.
- Stability of the top flange for loads producing compression, especially during the construction stage or for non-composite systems.
- Control of flange lateral bending effects.
- Distribution of vertical dead and live loads applied to the structure.

Typically, cross-frames play a more active role in horizontally curved steel girder bridges compared to straight girder bridges without significant skew. Curved girders are subjected to combined bending and torsion. Without cross-frames, the flanges of the I-section would have to be prohibitively large to control the flange lateral bending stresses (warping normal stresses) that are combined with the major-axis bending stresses. Cross-frames allow the girders to work together as a system to resist the torsion on the curved bridge and they limit the lateral bending stresses by supplying torsional supports along the span. Therefore, cross-frame members in curved bridges are considered primary members and should be designed for forces computed by appropriate analysis methods (see Section 2.2).

In curved I-girder bridges, the cross-frames should be orientated in a radial manner throughout the span, whenever possible (In curved and skewed bridges, cross-frames at the supports may be placed along the skew or in a radial manner and are often orientated in a radial manner within the span.) The spacing of the cross-frames,  $L_b$ , must control lateral buckling of the compression flange and limit the magnitude of the flange lateral bending stresses. Davidson et al. [5] developed an equation for the spacing required to limit the flange lateral bending stresses to a specified percentage of the flange major-axis bending stress. However, AASHTO specifies a maximum  $L_b$  limit as shown in the following expression:

$$L_b \leq 0.1R \leq \pi r_t \sqrt{\frac{E}{0.7F_y}} \leq 30 \text{ ft} \quad (11)$$

where  $R$  is the radius of curvature and  $r_t$  is the radius of gyration for lateral buckling. The reasoning for these limits is given in NSBA's *Steel Bridge Design Handbook: Structural Behavior of Steel* [6].

For straight girders with skewed supports, the relative displacement of the two ends of a cross-frame or diaphragm system can introduce significant live load forces into stiff bracing systems, especially near supports. The skew also affects the stability brace stiffness and strength requirements. As specified in *AASHTO LRFD BDS* Article 6.7.4.2, where the supports are not skewed more than 20 degrees, intermediate diaphragms may be placed in contiguous skewed lines parallel to the skewed supports. Where the supports are skewed more than 20 degrees, cross-frames must be placed perpendicular to the girders in contiguous or discontinuous lines. In cases where supports are skewed more than 20 degrees, it may be advantageous to place cross-frames in discontinuous lines to reduce the transverse stiffness of the bridge, particularly near interior supports. Placing the cross-frames in discontinuous lines can decrease cross-frame forces but increase flange lateral bending effects (see Sections 2.3.2 and 2.3.3). Recommended beneficial framing arrangements utilizing discontinuous cross-frame lines are discussed further in *AASHTO LRFD BDS* Article C6.7.4.2.

Diaphragms and cross-frames for rolled beams and plate girders should be as deep as practicable, but as a minimum should be at least 0.5 times the beam depth for rolled beams and 0.75 times the girder depth for plate girders. Cross-frames should contain diagonals and both top and bottom chords even if analysis shows that a chord force is zero. The flexural stiffness of a cross-frame without a top or bottom chord is substantially reduced and may become ineffective as a stability brace. Several orientations are possible for a cross-frame, such as an X-shape with top and bottom chords, and K-shape where the diagonals intersect the bottom chord, or a K-shape where the diagonals intersect the top chord. Cross-frame truss assemblies are preferably field delivered as a single unit rather than individual pieces for erection efficiency as well as assisting the erector with girder alignment. Efficient cross-frames are typically as deep as practical so that the diagonals of the cross-frame have large enough angles to prevent the gusset-type plates at the ends of the cross-frame from becoming too large. For cases requiring relatively shallow cross-frames, the diagonals of X-systems may be subjected to large axial forces with large unbraced lengths. In these cases, K-frame systems should be considered.

### **2.1.2 Top and Bottom Flange Lateral Systems**

In steel I-girder bridges, the need for lateral bracing should be investigated for all stages of construction, and the final condition. Lateral bracing may be required to resist lateral forces from wind and during construction, when the deck is not in place. When lateral bracing is required, it should be placed either in or near the plane of the flange being braced. Connecting the lateral bracing directly to the flange with a bolted connection (with or without a connection plate) is a preferred practice, as it eliminates the need for connection elements on the girder web that can be sensitive to fatigue issues. In addition, connecting directly to the flange provides a direct load path that improves the structural efficiency.

To help prevent lateral movement of the structural system during construction, especially in spans greater than 250 feet, it may be desirable to consider providing either temporary or permanent flange level lateral bracing. Flange level lateral bracing may also be needed in deck replacement projects on long span bridges. In the final condition, the concrete deck resists lateral wind loads and prevents significant horizontal movement of the structure. However, if the deck requires

replacement and is removed, lateral deflections due to wind can be excessive in long span bridges without lateral bracing. The large lateral flexibility may make the construction workers uncomfortable or can result in system instability. Essentially, a lateral bracing system will stiffen a non-composite structure significantly, as compared to one without any lateral bracing.

As noted above, top flange level lateral bracing is preferred. When located in the same plane as the top flange, the bracing is near the neutral axis of the final composite structure. As such, the bracing located at the top flange will not be subjected to significant live load forces in the final condition. In general, forces during construction related to wind and dead load will govern the design of top flange level lateral bracing. If top flange lateral bracing is subjected to live load forces in the finished structure, fatigue aspects of the detailing should be considered. Also, when top flange lateral bracing is connected directly to the top flange, the deck formwork needs to be detailed to avoid interference with the bracing members. A top lateral bracing system also interferes less with future inspection access using traditional underbridge inspection equipment.

Bottom lateral bracing can provide a similar function as top lateral bracing, but the lateral trusses can experience large forces induced by vertical bending of the I-girders, similar to those reported in tub girders by Fan and Helwig [7]. These live load forces that result from the vertical bending need to be considered by the designer. In I-girder bridges, bottom lateral bracing creates a pseudo-closed section formed by the I-girders connected with bracing and the concrete deck. In curved bridges where torsion is always present, the lateral truss will contribute significantly to the torsional stiffness of the bridge system. In addition to significant bottom flange level bracing forces caused by the torsion and pseudo-box effects, cross-frame forces will also be larger as the cross-frames act to retain the shape of the pseudo-box section.

## **2.2 Cross-Frame Forces in Horizontally Curved Girders**

Cross-frames are primary members in horizontally curved I-girder bridges. The cross-frame forces from bending and torsion in all phases of construction and loading can be determined directly from a first-order structural analysis of the bridge system. (Here, first-order structural analysis refers to a typical design analysis for static and transient loads.) Guidelines for proper modeling of the cross-frames in 3D-FEA or grid analyses are described in NSBA's *Steel Bridge Design Handbook: Structural Analysis* [8] and in the AASHTO/NSBA [9]. The availability of computer programs to determine the forces during erection and staged deck pours is improving. Stability brace forces can be determined using equations and methods discussed in Section 2.3. Alternatively, brace forces can be determined by a large displacement analysis on straight and curved girders, provided the effects of imperfections are considered. The necessity of including the imperfections in the analysis is generally dependent on the degree of horizontal curvature. For straight and mildly-curved girders (radius approximately greater than 1200 feet), stability forces will typically dominate. Initial imperfections are not important for girders with significant curvature.

Cross-frame forces can be determined directly from 3D analysis methods, and somewhat directly from 2D analysis methods. Prior to the widespread use of refined analysis methods for curved-girder bridges, cross-frame forces in curved I-girder bridges could be determined by the approximate V-load method mentioned in Ref. [8]. The development of the V-load method is documented by Poellot [10]. In the V-load method, the lateral flange bending curvature effects

are approximated by applying equal and opposite lateral loads,  $q = M/R\rho$ , to each flange of an equivalent length straight girder, where  $R$  is the radius of curvature of the bridge and  $M$  is the girder moment due to gravity loading. Vertical V-loads that are equivalent to the overturning torsional moment in the curved system are also applied at the cross-frames. The cross-frames provide lateral support to each flange with equal and opposite reactive forces  $qL_b$ , where  $L_b$  is the spacing of the cross-frames. The distribution of the cross-frame end moments and shears across a transverse section of the bridge is determined by equilibrium considerations only. The distribution of cross-frame end moments and shears have been conveniently summarized by Liu and Magliola [11] for systems ranging from 2-girder to 8-girder bridges. Design examples applying the V-load method are available [10, 12]. The V-load method cannot be used if there is a flange lateral truss system present, as the lateral truss resists the lateral flange bending effects and thus the V-load method will yield inaccurate results. [13]. Other potential cross-frame forces from stability requirements, wind, overhang brackets and other lateral loads should be added algebraically to the cross-frame forces determined via the various analysis methods.

In relatively flexible systems, second order effects can be significant. For example, curved I-girders with flange to depth ratios ( $b_f/D$ ) near the *AASHTO LRFD BDS* limit of  $1/6$  [1] specified in Article 6.10.2.2 will be relatively flexible and are likely to experience significant second order effects, particularly during erection when the full bracing is not yet installed. Research on curved girders by Stith et al. [14] found that proportioning girders with  $b_f/D$  ratios of approximately  $1/4$  or greater significantly reduces second order deformations during steel erection. In these cases, cross-frame forces due to horizontal curvature often can be predicted from a first-order structural analysis of the curved system with sufficient accuracy. These forces can be determined directly using commercial structural analysis programs or by using the approximate V-load method.

### **2.3 Stability Bracing of I-Girders**

For bridges with straight I-shaped girders, some type of bracing system will most likely be necessary to control lateral buckling of the compression flange(s) during construction. Note that the inflection point should not be considered to act as a brace point, in accordance with Article C6.10.8.2.3 of the *AASHTO LRFD BDS* [1].

This section provides a discussion of design recommendations for torsional and lateral bracing, related to the required stiffness of the various bracing components. While engineers historically have not typically performed these calculations, they are provided so that engineers can verify that the stiffness provided by the cross-frame and connection details is sufficient. The details and equations provided in this section and the related subsections can be used to determine the stability bracing forces. Using these equations, the stability bracing forces are additive to the bracing forces resulting from a first-order type of analysis (dead load, live load, etc.). For more complex bridges, or as an alternative to using the equations discussed in Section 2.3, a large displacement analysis can be used to determine the bracing forces.

Guidance on the practical implementation of stability bracing forces in bridge design is provided in the Pennsylvania Department of Transportation's Bridge Design Standard Drawing BD-619M [15]. BD-619M provides design guidance on combining the stability bracing forces with first-order analysis bracing forces in the context of the *AASHTO LRFD BDS* limit state load combinations. More recent guidance is provided in NCHRP Report 962 [16].

For continuous straight spans, bottom flange compression will generally require cross-frames or diaphragms to provide discrete bracing of the otherwise unbraced compression flange. In composite construction, the hardened deck prevents the top flange from twisting and lateral movement and also provides a bracing effect to the bottom flange if web distortion (Figure 5) is considered. For rolled sections, web distortion is not a significant issue because the web slenderness ratio is low ( $d/t_w < 60$ ).

For plate girders with stiffeners designed to control web distortion that are in contact with or welded to the top flange, no live load lateral buckling can theoretically occur in the negative moment region. For unstiffened plate girders in continuous composite construction, web distortional buckling as shown in Figure 5 occurs along the bottom flange, not lateral buckling. Span length is not a significant variable for distortional buckling, so the classical lateral buckling moment given by Equation 10 does not apply. The web distortional buckling moment for unstiffened bridge girders in negative moment regions can be conservatively predicted by the formulas given in Ref. [17]. However, the practice of considering only the transverse stiffeners and web distortion as discussed above is currently not a common practice in bridge engineering nor is it in conformance with the *AASHTO LRFD BDS*. It may only be potentially suitable for special situations. For example, a bridge in service could be hit by an over height vehicle and the cross-frames could be damaged. In this case, it may be necessary to remove the cross-frame and determine the buckling strength without the cross-frame in accordance with the formulas given in Ref. [18].

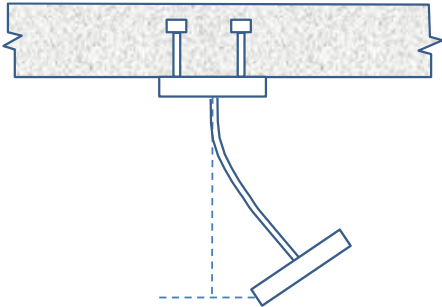


**Figure 5 Web Distortion**

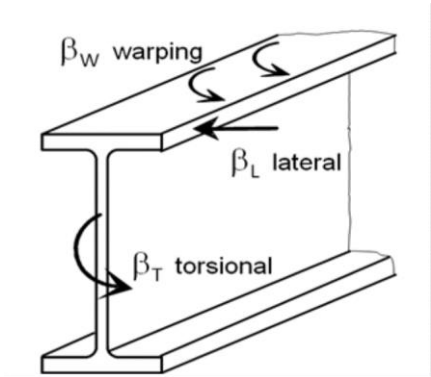


**Figure 6 Restraining Forces**

Stability bracing of beams is provided by lateral ( $\beta_L$ ), torsional ( $\beta_T$ ) and warping ( $\beta_W$ ) restraints as shown in Figure 6. Any one of these restraints alone can increase stability of the compression flange. Relative, nodal and lean-on systems as described earlier provide lateral and/or torsional restraint to single girders. Warping restraint is present only in continuous bracing systems. Lateral and warping restraints control the lateral movement of the flange to which they are attached.

Permanent metal deck forms (PMDF) that act as shear diaphragms and are attached directly to the top flange of a girder can also improve the lateral stability. Such systems provide mainly warping restraint to the top flange rather than lateral or torsional restraint. Stiffness and strength design recommendations for PMDF-braced beams are given elsewhere [19]. The diaphragm strength requirement, which is limited by the fastener capacity, generally controls the design. However, permanent metal deck forms in steel-girder bridges are not typically attached directly to the top flange and instead often bear on flexible clip angles welded to the edges of the girder top flanges, which limits the lateral stability provided by the system. Therefore, *AASHTO LRFD BDS* Article 6.7.4.1 states that metal stay-in-place deck forms should not be assumed to provide adequate stability to top flanges in compression prior to curing of the deck.

Top or bottom flange lateral bracing in I-girder bridges is relative or lean-on; torsional bracing is nodal, continuous or lean-on. If two adjacent beams are interconnected by a properly designed cross-frame or diaphragm at midspan, that point can be considered a torsionally-braced point when evaluating the beam buckling strength. Since the beams can move laterally at midspan, the effectiveness of such a torsional bracing system is sometimes questioned. As long as the two flanges move laterally the same amount, there will be no twist. If *twist* is prevented, the beam can be treated as braced at that point. Tests and theory confirm this approach [20, 21].

A general discussion of beam lateral and torsional bracing and the development of the design recommendations with design examples for bridge girders are presented elsewhere [18]. The design recommendations for torsional and lateral bracing given in Sections 2.3.1 and 2.3.5 have been adopted by the AISC Specification. The Commentary on the AISC Specification should be consulted for discussion on implementing the stability bracing requirements. The provisions are limited to doubly- and singly-symmetric members loaded in the plane of the web. Beam loads are assumed to be applied at the top flange, which is typical in bridges. Stability braces must have sufficient stiffness and strength to be effective.

### **2.3.1 Torsional Bracing Design Requirements, $\beta_T$**

The most common form of bracing in steel bridge systems are cross-frames or diaphragms that restrain the twist of the girders and are thereby typically classified as torsional braces. Concrete bridge decks in composite systems also provide torsional resistance to the girders. As noted earlier, effective stability bracing must possess sufficient stiffness and strength. The required flexural stiffness and strength requirements for torsional bracing recommended herein are given by Eqs. (A-6-11a) and (C-A-6-11), respectively, taken from Appendix 6 of the AISC Specification [22] as follows:

$$\text{Stiffness:} \quad \beta_T = \frac{\bar{\beta}_T L}{n} = \frac{2.4LM_r^2}{\phi nEI_{y_{\text{eff}}} C_b^2} \quad (13)$$

$$\text{Strength:} \quad M_{br} = F_{br} h_b = \frac{0.005L_b LM_r^2}{nEI_{y_{\text{eff}}} C_b^2 h_o} \quad (14)$$

where  $\phi = 0.75$ ,  $M_r$  is the largest factored major-axis bending moment for the limit-state load combination under consideration,  $I_{y_{\text{eff}}} = I_{yc} + (t/c)I_{yt}$ ,  $t$  and  $c$  are as defined in Figure 7,  $L$  is the span length,  $L_b$  is the unbraced length,  $n$  is the number of span braces,  $h_o$  is the distance between flange centroids, and  $C_b$  is the moment gradient modifier for the full bracing condition. For a singly-symmetric section,  $I_{yc}$  and  $I_{yt}$  are the out-of-plane moments of inertia of the compression and tension flanges, respectively. If the cross section is doubly symmetric,  $I_{y_{\text{eff}}}$  becomes  $I_y$ . All torsional bracing (nodal and continuous) uses the same basic design formulas.  $\beta_T$  and  $\bar{\beta}_T$  are defined as the torsional stiffnesses of the nodal and continuous bracing systems, respectively (for continuous bracing,  $L/n$  in Equation 13 is to be taken equal to 1.0).  $M_{br}$  is the required strength of the nodal torsional brace (for continuous bracing,  $L_b$  in Equation 14 is to be taken as the maximum unbraced length permitted for the beam to resist  $M_r$ ). For cross-frames, the moment is converted to chord forces,  $F_{br}$ , by dividing  $M_{br}$  by  $h_b$ , the distance between the chords. When the values of the variables in the two unbraced segments adjacent to a nodal brace are different, the brace can be designed for the average of values of the strength and stiffness determined for both segments. It is conservative to use  $C_b = 1.0$ .

Equation 13 and a simplified form of Equation 14 appeared in the 2010 AISC Specification. The 2016 AISC Specification introduced an even simpler strength equation to replace Equation 14 (as it originally appeared in the 2010 specification), but its applicability for use in the design of steel bridges has not yet been conclusively demonstrated. Therefore, the original form of the strength equation without any simplification, as given above by Equation 14 (and as presently given by Eq. C-A-6-11 in the Commentary to the 2016 AISC Specification), is recommended herein for use in bridge design until further studies are completed. This original form of the strength equation gives less conservative results for singly symmetric sections than the simplified form of the strength equation that appeared in the 2010 AISC Specification. Further, research conducted under NCHRP Project 12-113 recommends an increase in the coefficients in Equations 13 and 14 to 0.36 and 0.008, respectively, to provide three times the ideal stiffness to limit the out-of-plane deformations to a value equal to the initial imperfection as the critical buckling load is approached [16]. The ideal stiffness is the brace stiffness required for a perfectly straight element to reach a specified buckling capacity between the brace points. Three times the ideal stiffness is felt to be more appropriate for flexural applications; the AISC equations are based on twice the ideal stiffness. As of this writing, Equations 13 and 14 (with the modified coefficients) are being considered for possible adoption into the next edition of the *AASHTO LRFD BDS*.

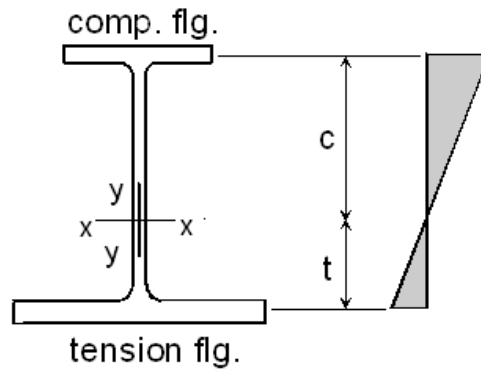


**Figure 7 Bending Stresses in Singly Symmetric Section**

In the development of the design recommendations outlined in this section, Yura et al. [21] extended the work of Taylor and Ojalvo [23] and showed that a torsional brace is equally effective if it is attached near the tension flange or the compression flange. A moment diagram with compression in both flanges (reverse curvature) does not significantly alter the torsional brace requirements. On the other hand, the stiffness of a torsional brace system  $\beta_T$  is greatly affected by web cross-section distortion at the brace point, as illustrated in Figure 5, and by the in-plane stiffness of the girders and is given by:

$$\frac{1}{\beta_T} = \frac{1}{\beta_b} + \frac{1}{\beta_{sec}} + \frac{1}{\beta_g} \quad (15)$$

where  $\beta_b$  is the attached brace stiffness,  $\beta_{sec}$  is the distortional web stiffness and  $\beta_g$  is the in-plane girder system stiffness (see Section 2.3.4). Because all of the stiffness terms are in series, the effective  $\beta_T$  is always less than the smallest of  $\beta_b$ ,  $\beta_{sec}$  and  $\beta_g$ . Brace member sizes that satisfy the torsional brace stiffness and strength criteria are usually small, but connection details must be carefully considered to control distortion.

### 2.3.2 Stiffness of Cross-Frame and Diaphragm Systems $\beta_b$

The  $\beta_b$  of some common torsional brace systems are given in Figure 8 and Figure 9. The choice between the two diaphragm cases shown in Figure 8 depends on the deck details. If the distance between the flanges of adjacent girders is maintained constant by the attachment of decking in addition to the diaphragm, then all the girders must sway in the same direction and the diaphragm stiffness is  $6EI_b/S$ . On the other hand, if adjacent flanges can separate as shown for the through girders, then the diaphragm stiffness will be  $2EI_b/S$ . For regions of the girders with the top flange in compression, placing a diaphragm above mid-height will typically cause the two compression flanges to displace laterally in the same direction bending the diaphragm in reverse curvature and resulting in stiffness of  $6EI_b/S$ . Values of the torsional bracing stiffness shown in Figure 9 assume that the connection between the girder and the brace can support a bracing moment  $M_{br}$ . Elastic truss analyses were used to derive the stiffness of the cross-frame systems shown in Figure 9. If the diagonals of an X-system are designed for tension only, then horizontal members are required in the

system. Although the top chord of the K-brace system has zero force, a top strut is still recommended to link the top girder flanges together (for the development of the stiffness  $6EI_b/S$ ).

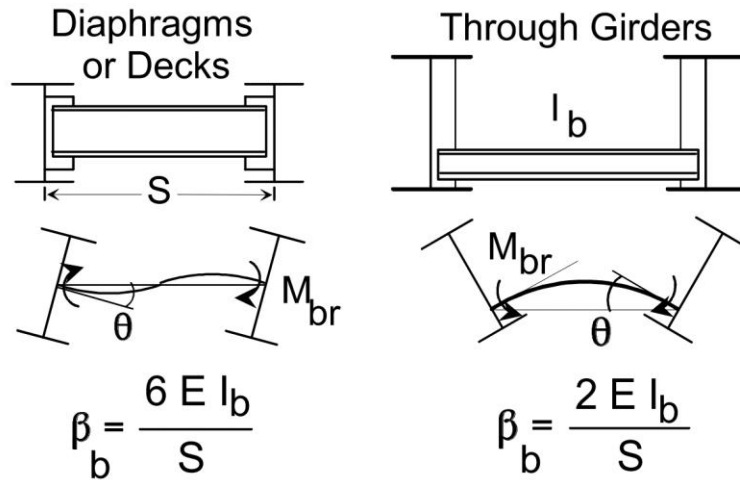


Figure 8 Diaphragm Stiffness,  $\beta_b$

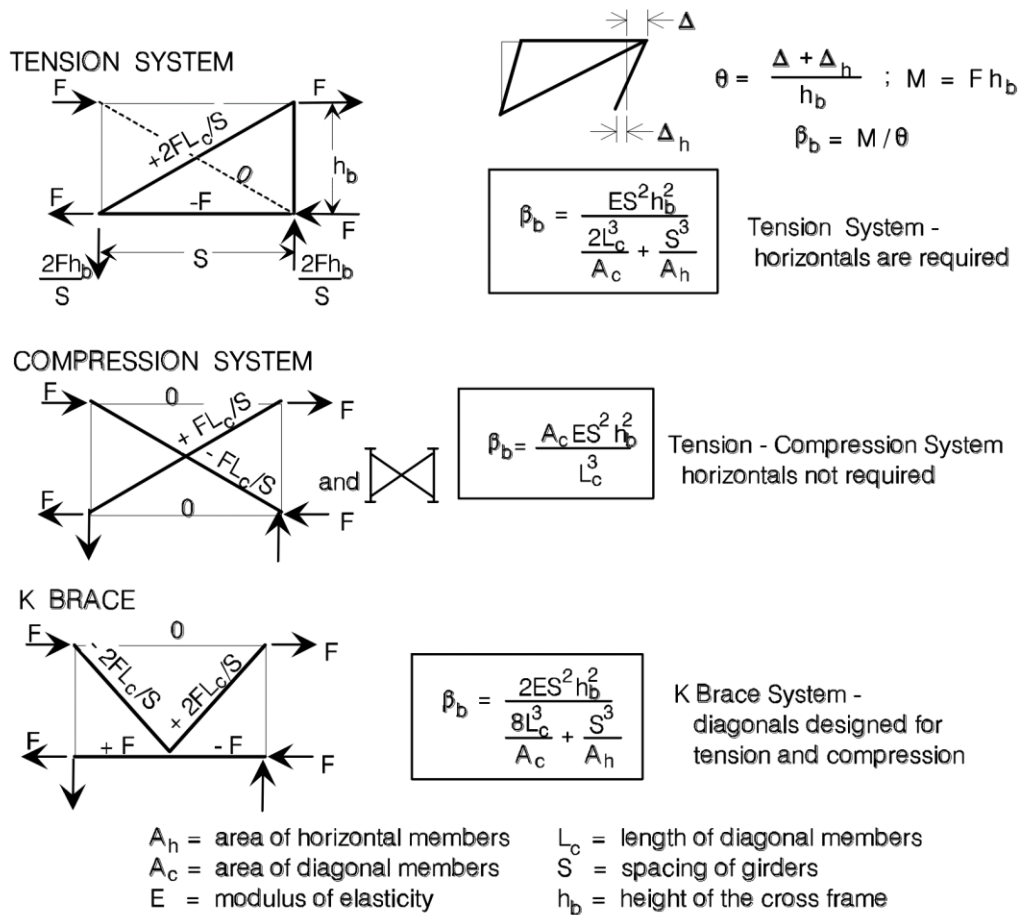


Figure 9 Stiffness Formulas for Twin Girder Cross-Frames [21]

Designs that utilize X-framing, such as the top two systems depicted in Figure 9 **Error! Reference source not found.**, may be treated as tension-only systems in which only one of the diagonals is relied upon for resisting the forces. The diagonal in compression is conservatively neglected. Structural analysis models should account for the tension-only concept when utilized. There have been cases where engineers conducting peer reviews may have been unaware of the tension-only philosophy used in the original design. As a result, the peer reviewer has requested costly retrofits because they claimed the designs were inadequate because of an apparent compressive force in one of the diagonals that exceeded the buckling capacity of that member. If one of the diagonals can support the entire load in tension, then the design is satisfactory.

In X-frame systems that rely on the compression strength of the diagonals and are connected at the intersection point, the out-of-plane and in-plane compressive strength can potentially be determined using an effective length of one-half the total diagonal length, as discussed further in Article C6.9.4.4 of the *AASHTO LRFD BDS* [1]. It has also been shown [24, 25] both theoretically and experimentally for  $T > 0.6C$  and no compression member splice that the effective length is  $0.5L$ . These studies neglect catenary action of the tension member, which is also effective in helping to provide the necessary bracing force at the intersection. However, Article C6.9.4.4 currently takes a more conservative approach and recommends that the full length of the diagonal be used for the effective length until further validation studies are completed.

### 2.3.3 Web Distortional Stiffness, $\beta_{sec}$

In Figure 5, the top flange is prevented from twisting by the bridge deck, but web distortion may permit a relative displacement between the two flanges. A stiffener (i.e., connection plate) at the brace location as shown in Figure 10 can be used to control the distortion. Note that in most bridge applications, the connection plate is to be full depth and positively attached to both flanges to account for potential fatigue issues related to distortion-induced fatigue. .

Cross-sectional distortion significantly impacts the behavior of beams with relatively shallow braces with respect to the beam or girder depth. The portion of the web that impacts distortion is the region above and below the brace. Therefore, web distortion essentially cannot occur for cross-frames or diaphragms that are nearly the full depth of the web. For braces that are less than the full web depth, distortion is controlled with the connection plates. The impact of cross-sectional distortion stiffness is accounted for with the term,  $\beta_{sec}$ , in the calculation of the actual overall bracing system stiffness. The  $\beta_{sec}$  effect on the torsional brace system stiffness, related to the out-of-plane bending stiffness of the web plus any web stiffening, is given by the following expression:

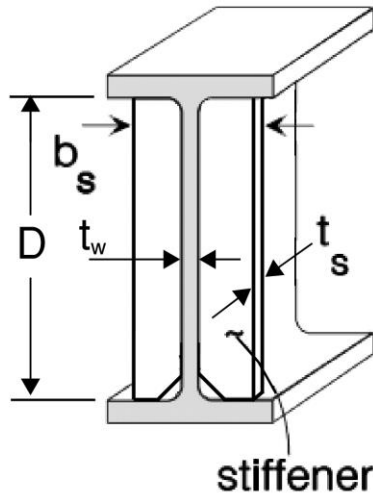


**Figure 10 Web Stiffener Geometry**

$$\beta_{\text{sec}} = 3.3 \frac{E}{D} \left( \frac{(1.5D)t_w^3}{12} + \frac{t_s b_s^3}{12} \right) \quad (16)$$

where  $t_w$  is the thickness of web,  $t_s$  is the thickness of the connection plate,  $D$  is the web depth, and  $b_s$  is the total width of the connection plate(s) on either side of the web as shown in Figure 10. The two terms within the parenthesis are the moments of inertia of the web, with an effective width of  $1.5D$ , and the connection plate(s). For continuous bracing use a unit width instead of  $(1.5D)$  in Eq. (16) and the torsional brace stiffness per unit length ( $\bar{\beta}_b$ ) in place of  $\beta_b$  in Eq. (15) to determine the required continuous brace system stiffness,  $\bar{\beta}_T$ . Equation (16) is similar to the expression for the bending stiffness of a member with the far end pinned,  $3EI/L$ .

For rolled sections, Figure 11 shows some of the geometrical decisions on the layout that need to be made in detailing diaphragms and cross-frames.

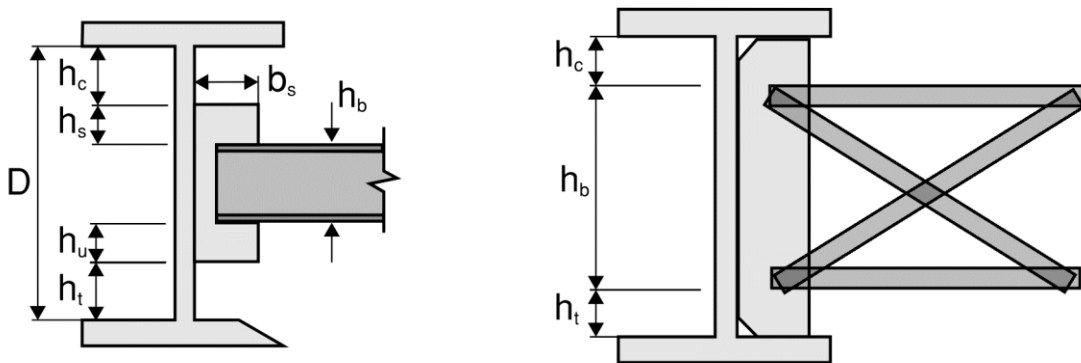


**Figure 11 Diaphragm and Cross-Frame Geometry for Rolled Sections**

The detailing can significantly affect the stiffness of the bracing system. The portion of the web along the depth of the brace (i.e., within the brace depth,  $h_b$ ) will not affect the stiffness of the brace since that portion of the web cannot distort. *AASHTO LRFD BDS* Article 6.7.4.2 requires a diaphragm or cross-frame in an I-girder bridge to extend at least  $\frac{1}{2}$  of the beam depth for rolled beams and  $\frac{3}{4}$  of the girder depth for plate girders; however, with adequate web stiffening effective bracing can be achieved with smaller depth braces. For example, in through-girder systems the floor beams are relatively shallow compared to the girders. With proper web stiffening, the floor beams provide good torsional restraint to the girders

Diaphragms are usually W-shapes or channel sections connected to the beam web through connection plates or end angles. Typically, a full-depth connection plate positively attached to both beam flanges is used. However, *AASHTO LRFD BDS* Article 6.6.1.3.1 does permit less than full-depth end angles or connection plates to be bolted or welded to the beam web to connect intermediate diaphragms in straight rolled-beam bridges with limited skew under certain conditions. This provision reflects the fact that less than full-depth end angles or connection plates have been bolted or welded to the webs of rolled beams to connect intermediate diaphragms for a number of years without noted issues. Rolled beams typically have thicker webs resulting in larger resistance to out-of-plane distortion and larger lateral-torsional buckling resistance. The end angles or plates must be at least two-thirds the depth of the web to provide some additional torsional resistance to the beam. A minimum gap of 3.0 inches is to be provided between the top and bottom of the end-angle or plate welds, or top and bottom bolt holes (as applicable), and each flange to preclude potential problems with distortion-induced fatigue.

For cross-frames or diaphragms whose depth is at least 0.8 times the beam or girder depth, attached to full-depth connection plates positively attached to both flanges as specified in *AASHTO LRFD BDS* Article 6.6.1.3.1, the term,  $\beta_{sec}$ , is sufficiently large such that web distortion is generally not an issue [19]. In such cases,  $\beta_{sec}$  is taken equal to infinity. Otherwise, as illustrated in Figure 11, the web is broken up into segments that depend on the stiffening conditions. For example, considering the section depicted in Figure 11, the web can be divided into an unstiffened compression region ( $\beta_c$ ), an unstiffened tension region ( $\beta_t$ ), a stiffened region above the brace ( $\beta_s$ ), and a stiffened region below the brace ( $\beta_u$ ). The stiffness values of the various portions of the web,  $h_i = h_c, h_s, h_t$  and  $h_u$ , are evaluated separately by:

$$\beta_c, \beta_s, \beta_t, \beta_u = \frac{3.3E}{h_i} \left( \frac{D}{h_i} \right)^2 \left( \frac{(1.5h_i)t_w^3}{12} + \frac{t_s b_s^3}{12} \right) \quad (17)$$

where  $t_s$  is the thickness of the connection plate or projecting leg of the end angle,  $b_s$  is the total combined width of the connection plates or projecting leg sizes of the end angles on each side of the web, and  $1/\beta_{sec} = \Sigma(1/\beta_i)$ . For continuous bracing, replace  $1.5h_i$  with a unit width and neglect the  $t_s$  term if there is no connection plate at that location. The portion of the web within  $h_b$  can be considered infinitely stiff. For less than full-depth connection plates or end angles used to connect diaphragms as shown in the left-hand side of Figure 11,  $h_i$  is taken as the distances along the web from the top and bottom of the connection plate or end angle to the adjacent flange (i.e.,  $h_i = h_c$  and  $h_t$ ); otherwise, if the connection plate is full-depth,  $h_i$  is taken as the distances along

the web from the top and bottom of the diaphragm member to the adjacent flange [i.e.,  $h_i = (h_s + h_c)$  and  $(h_u + h_t)$ ]. For the shallow cross-frame shown in the right-hand side of Figure 11 with the full-depth connection plate,  $h_i$  is taken as  $h_c$  and  $h_t$ .

The diaphragm does not have to be located close to the compression flange. As noted above, the location of the diaphragm may affect the brace stiffness ( $2EI_b/S$  vs.  $6EI_b/S$ ); however, for a given brace stiffness value, the location of a diaphragm or cross-frame on the cross section is not very important. The most effective cross-section location for diaphragm/cross-frames to minimize distortion and stiffener sizes is centered about the beam mid-height. The minimum depth requirements for diaphragms and cross-frames in I-girder bridges, mentioned previously, make the placement effect somewhat less significant.

### 2.3.4 In-Plane Stiffness of Girders, $\beta_g$

In cross-frames and diaphragms the brace moments  $M_{br}$  are reacted by vertical forces on the main girders as shown in Figure 12. The vertical couple causes a differential displacement in adjacent girders that reduces the torsional stiffness of the cross-frame system. These forces increase some main girder moments and decrease others and cause a relative vertical displacement between adjacent girders. The effect is greater for the two linked “twin girder” systems shown in Figure 12B compared to the fully interconnected system depicted in Figure 12A. For a brace only at midspan in a multi-girder system, the contribution of the in-plane girder flexibility to the brace system stiffness is [21]:

$$\beta_g = \frac{24(n_g - 1)^2}{n_g} \frac{S^2 EI_x}{L^3} \quad (18)$$

where  $I_x$  is the strong axis moment of inertia of one girder,  $n_g$  is the number of girders connected by the cross-frames, and  $L$  is the span length. As the number of girders increase, the effect of girder stiffness will be less significant. For example, in a two-girder system the term  $24(n_g-1)^2/n_g$  is 12 while for a six-girder system the factor becomes 100. Helwig et al. [26] showed that for twin girders the strong axis stiffness factor  $\beta_g$  is significant and Eq. (18) can be used even when there is more than one brace along the span. If  $\beta_g$  dominates the torsional brace stiffness in Eq. (15), then a system mode of buckling that is discussed later in this section is possible.

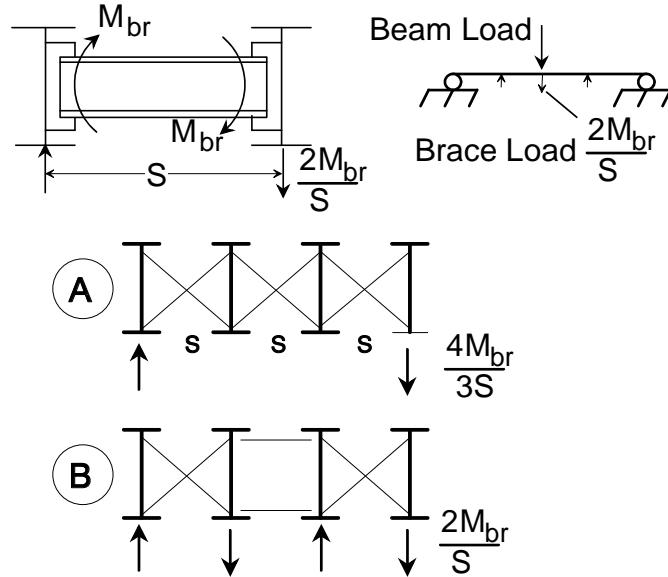


**Figure 12 Beam Load from Braces**

### 2.3.5 Connection Stiffness, $\beta_{\text{conn}}$

The diaphragm and cross-frame stiffnesses given in Figure 8 and Figure 9 assume that the attachment connections are not flexible. Clip angles welded only along the toe and tee stubs with bolted flanges will flex when tension is applied to the outstanding leg or tee stem. This flexibility,  $\beta_{\text{conn}}$ , will reduce the system stiffness. If partially restrained connections are used, the flexibility of the two connections should also be included in determining the system stiffness by adding the term,  $2/\beta_{\text{conn}}$ , to the right side of Eq. (15). Field studies [27] have reported a reduction of 40-70% in the stiffness of the non-permanent external cross-frames between tub girders due to tee stub flange flexibility. Bent gusset plates or connection plates used as an option to connect skewed cross-frames to girders when the skew angle exceeds 20 degrees from normal can also reduce the system stiffness.

The brace force design requirements are directly proportional to the magnitude of the initial out-of-straightness of the girders [28]. The brace force design requirements above are based on an out-of-straightness of  $0.002L$ . If oversize holes are used in the bracing details, the brace forces will be increased if slip occurs in the connection. This can be considered in design by adjusting the magnitude of the lateral and torsional brace force requirements by the modification factor,  $(1 + \text{oversize} / (L_b/500))$ .

The attachment of a single-angle or a tee-section member to a connection plate whether by direct connection or through an intermediate gusset plate introduces an eccentricity into the member and the connection simultaneously, which reduces the stiffness of the member. *AASHTO LRFD BDS* Article 4.6.3.3.4 states that the influence of the end-connection eccentricities is to be considered in the calculation of the equivalent axial stiffness of single-angle and flange-connected tee-section cross-frame members. Article C4.6.3.3.4 further states that in lieu of a more accurate analysis, the equivalent axial stiffness,  $(AE)_{\text{eq}}$ , of equal leg single angles, unequal leg single angles connected to the long leg, and flange-connected tee-section members may be taken as  $0.65AE$ . Engineers

should consider this guidance in the evaluation of the cross-frame stiffness,  $\beta_b$ , and in the development of finite-element models that are often used to predict forces in curved and skewed bridges. An outcome of many such analyses is the prediction of significant cross-frame forces. These forces typically result due to the size of the member input into the model and the fact that traditionally engineers have modeled these members as truss-type elements using their full  $AE/L$  stiffness contribution. Using the modified stiffness generally results in lower forces being attracted to the cross-frame members, lesser demands, and thus potentially smaller member sizes and connections.

## 2.4 Effects of Support Skew

Due to geometric requirements with either intersecting roadways or the terrain of the job site, the support lines of bridge systems often must be offset as depicted in the plan view in Figure 13.

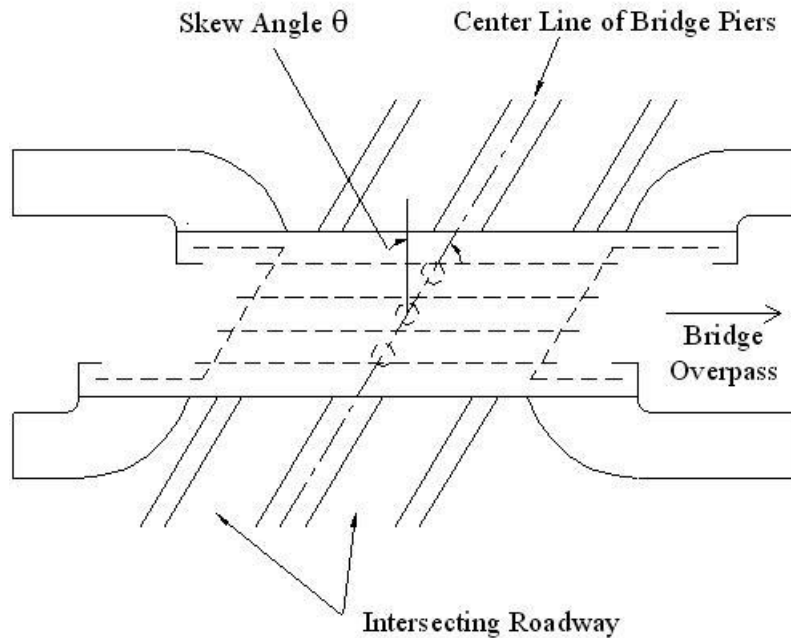


**Figure 13 Plan View of Bridge with Skewed Supports**

Since skew angles increase the interaction between the steel girders and the braces, the behavior of bridges with skewed supports becomes more complicated than that in bridges with normal supports. The interaction between the girders and braces often results in large live load forces in the cross-frames or diaphragms, which can lead to fatigue problems around the brace locations. The severity of the fatigue problem is dependent on the details that are used for the bracing. Figure 14 illustrates the two different orientations of braces for skewed bridges.

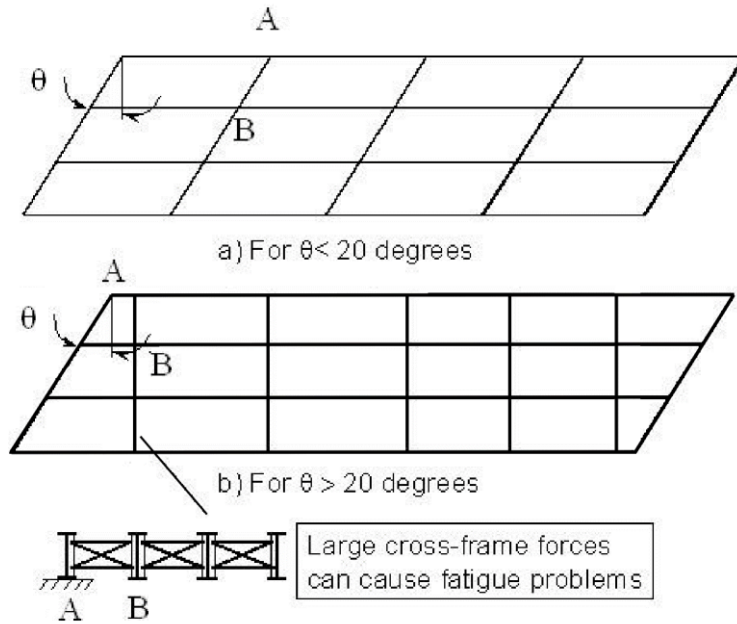


**Figure 14 Brace Orientations for Bridges with Skewed Supports**

If the skew angle is less than 20 degrees, the *AASHTO LRFD BDS* [1] allows the bracing to be parallel to the skew angle. For skew angles greater than 20 degrees, the *AASHTO LRFD BDS* requires the bracing to be perpendicular to the longitudinal axis of the girder. For braces parallel to the supporting abutments, points A and B at the ends of the brace will have similar vertical displacements during truck live load. However, when braces are normal to the girder lines, the two ends of the braces will have different vertical displacements during truck loading. This differential vertical displacement can result in large brace forces, which can lead to fatigue problems. Alternative bracing layouts to help minimize live load induced forces are to use either lean-on bracing or a staggered cross-frame layout as discussed in the next section. Alternatively, *AASHTO LRFD BDS* Article C6.7.4.2 discusses omitting individual cross-frames in perpendicular contiguous cross-frame lines, particularly near the obtuse corners of skewed supports, to reduce forces. Additionally, for perpendicular frames, the commentary discusses offsetting the first intermediate cross-frame line from the skewed support and provides recommend distances. This offset can be seen in Figure 14b.

When the cross-frames are oriented perpendicular to the longitudinal axis of the girders as shown in Figure 12(b), the provisions outlined in the previous sections for the stability stiffness and strength requirements are directly applicable with no correction required for the skew angle. The braces will develop additional forces due to differential displacement from the skew angle. For skew angles larger than approximately 45 degrees, the forces induced due to the differential displacement will be of similar magnitude or even larger than stability induced forces. During construction of the concrete bridge deck, these forces can be predicted with reasonable accuracy from a first-order analysis on a relatively simple computer model of the steel girders and bracing system. The forces from such an analysis are additive to the stability forces predicted from Eq. (14) and Figure 9.

When the cross-frames are oriented parallel to the skew angle as depicted in Figure 12(a), the skew angle has an impact on both the stability stiffness and strength requirements of the bracing. Wang and Helwig [29] present expressions for the stiffness and strength requirements of braces in bridges with skewed supports. The required stiffness of the braces is given in the following expression:

$$\beta_{bSkew} = \frac{\beta_b}{\cos^2 \theta} \quad (19)$$

where,  $\beta_{bSkew}$  is the stiffness requirement of the skewed brace,  $\beta_b$  is the required stiffness that results from Eq. 13, and  $\theta$  is the skew angle. Once the required skewed brace stiffness is determined, the stiffness equations given in Figure 9 can be used to size the diagonals and struts of the cross-frame. Although “s” in the stiffness equations is typically thought of as the girder spacing, for a skewed brace the value of “s” should be taken equal to the length of the cross-frame in the skewed orientation (equal to the girder spacing divided by  $\cos\theta$ ).

The strength requirement of the skewed brace is given in the following expression:

$$M_{brSkew} = \frac{M_{br}}{\cos \theta} \quad (20)$$

where  $M_{brSkew}$  is the brace moment applied to the skewed brace and  $M_{br}$  is the required brace moment from Eq. (14).

If the cross-frame is properly sized for the stiffness and strength requirements considering the skewed geometry, there is no technical reason why a cross-frame cannot be oriented parallel to the skew for angles larger than 20 degrees. The engineer needs to recognize that the stiffness of the cross-frame is affected by the skew as a function of the above equations and also that the parallel brace can become relatively long for larger skew angles. If the longer geometry is considered in the equations the brace will have the proper stiffness and strength.

For larger skew angles, the intermediate cross-frame lines will typically be oriented perpendicular to the longitudinal axis of the girders, but at the supports the cross-frames are usually parallel to the skew angle. One detail that can reduce the provided stiffness occurs when cross-frames parallel to the skew angle use a bent gusset plate at the end of the cross-frame member. Many designers depict a bent plate to make the connection between the brace and the connection plate (web stiffener), as illustrated in Figure 15 for a bridge with support skew of nearly 60 degrees. Such a detail allows the fabricator to utilize a connection plate that is perpendicular to the web plate; however, the bent plate connection can dramatically reduce the effectiveness of the brace due to the flexibility introduced by the eccentric connection. One solution to eliminating the bent plate is orienting the connection plate parallel to the skew angle; however, such a detail can be complicated for larger skew angles as access to the weld in the acute angle becomes problematic. In addition, fatigue tests and analytical investigations on stiffeners orientated parallel to the skew and welded to the flanges showed a lower fatigue life compared to perpendicular stiffeners [30, 31]. Another option is to use a full depth bent connection plate on the girder, where the bend line is located at the outer edge of the flange, reducing or eliminating any welds in the longitudinal direction. This option is more appropriate when using a full-depth diaphragm.



**Figure 15 Bent Plate Connection Detail Frequently Used in Bridges with Skewed Supports**

Although currently not a standard practice, an alternative to the bent plate detail in skewed bridges, Quadrato et al. [30] proposed the detail depicted in Figure 16 which shows a plan view of an I-shaped girder with a half-pipe (or half-round) bearing stiffener. The round pipe allows a perpendicular connection between the skewed support cross-frame and stiffener for any skew angle. The split pipe stiffener serves as both the bearing stiffener and connection plate. The pipe stiffener increases the warping resistance of the girder and thus improves the buckling resistance of the girder. Further information regarding the increase in warping resistance can be found in Quadrato et al. [30]. Additionally, with regard to fatigue behavior, analytical and experimental research has shown that the pipe stiffener weld detail to the girder flanges is no worse than a typical plate stiffener welded to the girder flanges [32]. However, the Engineer needs to be aware that currently, the pipe material may not be approved for use in bridges and may require special approval from the Owner.

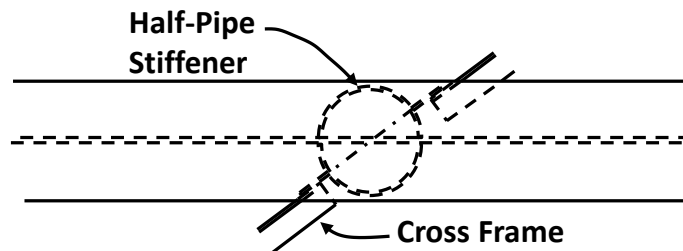


**Figure 16 Half-Pipe Web Stiffener**

## 2.5 Lean-On and Staggered Bracing

### 2.5.1 Lean-On Bracing

A common practice in the design of frames in building applications is to provide lateral stability by using lightly loaded columns to restrain other columns such as the case depicted in Figure 17.

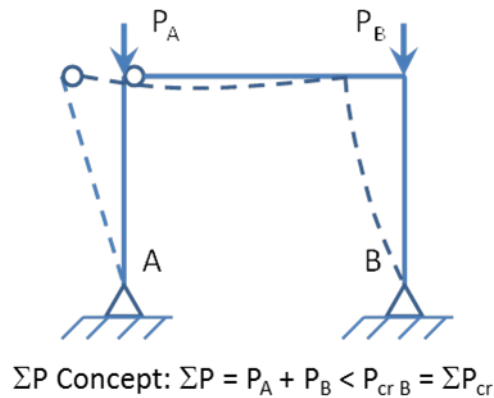


**Figure 17 Summation of  $\Sigma P$  Concept for Sidesway Frame Stability**

Column A has pins at both ends and therefore has no lateral stiffness. However, the column can be laterally stabilized by leaning on Column B, provided that column is designed to possess adequate lateral stiffness to support the total frame load. The figure demonstrates the  $\Sigma P$  concept that was presented by Yura [33] in which the frame is laterally stable in the sidesway buckling mode provided the sum of the applied load is less than the sum of the sway mode contribution of the columns in the plane of the frame. In the case depicted in Figure 17, Column A contributes no lateral stiffness to the frame and therefore Column B must be able to support the entire frame load. However, leaning columns such as Column A, must be able to support their axial force in the no-sway mode.

The  $\Sigma P$  concept also applies to beam systems such as the two beams depicted in Figure 18.

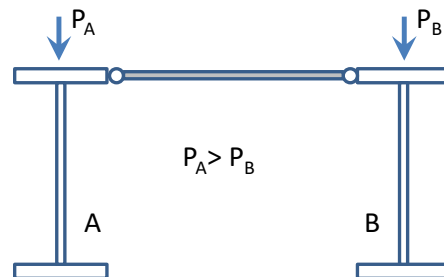


**Figure 18 Beams Linked Together at Compression Flange**

The beams are simply supported with gravity load that causes compression in the top beam flange. The two beams are connected at the top flange through a “truss bar” that does not restrain the flange rotation, but instead causes the two flanges to have essentially the same lateral displacement.

The respective loads on the two beams are  $P_A$  and  $P_B$ , in which the load on beam B is less than the members buckling load. Beam A can therefore rely, or “lean on” Beam B for stability and the  $\Sigma P$  concept, would simply require that the sum of the two applied loads are less than the sum of the two beams buckling loads. The spacing between the links must be close enough that beam A cannot buckle between the links.

The  $\Sigma P$  concept for beams is demonstrated numerically from the graph shown in Figure 19 [21].

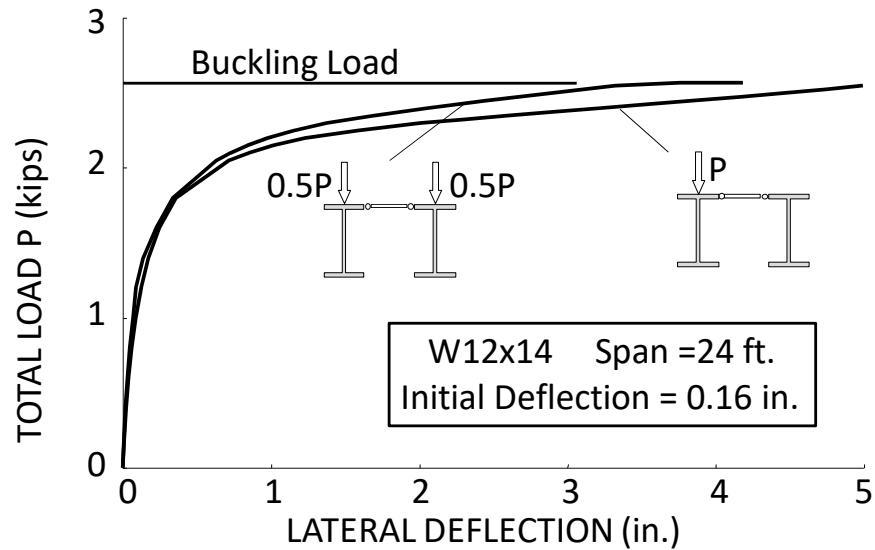


**Figure 19 Graph of  $\Sigma P$  Concept for Beams**

The graph shows results from a three-dimensional finite element analysis for two beams linked together at the top flange. The buckling load is indicated by the horizontal line in the graph that was determined from a critical load analysis (eigenvalue buckling analysis). The critical load does not reflect the impact of imperfections on the behavior. The two solid lines represent the results from a large displacement analysis on an imperfect system. The curves approach the critical load results (buckling load) at relatively large displacements. In one of the large displacement graph cases the two beams are equally loaded with  $0.5P$ , while in the other case only one of the beams was loaded with a load of  $P$ . The graphs show that the total load both beam systems can support is approximately 2.5 kips despite extremely different load distributions.

The above cases demonstrate the bracing scenario where lightly loaded beams can provide bracing to other, more heavily loaded beams. The lean-on concepts also apply to cases where beams can lean-on braces such as cross-frames or diaphragms. Cross-frames and diaphragms represent relatively costly structural components in steel bridges from the perspective of both fabrication and erection. The braces can often be difficult to install in the bridge due to fit-up problems and also may attract significant live load forces, particularly in bridges with large support skews. Therefore, minimizing the number of cross-frames on the bridge can lead to better overall bridge behavior as well as reduced maintenance costs. The typical practice in steel-bridge behavior is to place cross-frames between each of the girders at a uniform spacing along the length of the girders. Although this practice results in effective braces for providing overall stability to the bridge

girders, the resulting system is not necessary structurally efficient. Cross-frames and diaphragms fit into the category of torsional braces since they resist twist of the girders. Improved structural efficiency is possible by utilizing lean-on bracing concepts in which several girders can be braced across the width of the bridge by a single cross-frame. Lean-on bracing systems allow the designer to eliminate cross-frames on parts of the bridge where the brace is difficult to install or where large forces in the finished bridge may result from truck traffic, thereby potentially leading to poor long-term fatigue behavior. In a given bracing line, a cross-frame may be selectively positioned, and 3 or more girders can lean-on that brace as depicted in Figure 20. Girders that lean on the brace require top and bottom struts to control girder twist.

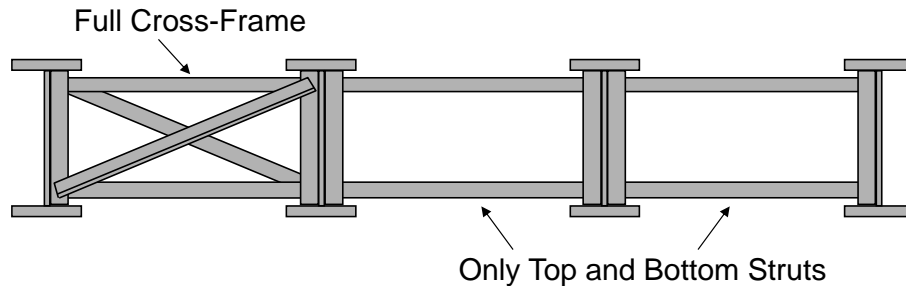


**Figure 20 Lean-on Cross-Frame Bracing**

Helwig and Wang [34] developed recommendations for straight girders with skewed supports so that intermediate cross-frames (between the supports) can be selectively located to minimize forces induced in the cross-frames. For example, the plan view of the bridge in Figure 21 shows a possible layout that will reduce the number of cross-frames and minimize the live load induced forces.

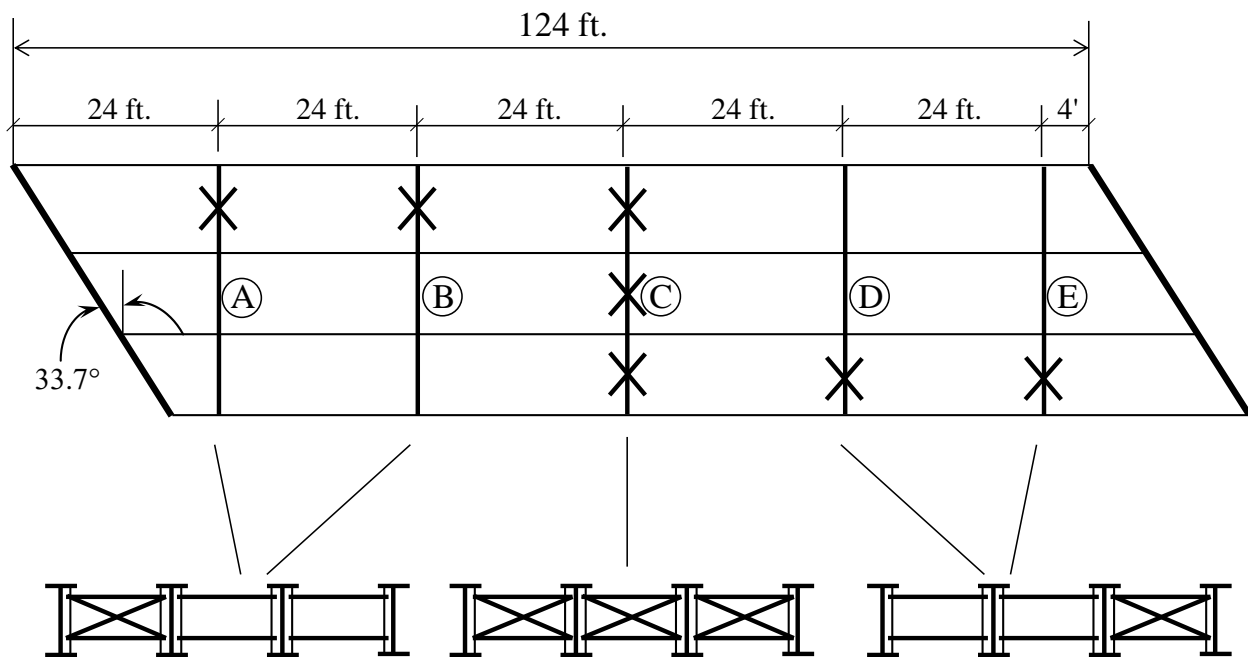


**Figure 21 Plan View of Bridge with Lean-On Cross-Frame Bracing**

In a given cross-frame line, the full cross-frame is located between the girders that will place the cross-frame as far away from the support as possible. In cross-frame lines A and B, this puts the cross-frame near the top of the figure, while in lines D and E, the braces are near the bottom of the plan view. Near midspan, at least one full line of cross-frames should be provided to link the girders together and control differential displacement. In addition, the cross-frame lines near the supports (lines A and E) should not frame directly into the support, but instead be offset by approximately 4 or 5 feet. Offsetting the bracing line from the skewed support reduces the forces induced in the cross-frame, while still producing effective bracing.

In systems with a large number of girders across the width, a contiguous line of cross-frames near midspan may not be necessary. Instead, the cross-frames can be distributed across the width of the bridge as shown in Figure 22, which shows a plan view of a straight two-span bridge with a 54-degree skew. The bridge was one of three straight bridges in Lubbock, Texas that was constructed using lean-on bracing. The circled cross-frames were cross-frames that were necessary to provide stability to the partially erected bridge.

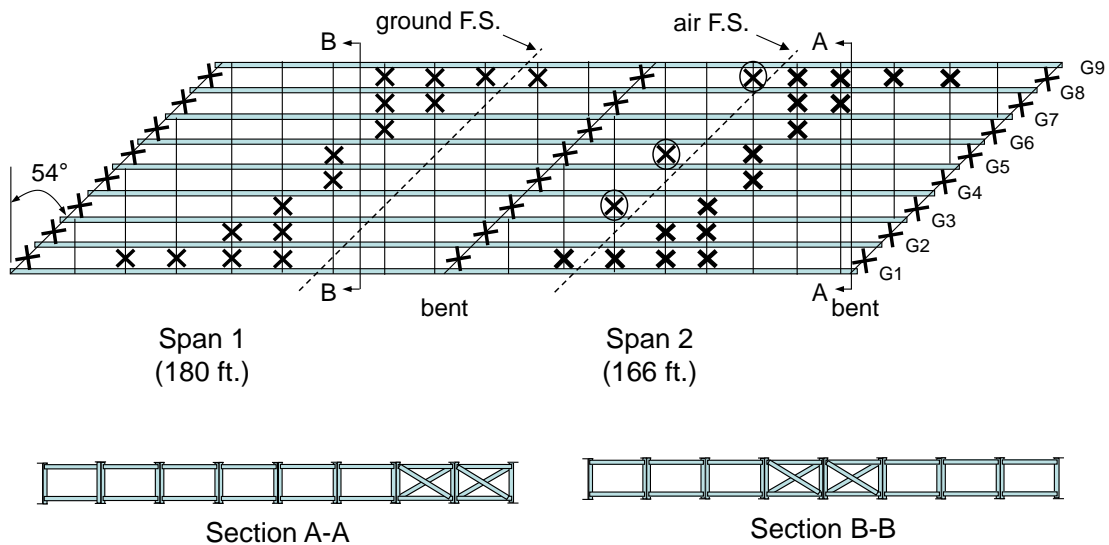
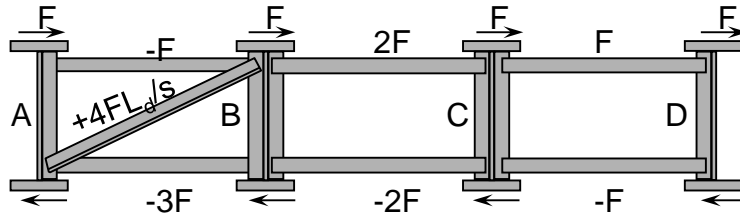


**Figure 22 Lean-on Bracing Layout in Bridge with Large Numbers of Girders**

Because there are several girders restrained by a single cross-frame in lean-on systems, the individual cross-frames need to be sized for the increased demand on the bracing. Figure 23 [34] demonstrates the distribution of forces across the bridge in a cross-frame system with lean-on bracing.



Lean-On Cross Frame Stiffness and Strength Requirements

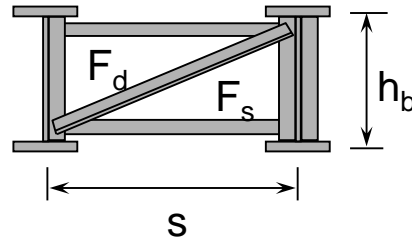
Define  $n_{gc}$  as the number of girders per cross-frame.

Brace Strength:

$$F_d = \frac{n_{gc}FL_d}{S}$$

$$F_s = (n_{gc} - 1)F$$

$$F = M_{br} / h_b$$



Brace Stiffness:

$$\beta_b = \frac{ES^2h_b^2}{\frac{n_{gc}L_d^3}{A_d} + \frac{S^3}{A_c}(n_{gc} - 1)^2}$$

**Figure 23 Stiffness and Strength Requirements for Lean-On Cross-Frames**

The cross-frame is idealized as a tension-only system. The expressions in the figure show the corresponding stiffness of the cross-frame as well as the maximum forces in the struts and diagonals of the cross-frame. In most situations, although the forces vary, the same size struts will be used throughout.

One other modification that is necessary with lean-on bracing is a reduction in the in-plane stiffness of girders. Since the bridge is not fully connected throughout, Helwig and Wang [34] recommended that the in-plane stiffness of the girders be reduced by 50% in the brace system stiffness calculation. This leads to the following expression for systems with lean-on bracing:

$$\beta_{g \text{ Lean-on}} = \frac{12(n_g - 1)^2}{n_g} \frac{S^2 EI_x}{L^3} \tag{21}$$

Note that  $n_g$  in the above cross section is the total number of girders across the width of the bridge and should not be confused with  $n_{gc}$  in the lean-on calculations.

### 2.5.2 Staggered Bracing

Another cross-frame configuration that is sometimes utilized in straight bridges with large support skews is the staggered layout depicted in Figure 24.

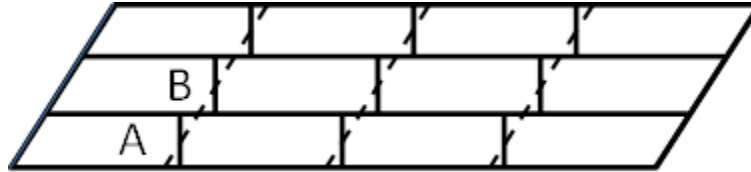


**Figure 24 Staggered Cross-Frame Layout**

In the staggered layout, the cross-frames are oriented perpendicular to the longitudinal axis of the girders; however, the individual cross-frames are staggered along a line parallel to the skew angle. The advantage of this layout is that the differential deflections at the ends of the cross-frame lines are relatively similar since the centers of the individual cross-frames are located at approximately the same longitudinal location on the bridge. Therefore, the behavior is similar to the parallel layout; however perpendicular connections can be used. The basic stiffness and strength expressions for the bracing are essentially the same as outlined for the cross-frames along contiguous lines.

Additionally, a staggered cross-frame arrangement as shown in Figure 24 will result in flange lateral bending, as the cross-frame members apply lateral loads to the girder flanges. In cases of smaller bridges or bridges with small skews, the lateral flange bending effects will be less than those that result from longer span bridges, or bridges with larger skews. The differential deflections between the adjacent girders where the cross-frames connect play a significant role in the cross-frame forces and the subsequent flange lateral bending effects.

### 2.6 System Buckling of Interconnected Girders

Cross-frame and diaphragm systems provide bracing by restraining twist of the interconnected girders. The generally accepted belief among designers is that reducing the spacing between these braces will improve the buckling capacity of the girder systems. This belief holds true for many applications. However, there have been a number of applications in which the buckling behavior of the girder system can be relatively insensitive to the spacing or size of the braces. For example, the two-girder widening shown in Figure 25 had relatively close cross-frames, however the girder experienced significant twisting during placement of the concrete deck as evidenced by the 10-inch lateral deformation of the bottom flange relative to the plumb line. The load on the twin girder system was balanced and did not have an eccentricity. The mode exhibited by the bridge widening is a buckling failure of the entire girder system as described below.



a) Twin Girder Widening



b) System Buckling

**Figure 25 System Buckling of a Twin Girder Widening, where the system has buckled out of plane nearly 10 inches during deck placement**

The buckling mode that is typically envisioned in a properly braced girder system is depicted in Figure 26a, which shows a plan view of a twin girder system. By reducing the spacing between the braces, the engineer can reduce the size of  $L_b$  and thereby improve the buckling capacity of the girders that results from lateral-torsional buckling expressions such as Eq. (10). However, in girder systems with a relatively large length to width ratio ( $L_g/s$ ), the controlling mode is the buckled shape depicted in Figure 26b. In the system buckling mode, the girder system behaves as a unit and the resulting resistance is not significantly affected by the spacing or size of the braces.

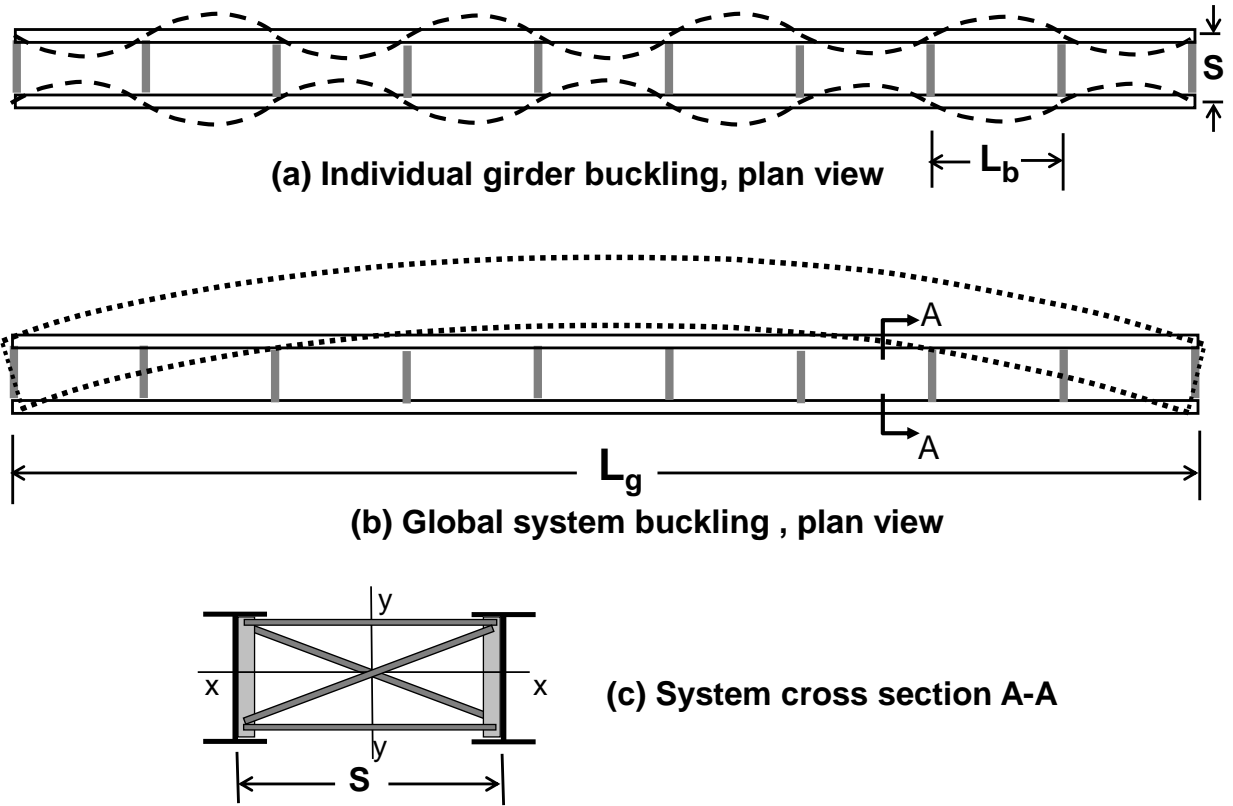


**Figure 26 Comparison of Individual Buckling Mode and System Buckling Mode**

Yura et al. [35] presented the following solution for doubly-symmetric girders that can be used to evaluate the buckling capacity of a girder in the system buckling mode:

$$M_{gs} = \frac{\pi^2 SE}{L_g^2} \sqrt{I_y I_x} \quad (22)$$

where:  $s$  is the girder spacing,  $L_g$  is the total length of the girder,  $E$  is the modulus of elasticity of the steel girder, and  $I_y$ , and  $I_x$  are the respective moments of inertia of a single girder about weak and strong axes. The expression estimates the capacity of one of the girders for comparison with the girder design moment.

For singly-symmetric girders,  $I_y$  in Eq. 20 can be replaced with  $I_{eff}$  [35]:

$$I_{eff} = I_{yc} + \frac{t}{c} I_{yt} \quad (23)$$

where  $I_{yc}$  and  $I_{yt}$  are the respective moments of inertia of the compression and tension flanges about an axis through the web, and  $c$  and  $t$  are the respective distances from the centroidal axis to the compression and tension flanges. For a doubly-symmetric section,  $I_{eff}$  given by Eq. (23) reduces to  $I_y$  since  $c = t$ .

Equation 20 provides a closed form solution that can be used to evaluate the system buckling capacity of twin girder systems. For a three-girder system, replace  $I_{yc}$  in Eq. (23) with  $3/2I_{yc}$ , and define  $S$  in Eq. (22) as  $2S$ , which is the distance between the two exterior girders. For four girders, replace the corresponding values of the  $I_{yc}$  and  $S$  terms with  $2I_{yc}$  and  $3S$ . Equation (22) shows that for a given girder span ( $L_g$ ), the system buckling mode can be improved by either increasing the stiffness of the individual girders or by increasing the girder spacing. Alternative methods of improving the buckling capacity include adding a top and bottom flange lateral truss near the ends of the girders as is discussed later in this volume.

Equation (22) is written as follows in Article 6.10.3.4.2 of the *AASHTO LRFD BDS* [1]:

$$M_{gs} = C_{bs} \frac{\pi^2 w_g E}{L^2} \sqrt{I_{eff} I_x} \quad (24)$$

where  $C_{bs}$  is a system moment gradient modifier,  $w_g$  is equal to the girder spacing for a two-girder system or the distance between the two exterior girders of the unit under consideration for a three-girder system, and  $L$  is the length of the span under consideration.  $I_{eff}$  is to be taken as  $I_y$  for doubly symmetric girders and from Eq. (23) for singly symmetric girders.

Equation (24) is for application to spans of straight I-girder bridge units with three or fewer girders, interconnected by cross-frames or diaphragms, in their noncomposite condition during the deck placement. The equation applies to units that are not braced by other structural units and/or by external bracing within the span, and to units that do not contain any flange level lateral bracing or lateral bracing from a hardened concrete deck within the span. Such units are particularly susceptible to significant global lateral-torsional amplification of the lateral and vertical displacements of the unit during the deck-placement operation. Situations exhibiting potentially significant global second-order amplification include phased construction involving narrow unsupported units with only two or three girders and possibly unevenly applied deck weight. Once a concrete deck is acting compositely with the steel girders, a given span of a bridge unit is practically always stable as an overall system. Eq. (24) is not intended for application to I-girder bridge spans in their composite condition. Eq. (24) is also not applicable to I-girder bridge units with more than three girders, which are typically not susceptible to excessive global lateral-torsional amplification during the deck placement.

Considering all the girders across the width of the unit within the span under consideration, the sum of the largest total factored girder moments during the deck placement within the span under consideration should not exceed 70 percent of  $M_{gs}$  given by Eq. (24). Limiting the sum of the largest total factored girder moments across the width of the unit within the span under consideration to 70 percent of the elastic global buckling resistance of the span theoretically limits the amplification under the corresponding nominal loads to a maximum value of approximately 2.0. Should the sum of the largest total factored girder moments across the width of the unit exceed 70 percent of  $M_{gs}$ , the following alternatives may be considered: 1) the addition of flange level lateral bracing adjacent to the supports of the span may be considered; 2) the unit may be revised to increase the system stiffness; or 3) the amplified girder second-order displacements of the span during the deck placement may be evaluated to verify that they are within tolerances permitted by

the Owner. Yura et al. [35] suggest adjustments to be made when estimating the elastic global lateral–torsional buckling resistance of the system where a partial top-flange lateral bracing system is present at the ends of the span, along with some associated bracing design recommendations.

For cases where the girders are nonprismatic and/or the girder cross sections vary across the unit, it is recommended that length-weighted average moments of inertia within the positive-moment sections of all the girders in the span under consideration be used for  $I_x$ ,  $I_y$ ,  $I_{yc}$  and  $I_{yt}$ , as applicable, in calculating the elastic global lateral–torsional buckling resistance from Eq. (24). Also, in cases where the girder spacing is less than the girder depth, it is recommended that the more general elastic global lateral–torsional buckling equation provided in Yura et al. [35] be used, as Eq. (24) becomes more conservative in this case.

The system moment gradient modifier,  $C_{bs}$ , in Eq. (24) accounts for the beneficial effect of the moment gradient within the span on the elastic global lateral–torsional buckling resistance of the span acting as a system, which is particularly significant for continuous-span units. A  $C_{bs}$  value of 1.1 applies to simply supported units and should also be applied if investigating continuous-span units that are in a partially erected condition. A  $C_{bs}$  value of 2.0 applies to fully erected continuous-span units.

$M_{gs}$  should only be used as a general indicator of the susceptibility of horizontally curved I-girder systems to second-order amplification under noncomposite loading conditions. Narrow horizontally curved I-girder bridge units as defined herein in their noncomposite condition during the deck placement may be subject to significant second-order amplification and should instead be analyzed using a global second-order load-deflection analysis to evaluate the behavior. As an alternative, the addition of flange level lateral bracing adjacent to the supports of the span may be considered, or the unit can be braced to other structural units or by external bracing within the span.

## 2.7 Lateral Bracing Systems

Common bracing systems that may be used in bridges consist of lateral trusses that control the relative movement of two points along the girders. Relative bracing systems generally consist of a combination of struts and diagonals as depicted in the plan view shown in Figure 27. As noted in the previous section, the lateral truss-type bracing depicted in Figure 27 may be used on the bottom flanges of some I-girder systems to enhance the resistance to lateral loads from sources such as wind. As is covered in detail later in this volume, these types of lateral trusses are extremely important to stiffen tub girders during construction. The struts are oriented perpendicular to the longitudinal axis, while the diagonals connect two points at different lengths along the bridge. The spacing between the two points defines the unbraced length. As the name implies, the bracing system controls the relative movement of the two points. For example, the diagonal and two struts in Figure 27 combine to form a relative bracing system.

The stiffness of the lateral bracing is a function of both the strut and the diagonal sizes, and the bracing can be designed to control the movement of Point C relative to Points A and B. The actual bracing system may vary in terms of the number or orientation of the diagonals. In some cases, two diagonals may be used, and the stiffness of the system is dependent on the buckling capacity of the diagonals. A “tension-only” system with two diagonals is sometimes specified such that the

compression resistance of the diagonal is conservatively neglected since (depending on the type of member selected) the buckling resistance may be low. However, since the lateral truss often is connected near the top or bottom flange of the girders, the designer needs to be aware of forces that can be induced in the bracing due to stresses from vertical bending of the girders. These stresses develop due to longitudinal strain compatibility between the bracing system and the girder flanges that experience compression or tensile stresses due to girder flexure. The nature of the stress induced in the lateral truss is the same state of stress in the girder where the truss is connected. For example, if the lateral truss is located at the top flange near the midspan region, gravity load stresses in the girders will induce compression in the truss. Generally, if a perpendicular cut everywhere along the unbraced length passes through the brace, then the brace system is relative.

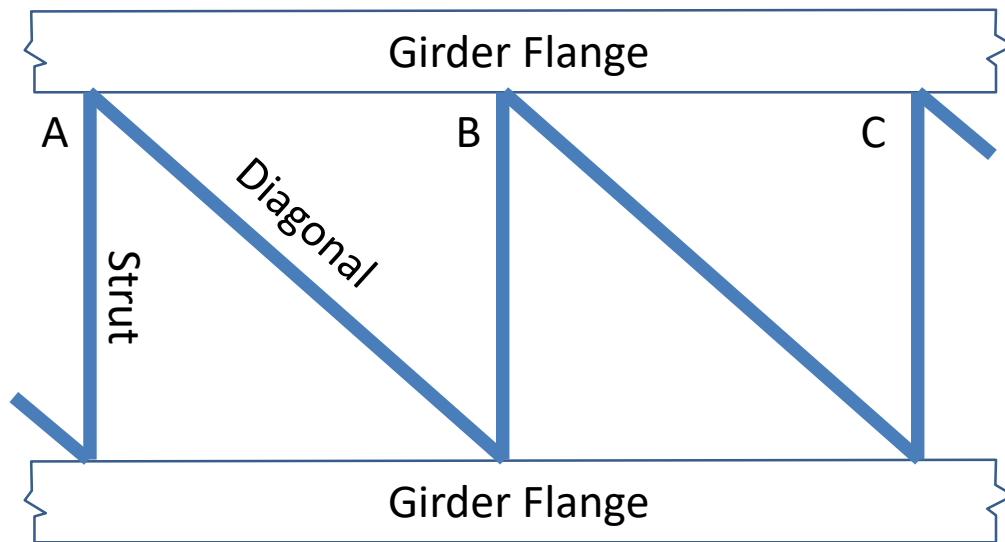


**Figure 27 Plan View of Typical Lateral (Relative) Bracing System**

Refer to the discussion at the end of Section 2.3.2 for information that may be relevant to the design of lateral bracing systems that utilize X-framing.

Winter [36] demonstrated that effective stability bracing must satisfy both stiffness and strength requirements. He demonstrated the concept with a simple rigid link model that could be used to determine the ideal stiffness requirements of the bracing as well as the impact of imperfections on the brace strength requirements. The bracing requirements for relative bracing based on Winter's approach [36], are:

$$\text{Stiffness:} \quad \beta_L = 4M_f C_d / \phi L_b h_o \quad (25)$$

$$\text{Strength:} \quad F_{br} = 0.008M_f C_d / h_o \quad (26)$$

where  $\phi = 0.75$ ,  $M_f$  is the maximum moment within the unbraced length ( $L_b$ ),  $h_o$  is the distance between flange centroids and the constant  $C_d = 1.0$  for single curvature bending and 2.0 for reverse curvature. The flange compressive force is conservatively approximated as  $M_f / h_o$ .

These provisions are applicable for lateral bracing attached near the compression flange (except for cantilevers where top flange bracing is more effective). Braces that are adjacent to an inflection point must be attached to both flanges and the stiffness and strength requirements are greater as given by the  $C_d$  factor. It should also be noted, that in most I-girder bridges, the design of the lateral bracing members will be governed by the applied loads, and not necessarily the bracing requirements presented above.

## **2.8 Continuous Bracing**

In a continuous bracing system with sufficient strength and stiffness, compression flange lateral buckling cannot occur because of the very close spacing of the connection points. A concrete bridge deck attached to the top flange through shear studs is an example of a continuous system. The hardened concrete bridge deck has very large in-plane shear stiffness and bending stiffness that effectively prevents top flange twist and lateral movement of the girders when attached by shear studs or flange embedment.

During a deck pour, the concrete has no stiffness, but the permanent metal deck forms (PMDF) do have significant stiffness and strength. In building construction, it is standard practice to use the PMDF as beam bracing when the ribs are perpendicular to the beam because the PMDF is attached directly to the top flange through the field welding of the shear studs.

In bridge construction, the connection of the deck forms requires leveling angles to account for flange transitions or differential camber. The leveling angles introduce flexible connections that reduce the effectiveness of the forms for bracing; however, the forms still do provide some help to the girder stability. A report [4] on a stability failure during a deck pour indicated that PMDF increased the girder buckling capacity 50% compared to an unbraced girder, but the increase was insufficient to support the entire deck weight. Field tests [27] on a U-shaped girder with the PMDF attached directly to the flanges with powder-actuated fasteners showed good performance. Improved PMDF attachment details have been successfully implemented on short span bridges [37, 38] that eliminated all the intermediate cross-frames. Currently, AASHTO does not allow the Engineer to consider the stability that can be provided by the PMDF's, as discussed in Section 6.7.4.1 of the *AASHTO LRFD BDS*.

### 3.0 BRACING OF TUB GIRDER SYSTEMS

U-shaped steel girders (tub girders) composite with a hardened concrete deck form a closed-box, torsionally strong bridge system. A typical cross section of a twin tub girder system is shown in Figure 28. Single tub girder systems are sometimes used for single-lane bridges. Prior to the development of composite action, the tub girder itself is a torsionally-weak, open steel section that must be braced to support the erection and construction loads. The three typical types of bracing systems are: interior diaphragms (ID), a top flange lateral truss (LT) and external intermediate cross-frames (EC) between adjacent tub girders (see Figure 29).

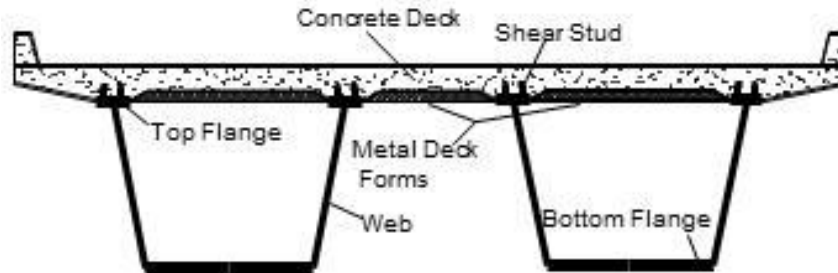


**Figure 28 Twin Tub Girder System**

The three bracing systems used with tub girders are designed to achieve one or more of the following objectives mainly during the construction stage:

1. Control box girder distortion (ID)
2. Control lateral buckling of the individual top flanges (ID, LT)
3. Increase the torsional stiffness and strength (LT, EC)
4. Control global lateral buckling of the tub girder (LT)
5. Support sloping webs in trapezoidal cross sections (ID, LT)
6. Control warping normal stresses (ID)
7. Maintain alignment in multi-girder systems (EC)

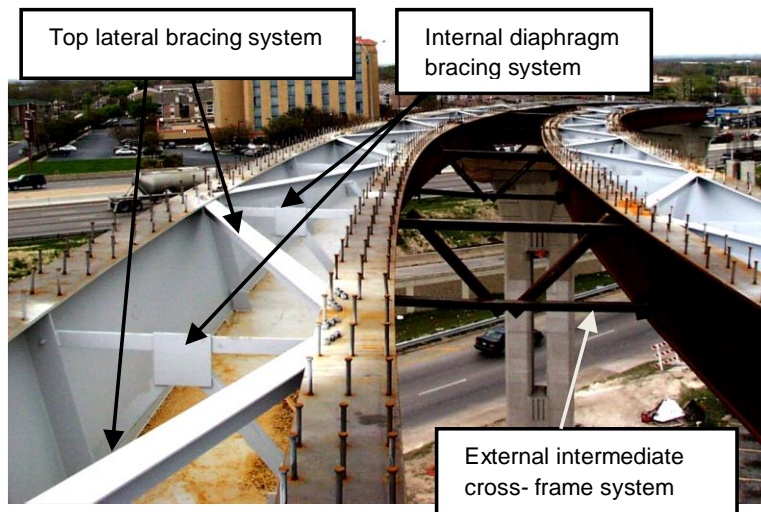


**Figure 29 Types of Bracing Systems for Tub Girders**

In the following sub-sections, the three types of bracing systems will be discussed, and design methods presented for spacing and proportioning the brace members.

### 3.1 Top Flange Lateral Truss

Horizontally curved tub girders are subjected to significant torsional loading that open steel sections cannot support by warping strength alone. By tying together the two top flanges of a tub girder with diagonals and struts to form a top flange lateral truss, the cross section becomes quasi-closed. When designing the top lateral bracing system, two major criteria must be considered, torsional rigidity and torsional strength. Torsional rigidity is related to the torsion constant  $J$  which is greatly enhanced by the top lateral system. A diagonal with an area of a few square inches will increase  $J$  by more than a thousand times (Eq. 4 divided by Eq. 3) if the top flange lateral truss is converted to an equivalent plate thickness,  $t_{eq}$ . As indicated by the expressions, the equivalent thickness is a function of the area of the diagonals, struts, the top flange areas, and the web areas. The top lateral members must have sufficient areas so that warping normal stresses can be neglected and torsional deformations can be kept small. The areas of the members must also be sufficient to resist the torsional forces imposed on the system. Vertical bending of the tub girders during construction can also develop forces in the top lateral system.

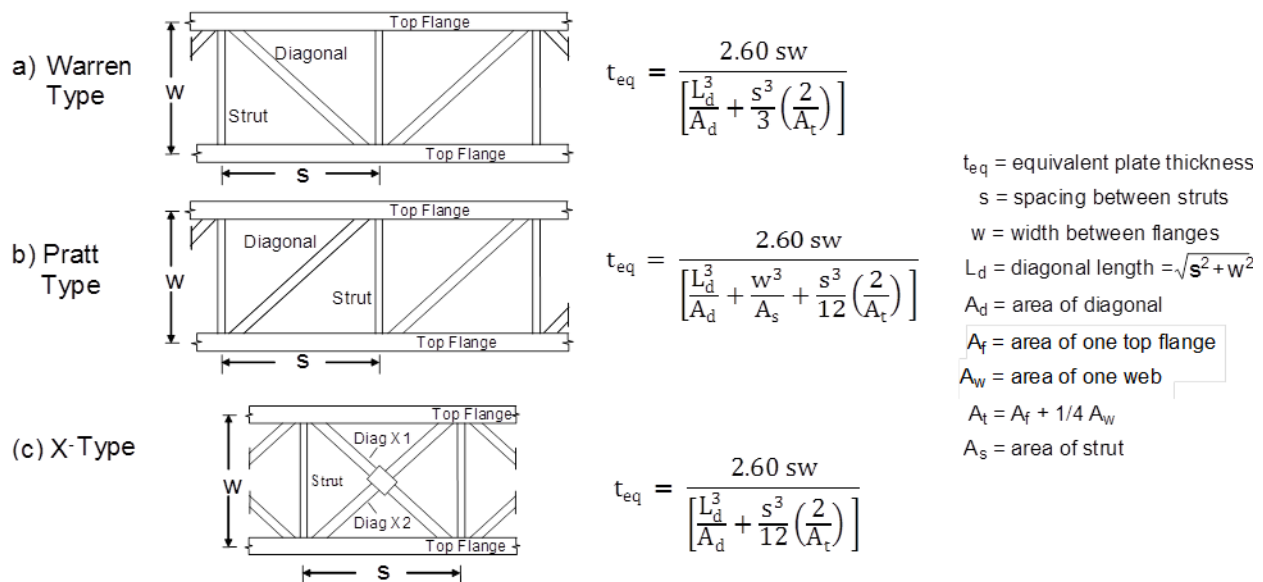


**Figure 30 Geometric Layout and Equivalent Plate Thickness of Top Lateral Systems [40]**

Three common geometric arrangements for the top flange lateral truss as shown in Figure 32 are the Warren, the Pratt and the X-type. The Pratt system is usually oriented so the diagonals are in tension. In the Warren system the diagonal at the location of maximum torque is usually oriented to be in tension. To maximize  $t_{eq}$ , the slope of the diagonals relative to the longitudinal axis of the girder should be between 35 and 40 degrees [39]. The truss arrangement should have an even number of panels within the span for improved performance especially for the Pratt and Warren types. The panel spacing is controlled by geometry or the unbraced length of the top flange.

The formulations for  $t_{eq}$  given in Figure 32 were derived by Kollbrunner and Basler [40]. If  $t_{eq}$  of all three geometric arrangements are the same, the angle of twist will be the same but the forces in the top lateral systems will vary as discussed in the next sub-section. To achieve the same torsional rigidity, the X-type requires the smallest total  $A_d$  within the panel and the Pratt system the largest. If the X-system diagonals are designed for tension only, then only one diagonal should be considered effective and  $t_{eq}$  is determined using the Pratt formula. Frequently, publications incorrectly define  $A_t$  in the  $t_{eq}$  formulations as the area of the top flange,  $A_f$ . When the top lateral truss is located below the top flanges,  $w$  is redefined as the width of the truss.

Article C6.7.5.3 of the *AASHTO LRFD BDS* [1] suggests as a guideline that  $A_d \geq 0.03w$  (all units in inches) in curved tub girders, based on work done by Heins [41] for X-type systems with two effective diagonals within the panel. Making the same Heins' assumptions for Pratt and Warren systems would require that  $A_d \geq 0.054w$ . The full derivation of the requirement for X-type systems can be found in Heins [41].

Wind and other lateral forces during the construction stage also can cause torsion in a tub girder because the shear center of the quasi-closed section is generally located below the bottom flange. The location of the shear center for a single tub or quasi-closed section is given in the Section 4.3. The applied torque is the resultant lateral force times its distance to the shear center. In straight tub girders with perpendicular supports, torsional loads do not dominate so a full length top lateral system may not be necessary. Lack of a top lateral system, however, makes the tub girder more susceptible to global lateral buckling as discussed later. If the supports are skewed, torsion must be considered.

### 3.1.1 Top Lateral Brace Forces

The forces in the members of a top lateral truss system can come from torsion, vertical bending, lateral bending, cross-section geometry, distortion and stability effects. Except for relatively straight girders, torsion effects dominate the forces in the bracing members. Figure 31 shows the forces determined from 3D-FEM analyses for a curved 180 ft simply-supported girder with three different top lateral truss arrangements [42]. The three different layouts consist of an X-type, a Pratt, and a Warren truss layout. The  $t_{eq} = 0.05$  in. is the same for all three systems. The brace member sizes within each arrangement are different in order to achieve a similar  $t_{eq}$  but are constant along the span. Only gravity load (steel and concrete deck self-weight) during construction was applied and there are no distortion forces, lateral forces or stability effects included in this comparison. The torsional forces in a lateral truss system are not significantly affected by the truss member sizes but the plots show that the forces in the three systems are different.

In the X-system two diagonals are considered effective within each panel. For clarity, the forces in the two diagonals within each panel, designated as diagonal 1 and diagonal 2, are plotted separately at the center of each panel along the span. For torsional loads only, the two diagonals should have the same magnitude of force, one in tension and the other in compression. At the left support, which is the location of maximum torque, the magnitudes of the two diagonal forces differ slightly but the disparity increases away from the supports because of in-plane bending. Although the tub girder alone is usually designed for the total bending gravity force during construction by

neglecting the top lateral truss, the top flange bending strain will induce forces in the diagonals for strain compatibility. The bending forces are maximum at midspan and small near the simple supports. On the other hand, torsional moments are maximum near the supports and zero at midspan so the diagonal forces at midspan are caused mainly by bending. Both diagonals within the panel have a 30-k compressive force at midspan. Note also that the maximum compressive force in a diagonal does not occur at the supports or midspan but at the fourth panel from each end. The largest compressive force is 25% higher than the maximum tension force in this example. Design approaches for X-type systems will be discussed later in this section.

The diagonals in the Pratt and Warren systems show similar force distributions along the span. The diagonals of the Warren truss alternate between tension and compression in adjacent panels, whereas the Pratt system has only tension in this example. The maximum diagonal force occurs at the end panels due to torsion and is approximately twice that in the X-type system since there is only one diagonal in each panel. At midspan the Warren system has a maximum compressive force of 10 kips and the Pratt system almost zero so the bending effect in these two systems is much smaller than in the X-type arrangement. In both of these single diagonal systems, lateral movement of the two top flanges occurs in the same direction due to bending, which reduces the in-plane axial stiffness of the top lateral truss. In the Warren system the lateral displacements (0.08 in.) occur in a local two-panel zigzag pattern along the span whereas the lateral displacements of each panel in the Pratt system accumulate in the same direction with a maximum lateral displacement at midspan (0.96 in) [43] as depicted in Figure 32. These lateral displacements induce local lateral bending stresses in the two top flanges of the tub girder at each strut location in the Warren system [6]. In the Pratt system, the local top-flange lateral bending effect is concentrated only at midspan where the truss diagonals change their orientation.

The strut force magnitude and distribution vary among the three systems. The struts are also usually part of the internal diaphragm system designed to control cross-section distortion and/or flange lateral buckling. No internal diaphragms were used in the span analyzed for Figure 31 in order to isolate certain types of forces in the top lateral system. In this case the strut forces can be due to torsion, bending and sloping webs. In all three systems the horizontal tension force that prevents the two flanges from spreading apart due to wet concrete load applied at the top flanges is a constant along the span and is usually quite small. The main strut forces are developed from torsion and bending. The strut forces due to torsion are zero in the X-type, are related to the algebraic sum of the transverse component of the two diagonal forces adjacent to the strut in the Warren system and are equal to the transverse component of the larger diagonal force framing into ends of each strut in the Pratt system (except at midspan). In the Warren system the strut forces due to torsion alternate from tension to compression along the span and are relatively small compared to the compressive strut forces in the Pratt system. Tub girder bending causes the large tensile forces in the struts near midspan of the X-type system (30 kips), 10-kip tensile forces in the Warren system and almost zero force in the Pratt system. In the Warren system the strut forces from all three sources (sloping webs, torsion and bending) are small and fairly constant along the length compared to the large strut forces generated in the X-type and Pratt systems.

The forces shown in Figure 31 do not include stability brace forces because a first order structural analysis was performed. Stability brace forces develop from the initial out-of-straightness of the structural components. These forces and deformations are not included in a first order structural

analysis. A top flange lateral truss system is a relative brace system that defines the unbraced length of the top flanges as the distance between panel points during the construction stage. For design, the stability brace force requirements shown previously should be added to the first order analysis forces from torsion and bending. Usually, the stability brace requirements will not alter the top lateral truss design because the largest stability forces occur at the location of the highest moment where the torsional forces are small. The stability brace requirements will only affect the top lateral design when the girders are relatively straight.

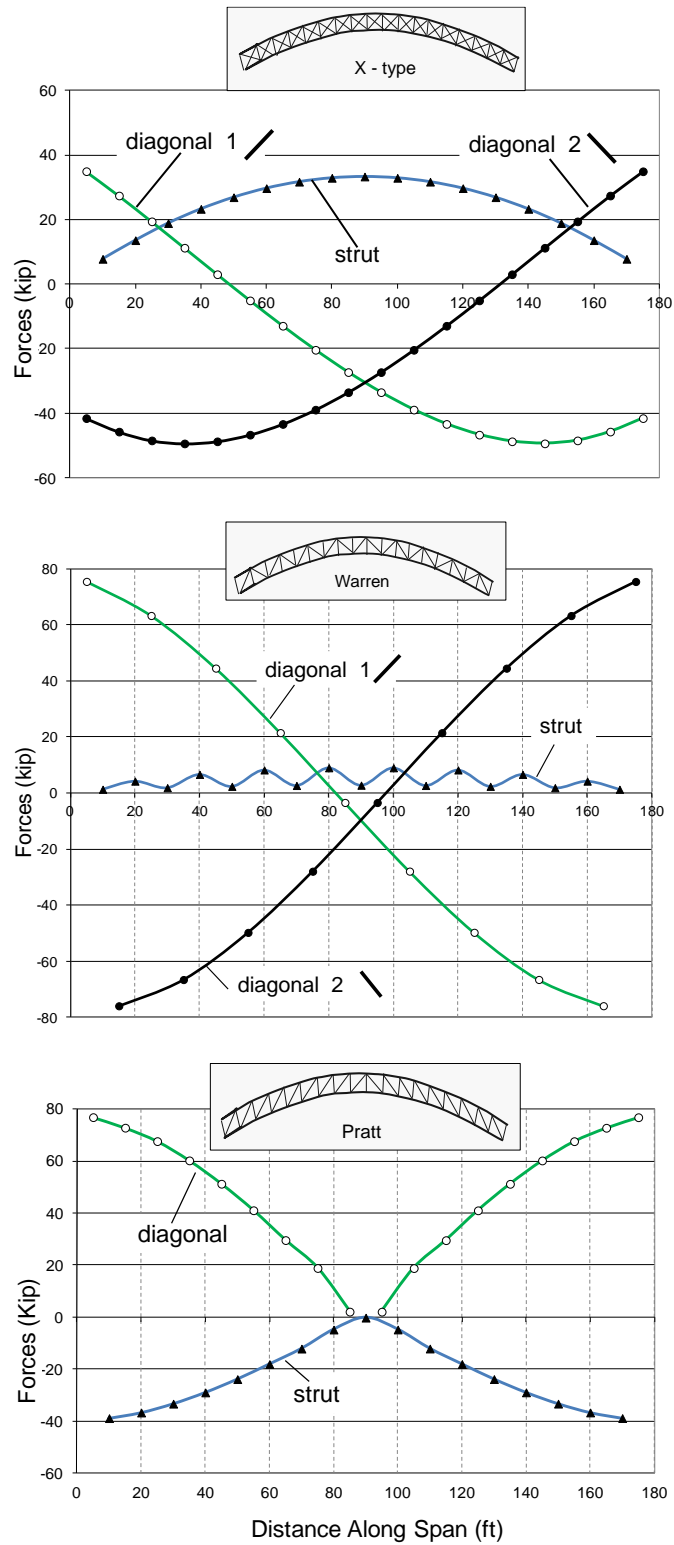


**Figure 31 Top Lateral Truss Forces for Various Tub Girder Bracing Systems**

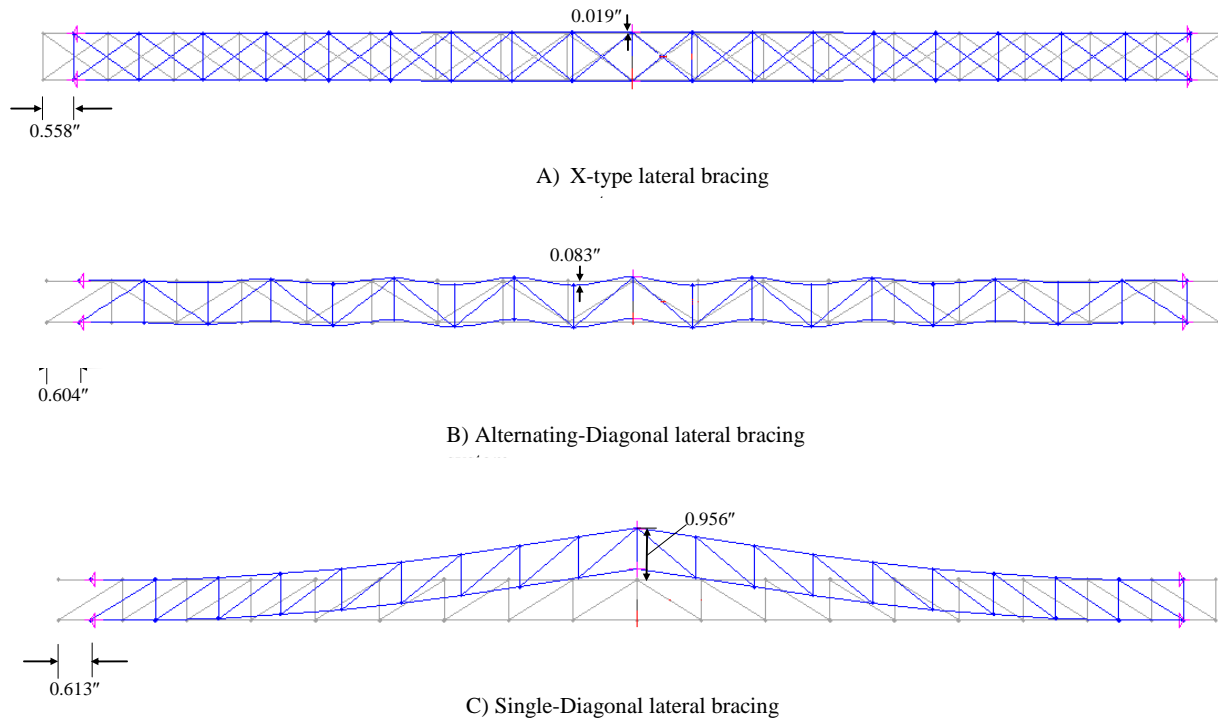


**Figure 32 Deformations of different box girder bracing systems**

### 3.1.2 Selecting the Top Lateral Bracing Layout

The layout of the top lateral bracing system is based primarily on effectively resisting the torsional forces during construction. Usually, the member sizes are kept constant along the span to minimize fabrication and detailing costs so the panels with the largest torsional moment near supports controls the initial member sizes. The diagonal forces within each panel due to torsion are similar for all three lateral systems. The Pratt system with the diagonals arranged for tension will require the smallest diagonal area. The X-type diagonals, one in tension and the other in compression, and the Warren system diagonals are controlled by compression. The two X-type diagonals will have a smaller total weight than the single Warren diagonal because the force and the unbraced length of the X-diagonal is one half that in a single diagonal system due to the bracing effect of the tension diagonal. The Warren compression diagonal would be designed for the slightly lower torsional moment in the panel adjacent to the one with the highest torsion where the diagonal is in tension. On the other hand, the strut forces from torsion are the highest in the Pratt truss and are zero in the X-type. The net effect based on brace system weight alone favors the Pratt tension system by approximately twenty percent over the Warren system. An X-type system over the entire span is the costliest system because of the greater number of pieces and connections.

The Pratt system is attractive for simple spans because it appears that the diagonals can be oriented in a tension only arrangement as shown in Figure 31 and the bending compatibility forces are negligible. However, even in a simple span, compression can develop if the pouring sequence starts at one end of the span. For example, the girder in Figure 31 will develop compressive top lateral loads (maximum value of 10 kips) in the three panels near midspan when half the span is loaded. Evaluation of the pouring sequence is important in Pratt systems. In continuous spans it is more difficult to guarantee that tension will always control in each panel. This dilemma can be

overcome by using a few X-type panels in locations where compression may develop in conjunction with the Pratt arrangement. The Warren diagonal design, which is controlled by maximum compression, offers more flexibility to handle variations in the pouring sequences that often occur in the field.

Torsional rigidity, which is affected by  $t_{eq}$ , should also be evaluated when designing the top lateral bracing system. As discussed earlier, for a targeted  $t_{eq}$  the X-type arrangement requires the least bracing weight, followed by the Warren and the Pratt systems. Comparing the Warren and the Pratt system designs for the maximum loads given in Figure 32, the Pratt was 17% lighter. The  $t_{eq}$  from the formulas in Figure 29 were 0.023 for the Pratt truss and 0.039 for the Warren truss indicating less rigidity for the Pratt system. For the Pratt truss design, a 3D-FEA analysis of the uniformly-loaded simple span gave a midspan rotation 2.3 times greater than the rotation with the Warren design. This rotation of the Pratt-system girder gave a 1.6 in. relative vertical displacement between the two top flanges of the tub girder. When torsional rigidity is a principal concern, both the Warren and X-type systems will be lighter than the Pratt arrangement with the Warren being more cost effective.

The X-type top lateral truss attracts larger bending compatibility forces than the Warren or Pratt systems as shown in Figure 31 because its geometric symmetry provides greater in-plane lateral stiffness. If these girder-bending induced forces are considered in design, the member sizes may be controlled by bending, not torsion. At locations of the highest girder bending stress where the torsional moment may be small, both diagonals within the panel can have compressive loads. In this case a diagonal is not braced at the intersection point because both diagonals can bend out-of-plane. The unbraced length is the full length of the diagonal.

### **3.1.3 Determining the Brace Forces**

The forces in the top lateral system due to torsion, girder bending and sloping webs can be determined directly if a 3D-FEA is used as illustrated in Figure 31. Field tests have shown [44] that the top flange lateral truss and external intermediate cross-frames most important function is during the construction stage. For construction stages, the designer should consider the forces in these top flange lateral truss and external intermediate cross-frames at the end of steel erection and during the deck placement sequence analysis. Most commercially available analysis software should have the ability to analyze the bridge for these conditions. Additionally, UTrAp is a no-cost 3D FEM tool that was specifically developed to analyze single and twin tub girder systems during construction [45]. The struts in the top lateral system may also function as the top chord of an intermediate cross-frame used primarily to control distortion. Distortional forces are discussed with intermediate cross-frames later in this volume. Structural models employed by grid analyses do not directly model the top flange lateral trusses. In this section analytical methods for determining the top lateral truss forces and the top flange lateral deflection bending stresses developed mainly by Fan and Helwig [6] will be summarized. The comparison between the forces from the analytical methods and 3D-FEM is very good.

### 3.1.3.1 Torsion

An approximate torsional analysis of a quasi-closed box girder can be performed using the M/R method (see reference [8]) to determine the torsional moment along the span coupled with the equivalent plate method for determining the geometric properties of the cross section. The resulting torsional properties are used in the structural analysis to determine the torsional moments in the girders. Once the distribution of torsional moment,  $T$ , is known, the shear flow,  $q$ , within each panel can be determined from Eq. 9 and used to determine the forces in the top flange lateral truss. The shear flow acting on the fictitious plate is then transformed into diagonal member forces in the lateral truss as demonstrated in Figure 33. The type of force (compression or tension) is important with regard to superimposing the torsionally-induced force with the other force components that will be discussed subsequently. Although a Warren truss is shown in Figure 34b, the same expression would be used for the Pratt truss except the forces would generally be all tension provided the diagonals are oriented properly.

After the diagonal forces from torsion have been established, the strut forces from torsion,  $F_s$ , are determined for the Pratt and Warren truss systems as shown in Figure 34. In the Pratt system the strut forces are equal to the transverse component of the larger diagonal force framing into the ends of each strut except where the diagonals in adjacent panels meet at one point (midspan in Figure 31). That particular strut would be in a Warren configuration. The simple expression for the strut force in the Warren truss shown in Figure 34 conservatively neglects the effect of the top flange lateral flexibility. More complex expressions that consider flange flexibility in the Warren system have been developed [46] but since the strut forces are small in typical bridges, this conservatism will not affect the design. The strut forces due to torsion are zero in the X-type. The signs of the forces (tension or compression) must be maintained so truss forces from sources can be properly superimposed.

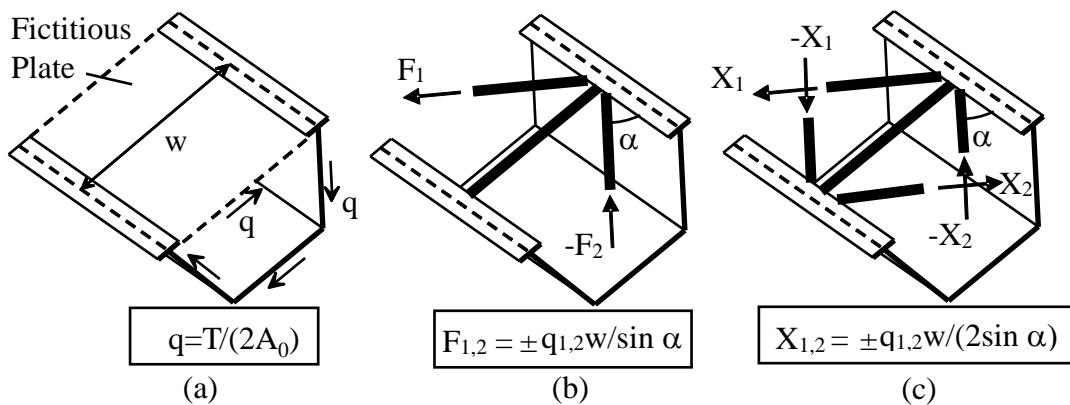


**Figure 33 Diagonal Lateral Brace Forces Due to Torsion in a Tub Girder**

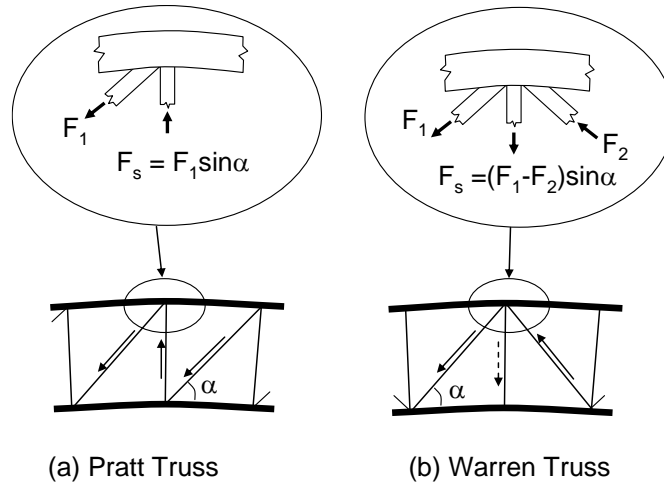


**Figure 34 Strut Forces from Torsion**

### 3.1.3.2 Sloping Webs

The sloping webs of trapezoidal girders also induce a lateral load component on the top flange. This lateral load component causes additional top flange lateral bending stress as well as axial forces in the struts of the lateral truss. The struts are typically designed to carry the horizontal component due to the sloping webs. Historically, some past design aides [8] provided recommendations that the top and bottom flanges each support half of the horizontal web components of the applied load. Based on this assumption, the half acting on the bottom flange does not generate any top flange lateral bending stress or forces in the struts. While this assumption would be relatively accurate for the girder self-weight, the sloping web component from external loads from sources such as the fresh concrete deck must be resisted by the top flange lateral truss. This can be demonstrated by considering a free body diagram of the top flange with an externally applied distributed load of  $p/2$  applied to each flange. Figure 35 demonstrates the transformation of the vertical load into a web shear and a horizontal component,  $f$  (force per unit length). For a truss panel length of  $s$ , the recommended design tensile force for the struts is equal to  $(f \times s)$ . The maximum lateral flange bending moment due to the top flange loading is  $(fs^2)/12$ , assuming the top flange behaves as a continuous beam supported at the strut locations.

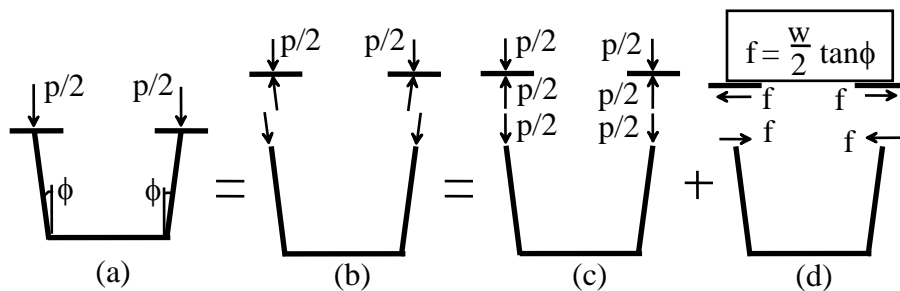


**Figure 35 Strut Forces from Top Flange Loads**

### 3.1.3.3 Vertical Bending

In addition to torsionally-induced forces, the top flange truss also develops forces due to vertical bending of the box girder. When the lateral truss system is attached to the top flanges of the tub girder, the longitudinal top flange deformations between panel points from bending stresses produces a compatible longitudinal deformation and corresponding force in the truss diagonals. As shown in Figure 36, the tub girder and the top lateral truss together resist the vertical bending. If the tub girder alone was designed to support the bending forces, the stress distribution through the depth of the tub girder would be represented by the dashed line. The forces in the diagonals reduce the tub bending stresses shown by the solid line. These strain-compatibility truss forces are generally undesirable since the primary purpose of the lateral truss is for torsional stiffening.

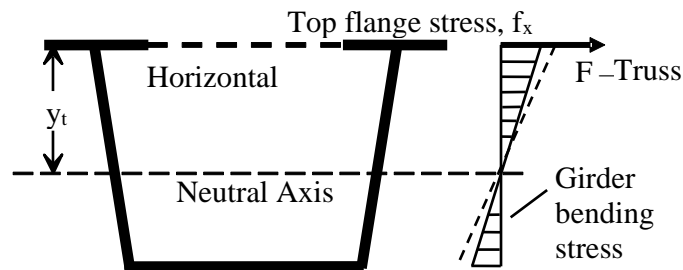


**Figure 36 Tub Girder Vertical Bending Stresses**

The bending compatibility forces can be significant as illustrated in Figure 32, especially for the X-type top lateral system. If the X-type redundant lateral system is not considered when proportioning the tub girder for bending, then the compatibility forces determined from an elastic analysis need not be considered in design. The diagonals can be designed for torsion alone. Within a panel the compatibility forces increase the force in one diagonal and decrease the force in the other diagonal by the same amount as shown in Fig 34. Torsion alone develops the same absolute magnitude of force in both diagonals. If the diagonals are designed only for torsion, one of the diagonals will reach its design limit first because of the added compatibility force, say 10 kips. The axial stiffness of that panel is then reduced and additional compatibility forces will also be reduced as additional load is applied to the bridge. The other diagonal in the panel has a smaller force than expected; the torsion force minus 10 kips. As additional bending and torsional forces are applied to the tub girder, the force in the highest stressed diagonal will not change (it is at its strength limit). The diagonal with the lower force will resist the torsion alone but it can support an additional torsion force equivalent to the compatibility force (10 kips). The compatibility forces do not affect the ability of a panel with two diagonals to resist the torsional moments. There may be some initial sag in both diagonals at locations of low torsion, but this does not affect structural performance of the tub girder system. Designing for compatibility forces in redundant systems is somewhat self-defeating. When the brace size increases, the compatibility forces also increase.

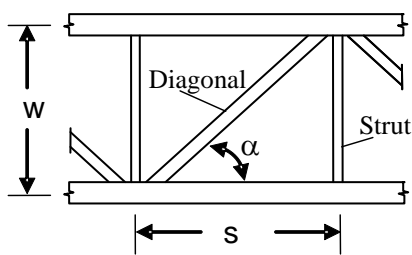
In the Warren truss and Pratt systems with a single diagonal within each panel, the bending compatibility forces must be considered because the system is not redundant. When the single diagonal in compression reaches its strength limit by forces from torsion and bending compatibility, only small additional forces can be applied.

Equations for predicting the truss forces induced due to vertical bending of the tub girder are available [6] and summarized in Figure 37. The Warren truss layout also results in a lateral load on the flanges that cause the flange stress denoted by  $f_{L \text{ bend}}$  in the figure. The formulations for the diagonal forces are related to the strut and diagonal sizes; the larger the members, the larger the forces in those members from tub girder bending. The top lateral compatibility forces will be compressive in the positive moment regions and tensile for negative moments.

The expressions given in Figure 37 for the Warren system were developed for the specific case of internal cross-frames positioned in every other panel, which is a spacing of  $2s$ , where  $s$  is the spacing between the struts of the top flange truss. Bending induced forces in the top flange Warren truss are sensitive to the spacing between the internal K-frames. When internal cross-frames are spaced at every panel point of the top flange truss (spacing of  $s$ ), the bending induced top lateral forces are actually larger [46, 47, 48] The  $2s$  (every other panel point) spacing of the internal K-frames in the Warren truss system is recommended. At the truss panel points between the internal K-frames only a strut is provided. The intermediate internal cross-frame spacing does not affect the forces in the X-type system.

There are currently no direct analytical solutions for the Pratt arrangement but 3D-FEA has indicated that the diagonal and strut forces due to bending are much smaller than those in the Warren system over most of the span. However, at locations where the Pratt diagonals change their orientation (maximum bending moment locations), the two adjacent diagonals meet at one point in a Warren configuration. At these locations, the bending compatibility forces are maximum and similar in both the Pratt and Warren orientations.

$D_{\text{bend}}$  = diagonal force due to girder bending  
 $S_{\text{bend}}$  = strut force due to girder bending  
 $f_{x \text{ top}}$  = top flange bending stress in panel  
 $s$  = panel length (spacing between struts)  
 $\alpha$  = Angle between diagonal and flange  
 $L_d$  = diagonal length  
 $w$  = strut length  
 $A_d, A_s$  = respective area of diagonal or strut  
 $b_f, t_f$  = respective width and thickness of girder flange  
 $f_{L \text{ bend}}$  = lateral bending stress in girder top flange



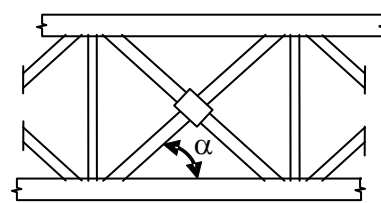
$$D_{\text{bend}} = \frac{f_{x\text{Top}} s \cos \alpha}{K_1}$$

$$K_1 = \frac{L_d}{A_d} + \frac{w}{A_s} \sin^2 \alpha + \frac{s^3}{2b_f^3 t_f} \sin^2 \alpha$$

$$S_{\text{bend}} = -D_{\text{bend}} \sin \alpha$$

$$f_{L \text{ bend}} = \frac{1.5s}{b_f^2 t_f} S_{\text{bend}}$$

**WARREN, (Pratt)**



$$D_{\text{bend}} = \frac{f_{x\text{Top}} s \cos \alpha}{K_2}$$

$$K_2 = \frac{L_d}{A_d} + \frac{2w \sin^2 \alpha}{A_s}$$

$$S_{\text{bend}} = -2D_{\text{bend}} \sin \alpha$$

**X-TYPE**

**Figure 37 Bending Induced Truss Forces**

### 3.1.4 Top Flange Truss Details

The number of panels and the orientation of the diagonals can have a significant effect on the efficiency of the design as well as the performance of the girder system. In specifying the number of panels along the span length, the angle of the diagonals  $\alpha$  defined in Figure 39 should be kept within the range  $35^\circ < \alpha < 50^\circ$ . The upper limit on this range is related to economics since larger values of  $\alpha$  will lead to more panels which results in more connections and larger fabrication costs. The lower limit on this range is related to the compression behavior of diagonals from both torsional and vertical bending. With a smaller angle of inclination, the diagonals become relatively long and therefore possess a lower buckling capacity. In general, diagonals with orientations outside of the recommended range are inefficient and should be avoided.

Structural T-sections are often used for the diagonals, while angles are commonly used for the struts. For practicality of the connections and safety of the construction workers, the T-sections should be oriented with the stem pointing downwards. The construction personnel often must walk on these members during erection and early stages of construction. In addition, the stem should be pointed downward to avoid clearance issues with the metal deck forms. In detailing the connections for the diagonals, care should be taken not to employ excessively thick connection plates or shims that will increase the eccentricity of the connection. The thickness of the connection plate should be approximately equal to the thickness of the WT flange.

The strut for the top flange truss frequently serves as the top chord member of an internal cross-frame if one is provided at the panel point. To avoid congestion at the intersection of the struts and the diagonals, some designers connect the strut to the web stiffener at an eccentricity denoted as  $e$  in Figure 38.

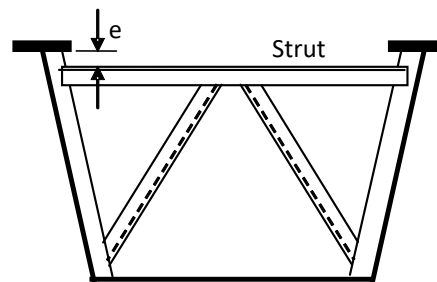


**Figure 38** Strut eccentricity in a tub girder cross section

This eccentricity generally has an insignificant effect on the performance of the top flange truss; however, the eccentricity should be limited to a maximum value of 3 or 4 inches. In many cases, lowering the strut due to concerns about congestion between the diagonals and the struts is unnecessary because of the inclination of the diagonals and the length of the connection. In cases where the Pratt truss geometry is specified, the effects of  $e$  are more significant than for the Warren and X-type layouts because the strut forces are much higher. With an eccentric connection such as the one depicted Figure 38, forces from the diagonal in the Pratt truss would be transferred into the web/stiffener of the girder, down to the strut and across the girder, back up the web/stiffener of the girder and into the diagonal of the adjacent panel.

### 3.1.5 Controlling Global Lateral Buckling

Lateral buckling of an I-shaped girder is a well-documented limit state included in the *AASHTO LRFD BDS*. Either intermediate diaphragms or top flange lateral truss systems are used for braces to establish the unbraced length of the compression flange. Global lateral buckling of the tub girder as a whole is not as well understood and there are no AASHTO provisions for this phenomenon. There have been two total collapses from global buckling of straight tub girders during the deck pour [4]. In both cases the girders had frequently spaced internal diaphragms but no top flange lateral truss system.

Open-section tub-girder cross sections are susceptible to lateral buckling due to the location of the shear center (see Appendix), which is well below the bottom flange. Global buckling of tub girders

is discussed by Yura and Widiyanto [49]. It is very unconservative (by approximately a factor of five) to use formulas developed for single web I-shaped members such as Eq. 10 for checking lateral buckling of twin web tub girders. Another unconservative approach is to assume that lateral buckling cannot occur if the tub girder is bent about its smallest principal axis. The Marcy bridge that collapsed had  $I_y/I_x = 1.75$ . A girder with a trapezoidal shape has reduced lateral buckling resistance compared to a rectangular girder.

The lateral buckling capacity of tub girders can be determined from a 3D-FEM buckling analysis (a free download is available for one such program [45]) or from the classic lateral buckling formula for singly-symmetric cross sections [28],

$$M_{cr} = \frac{\pi^2 EI_y}{L_b^2} \left[ \frac{\beta_x}{2} \pm \sqrt{\frac{\beta_x^2}{4} + \frac{GJ}{EI_y} \left( \frac{L_b}{\pi} \right)^2 + \frac{C_w}{I_y}} \right] \quad (27)$$

where  $\beta_x$  is the monosymmetric constant. Formulations for  $\beta_x$  and  $C_w$  for an open-section tub girder are given in Section 5.2 and 5.3. If Eq. (27) indicates that an open-section tub girder is inadequate during the construction stage, a partial or full-length top flange lateral truss system or external bracing will be required. The number of internal diaphragms does not affect global lateral buckling.

The effect of installing a top lateral X-type truss system along the entire length of a uniformly-loaded, straight 170 ft simple span tub girder to improve the global buckling strength is illustrated in Figure 39. The trapezoidal cross section used in the analysis was similar to the Marcy Bridge. The area  $A_d$  of the truss diagonals was varied, and a 3D-FEM buckling analysis performed. For an open section (no lateral system), the girder buckled at a top flange bending stress of 13 ksi. The addition of a top lateral system increases the buckling strength linearly as the size of the truss diagonals increases. Only a very small area for the top lateral bracing diagonals is required to increase the global buckling strength to adequate levels. For this particular girder, if the bracing area of the X-type system is larger than 0.08 in<sup>2</sup> ( $t_{eq} = 0.0015$  in.), then global LTB will occur at a stress higher than 50 ksi. Single diagonal bracing systems give similar results provided that the area of the diagonal is two times the area shown for the X-type system.

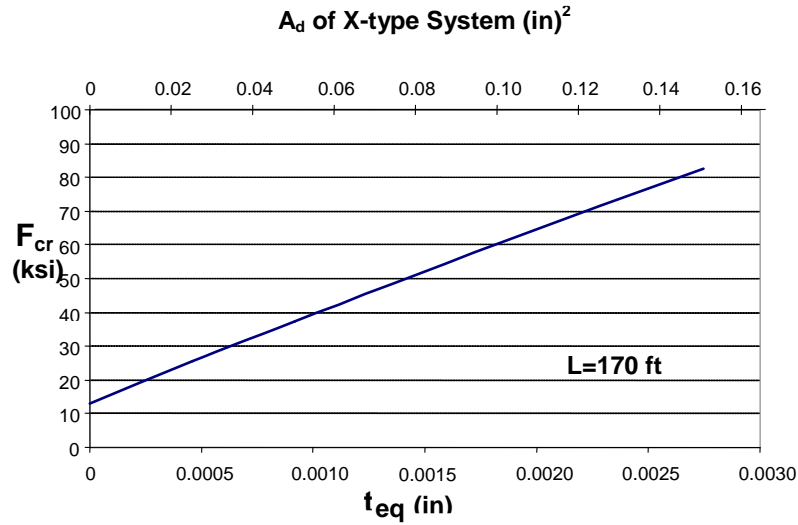


**Figure 39 Effect of  $t_{eq}$  on global buckling on a tub girder section using a X-type lateral bracing system**

Installing a top lateral bracing system along the entire span length for a condition that occurs during construction may be expensive. A study [49] indicated that bracing of the end panels where the flange stress is low is much more effective than bracing near midspan where the stress is maximum. The effect of the end panel bracing on the global buckling strength is shown in Figure 40.

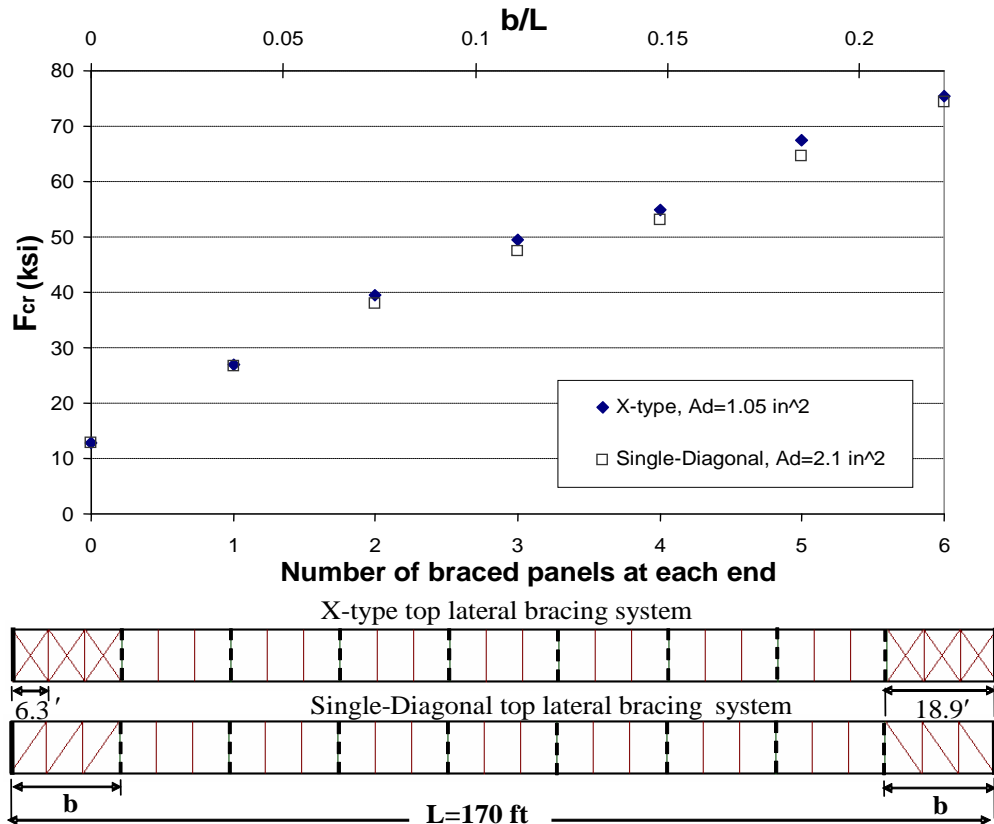


**Figure 40 Effect of Partial End Panel Bracing on Girder Buckling Stress**

Both the number of braced panels and the ratio of the length of the braced panels at each end,  $b$ , to the length of the girder,  $L$ , are shown. The diagonal areas of the X-type and Single-Diagonal systems are  $1.05 \text{ in}^2$  and  $2.1 \text{ in}^2$ , respectively, corresponding to the  $t_{eq}$  of 0.019 inches and 0.012 inches. To achieve  $F_{cr}$  higher than 50 ksi so that yielding will govern, only bracing of four panels at each end is required. Since the  $t_{eq}$  of both the X-type and the Single-Diagonal systems are about the same, the effectiveness of both systems is almost the same. A global buckling parameter study with span, number of braced panels, cross-section proportions and type of truss layout as variables and a constant  $t_{eq} = 0.02 \text{ in.}$  in the braced panels indicated that  $M_{cr}$  is linearly proportional with the increase of  $b$  up to  $b/L = 0.2$ . Additional braced panels do not have a large impact on the global lateral-torsional buckling strength.

### 3.2 Intermediate Internal Cross-Frames

The primary role of intermediate internal cross-frames/diaphragms in tub girders is to maintain the shape of the cross section against torsional forces that tend to distort the shape of the box girder. Typical geometric arrangements, commonly called K-, X- or Z-frames, employed as intermediate cross-frames are shown in Figure 41. Solid plate intermediate diaphragms are typically reserved for support regions. In the absence of a top lateral system, internal cross-frames act as torsional braces to control lateral buckling of the top flanges. Torsional bracing stability requirements were presented earlier. This section outlines the design requirements for internal cross-frames to

properly control distortion and provides recommendations on detailing practices for the internal cross-frames.

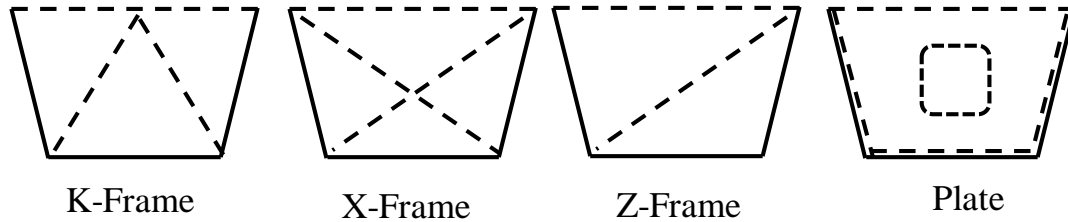


**Figure 41 Internal Intermediate Cross-Frame Layouts for Tub Girders**

### 3.2.1 Tub Girder Distortion

Depending on the distribution of the applied torsional loads, the cross-section of a quasi-closed tub girder may distort from its original shape. This distortion of the cross-section can lead to significant warping stresses, which are in addition to torsional warping stresses. Warping stresses that develop as a result of distortion of the cross-section are appropriately referred to as distortional warping stresses. While torsional warping stresses in box girders may be relatively small, without proper bracing distortional warping stresses can be quite significant.

Forces develop in the intermediate cross-frames and other bracing members due to the distortion of the box section. Torsion in box girders is usually the result of either horizontal curvature of the girder or unbalanced gravity loading that results in an eccentricity of the load on the cross-section. Depending on the type of loading, the torque on girders can be visualized as either a horizontal or vertical couple as depicted in Figure 42.

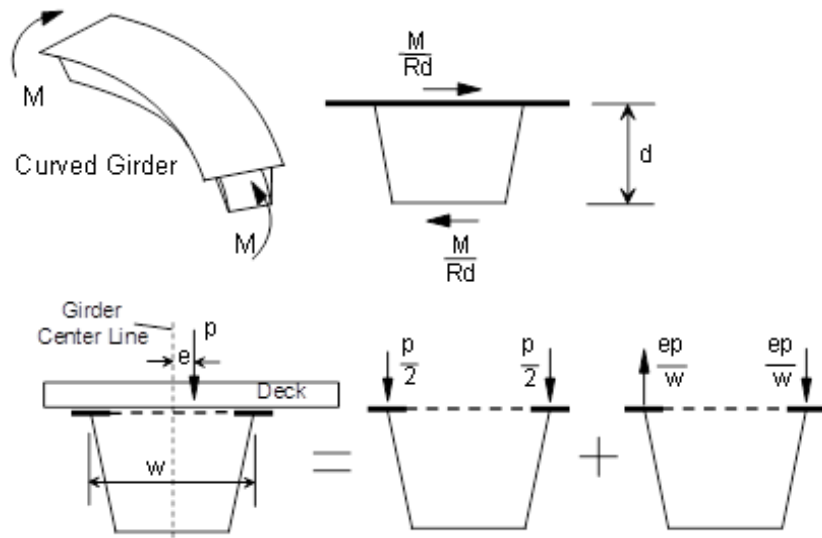


**Figure 42 Sources of Torsion in a Tub Girder**

The torsional moments in curved tub girders determined from the M/R method can be visualized as a horizontal couple. In the cases of unbalanced gravity loading, the effective eccentric loading can be idealized as two couples, pure flexural load plus a torque consisting of a vertical couple.

Cross-sectional distortion of box girders is induced by the components of the two torsional loads that are not directly distributed in proportion to a uniform Saint-Venant shear flow on the cross-section. All practical loading cases cause some form of cross-section distortion since the load application is never distributed in proportion to the Saint-Venant shear flow. Each torsional load can be divided into pure torsional components (kips per unit length),  $q_{h,v,T}$ , and distortional components,  $q_{h,v,D}$  as shown in Figure 43.

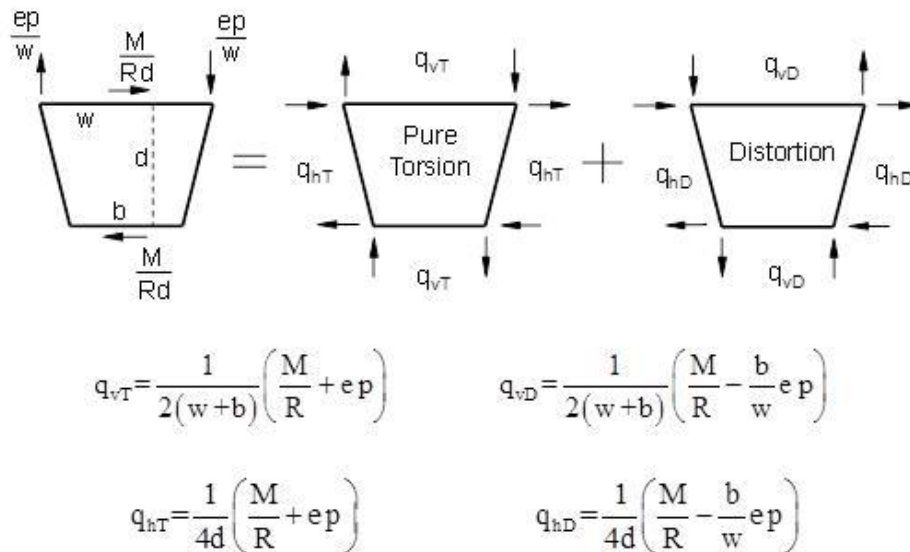


**Figure 43 Pure Torsional and Distortional Components in a Tub Girder**

The pure torsional components are distributed around the cross section in proportion to the St. Venant shear stresses. The distortional components of the applied loads on the right side of the figure yield zero net torque on the cross section. The horizontal and vertical torsional couples produce distortional components that are in opposite directions even though both torsional couples produce clockwise moments. Therefore, a distortional analysis requires a separation of the horizontal and vertical components and a sign convention for the eccentricity (see Figure 44).

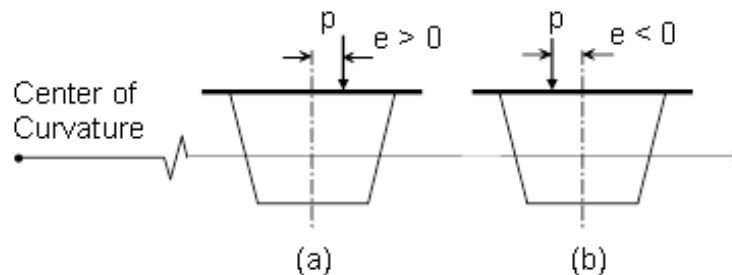


**Figure 44 Sign Convention for Eccentricity**

An approximate distortion analysis was developed by Fan and Helwig [50] for determining the forces, H and V, (see Figure 45) applied to intermediate cross-frames. H and V are equal to the  $q_{hD}$  and  $q_{vD}$  distortional unit forces, respectively, given in Figure 43 multiplied by the spacing

between intermediate cross-frames,  $S_K$ . These applied forces are applicable for any of the cross-frame arrangements shown in Figure 41. For the specific K-frame which is the most common, the H and K forces are converted to diagonal and strut forces as follows:

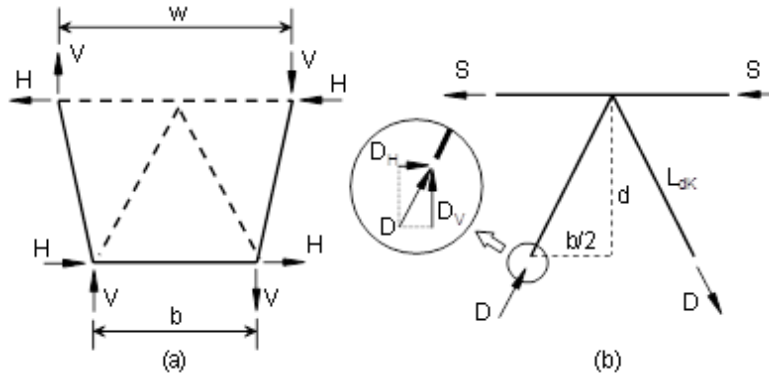


**Figure 45 Approximate Distortional Forces in Intermediate Cross-Frames in a Tub Girder**

$$D = \pm \frac{s_K L_{dK}}{2A_0} \left( \frac{M}{R} - \frac{b}{w} ep \right) \quad (28)$$

$$S = \pm \frac{s_K b}{4A_0} \left( \frac{b}{w} ep - \frac{M}{R} \right) \quad (29)$$

where:  $D$  = distortional induced force in the K-frame diagonal;  
 $S$  = distortional induced force in the K-frame strut;  
 $s_K$  = spacing between internal K-frames measured along the girder length;  
 $L_{dK}$  = length of the K-frame diagonal;  
 $A_0$  = area enclosed by box =  $(w+b)/2d$ ;  
 $w$  and  $b$  = box girder dimensions as depicted in Figure 45;  
 $e$  = effective eccentricity of resultant distributed load;  
 $p$  = distributed load (weight/ft.);  
 $M$  = box girder bending moment; and  
 $R$  = radius of horizontal curvature of box.

The  $M/R$  term in the parentheses is directed at the torsional effects of horizontal curvature while the  $ep$  term in the parentheses captures the effects of eccentric gravity loading. The plus/minus sign on the expressions indicates that the distortion induces tension and compression as indicated in Figure 45b. One diagonal experiences compression while the other experiences tension. In the case of the strut, equal magnitudes of tension and compression are induced on either side of the two diagonals. Since the struts serve as members of both the internal K-frames and the top lateral truss, these members have torsional components from box girder bending, torsion, and distortion. The components due to torsion and bending are uniform across the strut while the distortional components have equal magnitudes of tension and compression as indicated by the plus/minus sign in Eq. (29). The distortional component can therefore be isolated from the bending and

torsional component by averaging the magnitudes of the strut force on either side of the two diagonals.

Examples demonstrating the use of these preceding equations can be found in Fan and Helwig [50] and Helwig, et. al [51].

### **3.2.2 Internal Cross-Frame Details**

As discussed in the Section 3.1.3.3, the spacing of the intermediate internal cross-frames, should be  $s_k = 2s$ , where  $s$  is the panel spacing in the top lateral system in single diagonal systems. Not only is the cost reduced by using fewer intermediate cross-frames, but the forces in the top lateral system are also reduced. The panels adjacent to the cross-frames only have a single top flange strut.

A K-frame composed of angles is the preferred layout arrangement based mainly on its convenience when the interior of the closed box must be inspected. With an X-frame it is difficult to travel within the interior. Z-frames with only one diagonal provide less interference but the diagonal may be in compression. Since its diagonal is almost twice the length of a diagonal in a K-frame, a heavier frame will be required. The intermediate cross-frame should also be detailed to minimize fatigue issues since live loads can cause distortion.

### **3.3 End Diaphragms**

Diaphragms are provided at the supports of the tub girders. The diaphragms are required for torsional equilibrium of the girder system. Diaphragms resist the girder twist at the ends of the girders based primarily upon the shear stiffness of the diaphragm if the aspect ratio,  $L_d/h_d$ , is less than 4 [1]. The ends of the girders are typically closed by solid plates and the diaphragm that connects the adjacent girders is may be trapezoidal in shape. The detailing requirements of the support diaphragms depend on the aspect ratio of the end diaphragms. Although the end diaphragm is typically trapezoidal in shape and is often bolted to the two adjacent girders, for establishing the detailing requirements the effective length of the diaphragm can be assumed to be measured as the spacing between the center of the bearings of two adjacent girders as shown in Figure 46. For most tub girder geometries, the practical range of spacing between the bearing centerlines and therefore the effective diaphragm length is in the range of 14 ft.  $< L_d < 20$  ft. The lower range of the diaphragm depth so that shear stiffness dominates the behavior is 3.5 feet at the lower  $L_d$  range (14 ft.) and 5 feet at the upper  $L_d$  range (20 ft.). The end diaphragms are often deeper than these lower-bound values so shear stiffness will govern the behavior of these braces.

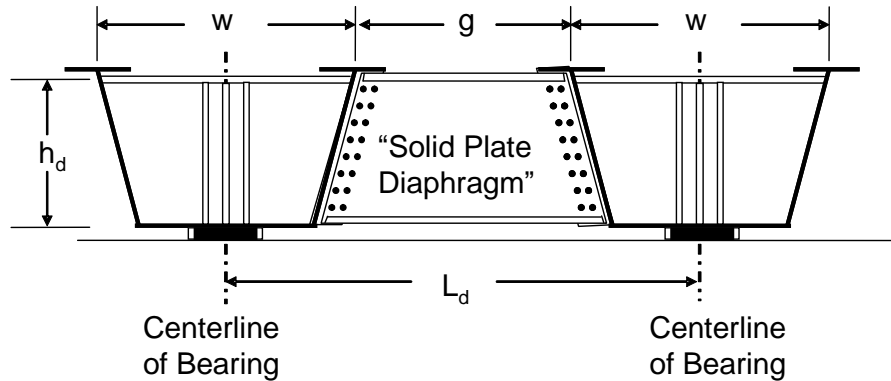


**Figure 46 Typical End Diaphragm Geometry**

The fact that most end diaphragms have aspect ratios less than 4 is important from a detailing perspective. The end diaphragms usually have top and bottom stiffening plates that increase the out of plane stiffness of the diaphragm plates. Many designers treat the top and bottom plates as flanges of a beam and then associate the connection requirements with what is frequently required in the beams of a frame. The flanges of beams in a frame are often fully connected to columns to create a “moment connection” between the beam and column. In the case of the plate diaphragms, the primary mechanism of restraint provided by the diaphragm comes in the shear stiffness of the plates and connecting the flanges has very little effect on the behavior of the system. This is illustrated in Figure 47, which shows a 3D-FEM of the end diaphragm in a twin box girder model. The end connections of the solid diaphragm were modeled with both continuous top and bottom plates as well as discontinuous plates. There was virtually no difference in the behavior of the two girder systems [47]. Only in cases where a relatively shallow diaphragm with an effective aspect ratio in excess of 4 should designers consider making the stiffening plates continuous across the ends of the girders. In most applications, simply bolting the end diaphragm will provide exactly the same behavior as if the top and bottom stiffening plates were connected. However, in cases where redundancy considerations are a significant concern, consideration should be given to making the stiffening plates continuous.

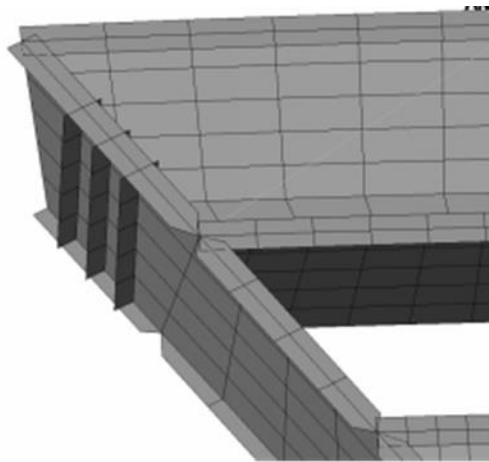


**Figure 47 Non-continuous flanges illustrated by a 3D FEM of the end diaphragm of a twin box girder model**

### 3.3.1 Diaphragm Strength Design Requirements

There are two criteria that the designer should consider when proportioning the solid end diaphragms for box girder applications. The most obvious consideration is the basic shear strength of the plate diaphragm. The other consideration is related to excessive shear deformations at the ends of the beams that can result in rigid body rotations of the girders along the length. The strength limit state is relatively well-understood; however, an expression based upon stiffness criteria is also presented in the following sub-section.

Figure 48 shows girder torsional demand that acts on diaphragms and the resulting shears that develop as a result of these torsional moments.

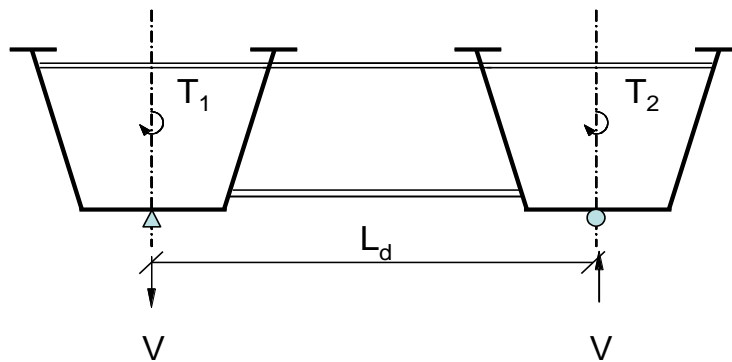


**Figure 48 Girder end torsional demand that acts on diaphragms and the resulting shears**

The moments  $T_1$  and  $T_2$  are the torsional moments that come as output from the results from a grid model. The girders are generally subjected to vertical gravity loading and although the net end reaction will typically be upwards, the diaphragm tends to redistribute the gravity load so that more of the gravity load shifts towards the exterior girder. Figure 48 shows the redistribution in the form of a downward shear on one girder and an upward shear on the other girder. The shear,  $V$ , represents the design shear for the end diaphragm. In terms of the girder end torques, the shear is:

$$V = \frac{T_1 + T_2}{L_d} \quad (30)$$

In a curved girder,  $L_d$  is the difference in the radii of the two girders. The design approach for shear is based upon a uniform shear stress through the depth of the plate. Referring to the area of the diaphragm plate as  $A_d = h_d t_d$ , the shear stress would be given as follows:

$$\tau = \frac{V}{A_d} = \frac{T_1 + T_2}{L_d A_d} = \frac{T_1 + T_2}{L_d h_d t_d} \quad (31)$$

Based upon a uniformly distributed load on a simply supported girder, the end torque (neglecting the presence of intermediate K-frames) is:

$$T_i = \frac{pL_i^3}{24R_i} = \frac{pL_i^2\beta_o}{24} \quad (32)$$

where  $p$  is the uniformly distributed load,  $L_i$  and  $R_i$  are the respective chord length and radius of curvature of the  $i^{\text{th}}$  girder, and  $\beta_o$  is the subtended angle within the span. This leaves the designer with several options to design the plate diaphragm for strength. The torque from Eq. (32) also provides a reasonable estimate of the design torques. Although the equation was derived for a simply supported girder, there is little torsional interaction between adjacent spans in box girders since the diaphragms are relatively stiff and the St. Venant stiffness tends to dominate the behavior. Therefore Eq. (32) provides reasonable estimates of the end torques on each girder. Alternatively, analysis results can also be used such as getting the torques from a grid analysis. With the end torques in the two adjacent girders, the diaphragm shear  $V$  can be found using Eq. (30) and compared with the shear strength (i.e.,  $\phi V_n$  from the *AASHTO LRFD BDS* [1]). For example, if the web slenderness satisfies the requirements for full shear yielding, the material shear strength  $\tau = 0.58F_y$  can be applied with Eq. (31) to give:

$$A_d = \frac{T_1 + T_2}{L_d(0.58F_y)} \quad (33)$$

where  $F_y$  is the material yield stress of the web of the diaphragm. For a diaphragm web not satisfying the slenderness limits for full yielding, the appropriate expression for shear buckling can be utilized.

### 3.3.2 Diaphragm Stiffness Design Requirements

Instead of the diaphragm strength limit, an alternative limit on the diaphragm may be shear deformation. Relative vertical deformation between the adjacent girder flanges can also occur due to deformations in the end diaphragms. To develop a deformational limit, some geometrical approximations of the portion of the end diaphragm restraining girder twist must be established. Although the diaphragm itself is usually viewed as a trapezoidal plate, since the plate is fully bolted to the two girders with slip critical bolts, the portion of the diaphragm resisting girder twist can be idealized as a rectangular plate extending from the middle of the two girder bearings as depicted in Figure 49 for a total diaphragm effective length of  $L_d$ .

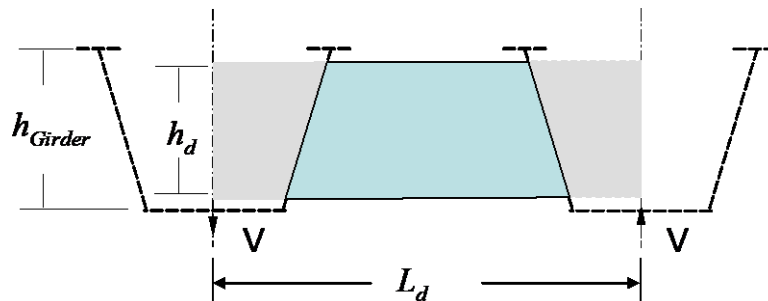
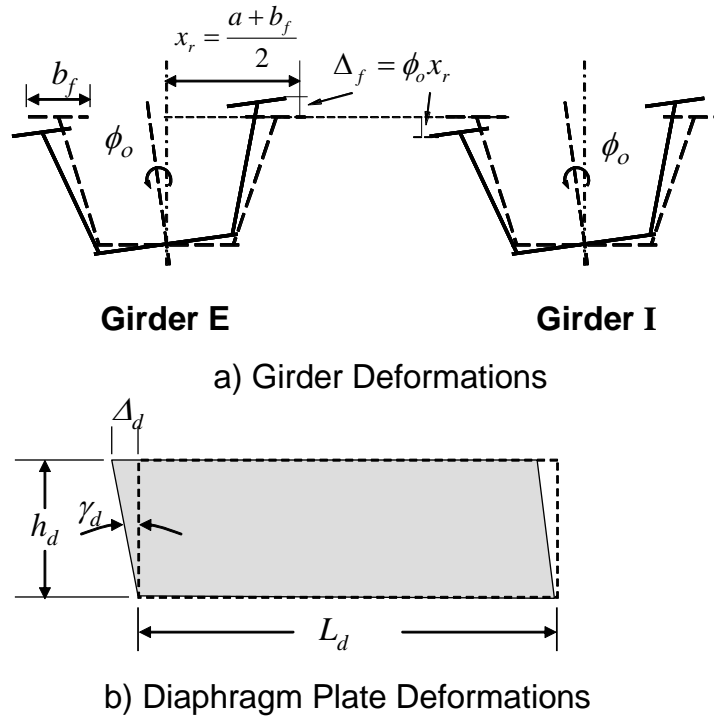


Figure 49 Idealized Rectangular Diaphragm Plate

Figure 50 shows the girder end deformations at the diaphragm and then the resulting deformations of the idealized rectangular diaphragm plate. As discussed above, the girder deformations result in a rigid body deformation that causes a relative vertical movement between the two flanges of the box girder. The vertical flange deformations are  $\Delta_f$  in Figure 50. The relative value between the two flanges is then given by the expression:

$$\Delta_{\text{Rel dia.}} = 2\Delta_f = 2\phi_o x_r \quad (34)$$



**Figure 50 Girder and Diaphragm Deformations**

where  $\phi_o$  is the end twist due to the shear deformations in the end diaphragm, and the distance  $x_r$  is defined in the figure. Since the end diaphragm deformations result in rigid body movements of the entire girder, these deformations are very undesirable and should be kept to a minimum. As a result, the diaphragms should be made relatively stiff to avoid large relative movements between the adjacent girder flanges. A value for the tolerable relative movement is a matter of judgment. In reference [51] a value of 0.5 in. was selected to control variations in the slab thickness due to girder flexibility along the span. Since a rigid body rotation at the supports contributes to the midspan relative deflection, the support deformations must be kept to a minimum. A limit of  $2\Delta_f < 5\% \times 0.50 \text{ in.} = 0.025 \text{ in.}$  at midspan was chosen. In reference [50], the  $\Delta_f = 0.0125 \text{ in.}$  limit was transformed into the following stiffness limit for the area of the diaphragm:

$$A_d = h_d t_d \geq \frac{(T_1 + T_2) x_r}{0.0125 G L_d} \quad (35)$$

The controlling diaphragm area would be the larger value from Eq. 35, or the strength criteria discussed in the previous sub-section.

### 3.4 Intermediate External Cross-Frames

The primary role of the intermediate external diaphragms is to control the relative deformation between adjacent curved girders during casting of the concrete bridge deck. In cases where the external bracing is not removed after construction, the external bracing will also contribute to the load transfer between adjacent tub girders. In a twin girder system depicted at midspan in Figure 51, Girder E is the exterior girder with the longest individual span. The girders will twist independently during construction if there are no intermediate external cross-frames connecting the two girders with Girder E having the larger angle of twist and vertical deflection compared to Girder I on the interior. Since the girders have some flexibility, there will be a relative vertical displacement  $\Delta_{rel}$  between points B and C in (c) that causes a variation in the deck thickness and reinforcement cover. The dashed lines in (b) and (c) represent a straight line between the finishing machine rails at points A and D. The displacement  $\Delta_{rel}$  must be controlled within some practical limit. Stiffer girders (larger  $t_{eq}$ ) can be one approach but may be cost-prohibitive and very stiff girders pose greater problems with bolted field splices during erection. External intermediate cross-frames shown in (b) can be used to improve the constructability. Studies [48, **Error! Reference source not found.**] have shown that only one or two cross-frames near midspan are sufficient to control  $\Delta_{rel}$ .

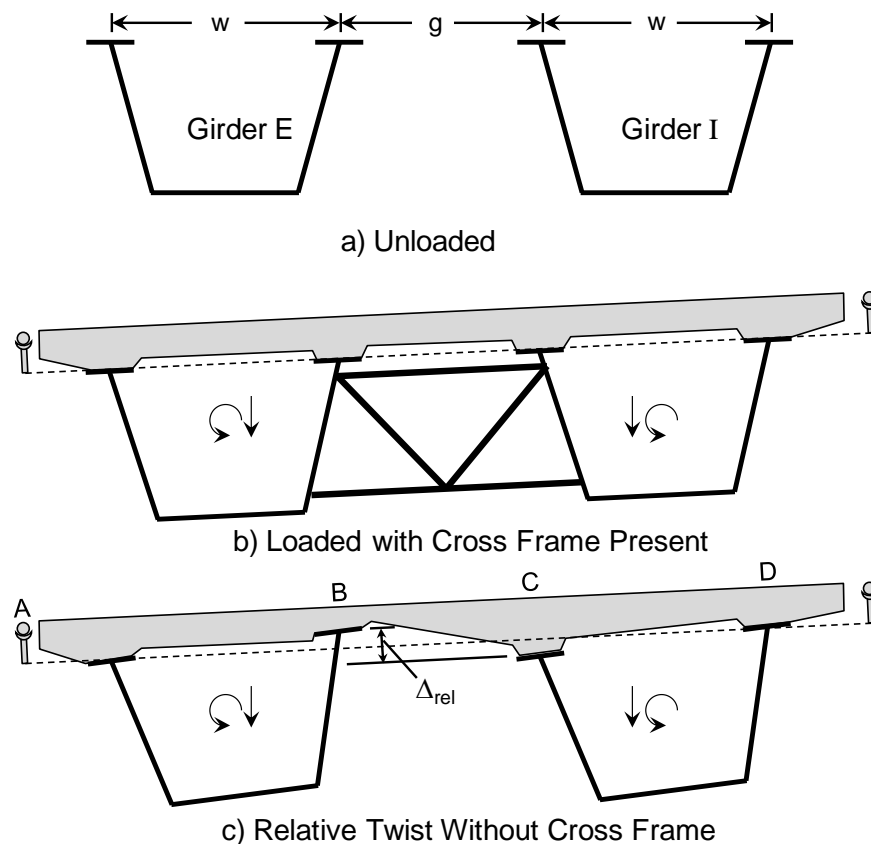


**Figure 51 Relative Deformation between Adjacent Girders**

Cross-frames should be concentrated towards the middle of the span instead of spreading the braces out equally along the bridge length. Although the deformations often do not differ substantially with the addition of several braces, the forces induced in the intermediate cross-frames will be smaller as more braces are added. However, the forces in the intermediate cross-frames from the construction loading are often relatively small except for spans with sharp curves ( $R < 250$  ft). With skewed supports, the forces in the cross-frames do become larger. Unless the support skew becomes large (greater than approximately 30 degrees), the forces can often be handled with members satisfying slenderness limits.

External intermediate K-frames are primarily needed on horizontally curved girders. In straight girders, if diaphragms are provided at the supports and a top flange lateral truss is utilized, the girders are very stiff and intermediate external diaphragms can be omitted. Diaphragms would be needed if a large unbalanced load (i.e., large torque) is applied or if the supports have significant skew. The problem with the large support skew is that the ends of the girders may tend to twist due to the angled diaphragm. The twist at the support results in a rotation of the girders that can result in problems with the uniformity in the slab thickness as outlined earlier. Most practical applications of straight girders do not need external bracing.

In most situations, external intermediate K-frames can be removed once the concrete deck hardens because field tests have shown that external K-frames have very little impact on live load distribution. The cross-frames are most often removed due to fatigue concerns.

### **3.4.1 Analysis Approaches for Intermediate External Diaphragms**

The treatment of the external braces in the structural analysis as well as the accuracy of the resulting forces depends heavily on the analysis method that is used. If a 3D-FEM is utilized, the braces can be modeled relatively accurately and the member forces can be obtained directly from the analysis. However, incorporating the external K-frames into a grid model poses a complicated geometrical problem. Although the internal and external K-frames are trusses made up of several members, the grid models treat these braces as a line element that spans between the centerlines of the adjacent girders. Therefore, estimating the stiffness of these external braces can be difficult. In addition, the analytical estimates of the intermediate diaphragm moments from a grid model may often be of questionable accuracy.

Another possible analysis approach is to designate the intermediate external K-frames solely as members to help control the constructability of the slab. With this approach, the analysis would be carried out only modeling the girders and solid diaphragms at the supports. The girders and support diaphragms would therefore be sized to support the entire load. This will often result in larger member sizes for the top flange lateral truss, when compared to an analysis that includes the external braces; however, the economics of the top flange truss should not change too dramatically. The cost of the top flange truss is mainly related to fabrication costs, which are often primarily a function of the number of pieces required to fabricate. Increasing the size of a member by a few pounds per foot should not have too large of an impact on the design economics; however, the behavior and safety of the design are much easier to predict with this approach. As mentioned above, a few external cross-frames concentrated near the middle of the span often provide excellent control over the relative twist between adjacent girders. In the following sections, approximate

methods developed in [51] will be summarized that can be used to determine the number of external cross-frames needed to control constructability and to predict the member forces in the external cross-frame.

### 3.4.2 Spacing of Intermediate External K-frames

The approximate approach outlined is for determining how many intermediate cross-frames are needed. The spacing equation is based on the following assumptions: a simple-span twin curved girder symmetrical system with radial supports, no relative twist between the two supports of the span and the two girders have similar cross-section properties. The vertical and horizontal deflections at the web-top flange intersection at midspan for points B and C from vertical load applied at the top flanges of the quasi-closed sections were determined. These calculations required that the angle of twist of each girder, which is a function of the individual span lengths, be determined along with the vertical displacement of both girders. Since the cross-sectional properties of the two girders is the same, the difference between the perpendicular displacements of points B and C relative to a straight line between screed rails,  $\Delta_{rel}$ , is mainly a function of the difference in span lengths between the two girders and the identical cross-sectional properties. The difference in span lengths is related to the spacing between the two girders,  $(w + g)$ , and the subtended angle  $\beta_o = L/R$  of the bridge plan. With some minor assumptions associated with the relative location of the screed rails on typical tub girder geometries, the relationship of the span length between external cross-frames and  $\Delta_{rel}$  is

$$L_{max} = \left[ \frac{1.2\Delta_{rel}}{\frac{5w\beta_o(w+g)}{384EI} \left( \frac{EI}{GJ} - 3 \right)} \right] \quad (36)$$

For design, the maximum permissible deviation in slab thickness  $\Delta_{rel}$  can be set equal to some maximum value, say 0.5 in., to determine  $L_{max}$ . If  $L_{max}$  is greater than the span length, no external intermediate cross-frames will be required for constructability.

### 3.4.3 Forces in Intermediate External K-frames

To develop expressions for the forces in the external diaphragm, the case of a single external K-frame located at midspan will be considered. The lengths,  $L_i$  and  $L_e$ , of the respective interior and exterior girders in these derivations are taken as the total arc length of the respective girders between the supports. The external diaphragm helps to restrain twist and vertical deflections of the box girders at the location of the braces. The basic geometry of the external K-frame and box girder system are shown in Figure 52. The angle of the diagonal of the K-frame is represented as  $\psi$ , while the depth of the K-frame is denoted as  $h_K$ . The rotation of the two girders and the K-frame system are assumed to be the same and are represented as  $\phi$ . The distance from the center of a girder to where the top chord of the K-frame connections is shown as  $L_T$ . The distances  $h_K$  and  $L_T$  will be used to represent the torque exerted by the external K-frame on the girders.

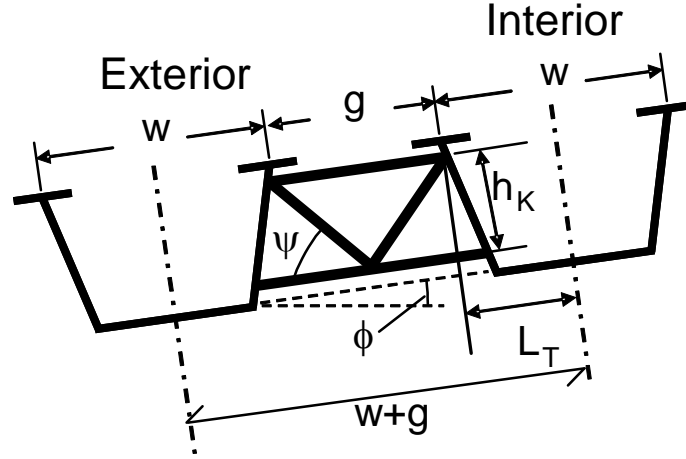


Figure 52 K-frame Geometry

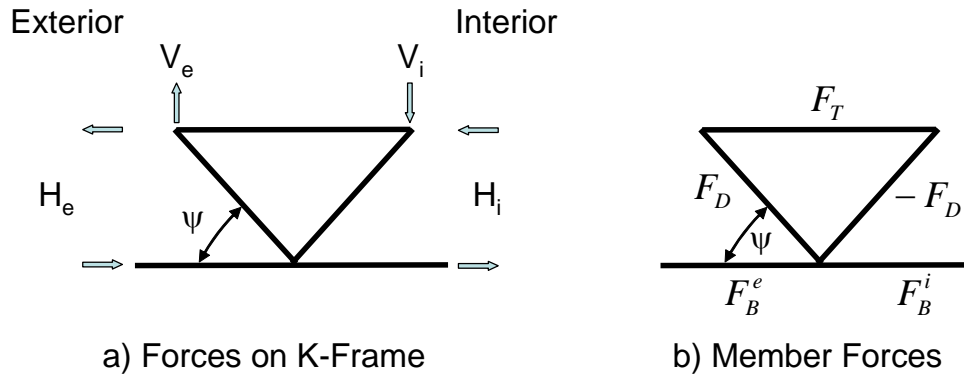


Figure 53 External K-Frame Forces

The K-frames exert restraining forces  $H$  and  $V$  on the girders in the respective horizontal and vertical directions. The equal and opposite forces that act on the K-frame are depicted in Figure 53a. The corresponding member forces that develop in the K-frames are depicted in Figure 53b.

$$F_D = 4GJ \frac{L_i \phi_{w,ext} + L_e \phi_{w,int} - K_1 \Delta_{w,rel}}{K_2} \quad (37)$$

$$F_T = \frac{4GJ(\phi_{w,ext} - \phi_{w,int}) - F_D L_K (L_e - L_i)}{h_K (L_i + L_e)} \quad (38)$$

$$F_B = \pm F_D \cos \psi - F_T \quad (39)$$

The variables in the above equations can be calculated as follows:

$$L_K = h_K \cos \psi + L_T \sin \psi$$

$$K_0 = 1 + \left(1 + \frac{EI}{GJ}\right) \left(1 - \cos \frac{\beta_0}{2}\right)$$

$$K_1 = \frac{L_i + L_e}{w + g}$$

$$K_2 = K_0 K_1 \frac{L_i^3 + L_e^3}{12(EI/GJ)} \sin \psi + 2L_i L_e L_K$$

$$\Delta_{w,rel} = K_0 \frac{5w}{384EI} (L_e^4 - L_i^4)$$

$$\phi_{w,int} = \frac{5wL_i^4}{384EIR_{int}} \left(1 + \frac{EI}{GJ}\right)$$

$$\phi_{w,ext} = \frac{5wL_e^4}{384EIR_{ext}} \left(1 + \frac{EI}{GJ}\right)$$

Comparison of the member forces with the forces from a 3-D FEA show reasonable agreement [47].

## 4.0 BRACING MEMBER DESIGN AND CONNECTION DETAILS

### 4.1 Design of Tees and Angles

For tension and compression members, the 2020 *AASHTO LRFD BDS* [1] has adopted the limit state provisions from the 2016 AISC Specification [22] and added mandatory  $L/r$  limitations. All  $\phi$ -factors in AASHTO [1] are generally larger than their counterparts in the 2016 AISC Specification [22]. Therefore, the use of the design capacities in the AISC Manual [52] for tension and compression members and their connections is conservative. If desired, engineers can adjust AISC Manual [52] tabulated values by the ratio of the respective  $\phi$ -factors ( $\phi_{\text{AASHTO}}/\phi_{\text{AISC}}$ ).

#### 4.1.1 Tension Members

Single angle, double angles, and tee-sections in tension are checked for the limit states of yielding on the gross section, fracture on the net section, block shear at the end connections and limiting slenderness ratio. When evaluating the slenderness ratio, any bracing member required to enable a main member to support the applied loads should be treated as a primary member. That is, if the main member cannot support the design loads without the bracing member, then the bracing is not a secondary member. Single and double angle members are usually connected at the ends through one of the legs. The eccentricity between the end connection and the angle centroid has little structural significance and is typically ignored. Tees are mainly connected through the flange. The bracing members are connected to the main member by connection plates on the webs or directly to the flanges. The eccentricity between the connection and the member centroid has little structural significance for tension members and can be ignored. Also, the U-factor reduction in the net section fracture capacity in AASHTO Section 6.8.2.1-2 [1] was developed from test data with specimens that had eccentricities.

#### 4.1.2 Compression Members

##### 4.1.2.1 Single angles

Single angles are commonly used in cross-frame members. Since the angle is typically connected through one leg only, the member is subjected to combined axial compression and flexure about both principal axes due to eccentricities of the applied compressive force. Additionally, the angle may be restrained by differing amounts about its geometric axes. As a result, the prediction of the nominal compressive resistance of these members can be difficult.

The methods specified in various design codes for the design of single angle compression members loaded through one leg can be divided into two categories: column approaches and beam-column approaches. The column approach, which is the simplest for design, was given in the first edition (1971) of the ASCE Standard 10-97, *Design of Latticed Steel Transmission Towers* [53]. Based on the results of many angle tests and full-size tower tests, angle design was based on axial load only with an adjusted  $L/r_z$  used with the normal column formula to account for eccentricities and end restraint. The British, European, South African, and Japanese steel design specifications use similar column approaches. The main variable among these different standards is the axis used to

define the critical column slenderness ratio. The ASCE method uses the minimum principal radius of gyration,  $r_z$ .

Prior to 2005, AISC [54] specified a beam-column approach that required the eccentricity to be defined explicitly about both principal axes and that second-order effects also be considered. For unequal-leg angles the orientation of the principal axes makes the geometry even more complex. Over the past thirty years, numerous experimental studies have shown the AISC method to be overly conservative [55]. In 2005, the AISC Specification [22] adopted a new design approach based on the ASCE 10-97 [56] Standard for angles loaded through one leg. The ASCE method is based mainly on tests with small (2.5 in.) equal leg angles. Tests with larger angles and unequal legs [57] showed that the capacity with the short leg connected was approximately 80% greater than tests with the long leg attached. The ASCE method predicted the same capacity for both cases since  $r_z$  is constant for both arrangements. Also, tests have shown that the dominant deformation is bending about the centroidal axis parallel to the attached leg, which will always be called the  $x$ -axis, so  $L/r_x$  should be the controlling slenderness ratio. Taking  $r_z/r_x = 0.63$  for all equal leg angles, the ASCE effective slenderness of  $KL/r_z$  for typical tower framing details (not highly restrained) was directly converted to an equivalent  $KL/r_x$  formulation [57]. There is an additional equation for the effective slenderness ratio,  $(KL/r)_{\text{eff}}$ , given for longer members. Using  $r_x$  instead of  $r_z$  made the ASCE formulation reasonably accurate for both equal and unequal leg angles.

The *AASHTO LRFD BDS* has adopted the AISC method [22] for single-angle members in Article 6.9.4.4, which significantly simplifies the design of single-angle members that are subject to combined axial and flexure, if they satisfy certain conditions. When these conditions are met, the simplified provisions permit the flexural effects due to eccentric loading to be neglected, and allows single angles to be designed as axial loaded compression members for flexural buckling only using an appropriate specified effective slenderness ratio,  $(KL/r)_{\text{eff}}$  in place of  $KL/r_s$ , in Articles 6.9.2.1, 6.9.4.1.1, and 6.9.4.1.2 to determine the nominal compressive resistance,  $P_n$ . Equations for  $(KL/r)_{\text{eff}}$  for equal-leg angles and certain unequal-leg angles are provided in *AASHTO LRFD BDS* Article 6.9.4.4.

A summary of stability issues for angle members is given in Ref. [58] and Chapter 11 of the SSRC Guide to Stability Design Criteria for Metal Structures [28].

#### 4.1.2.2 Tees and Double Angles

A tee flange is normally attached to a gusset or top flanges by welding or bolting as shown in Figure 54. The eccentrically loaded tee is subjected to a concentric load,  $P$ , and an end moment,  $eP$ , where  $e$  is the eccentricity. Unlike tension members, the effects of the eccentricity must be considered in the design of the brace because the compressive load amplifies the moments and deflections. In tension members, the bending deformations and moments along the span are reduced by the tension force. Designing tees and double angles for combined bending and axial compressive load by directly applying all the required design checks per the *AASHTO LRFD BDS* is a formidable task as tees and double angles do not have a similar effective slenderness ratio method that is used for angles. As such, the chosen member needs to satisfy the interaction equations for the combined effects of compression and flexure (Article 6.9.2.2).

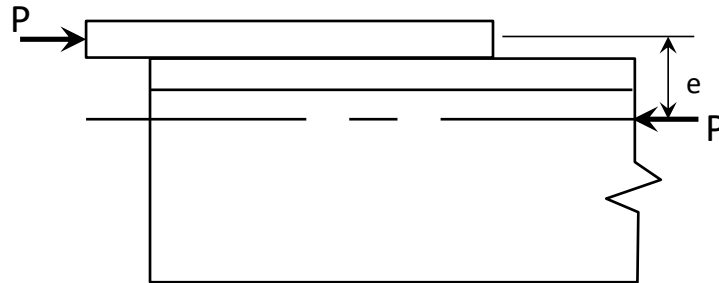


**Figure 54 Eccentrically loaded WT section**

The nominal compressive resistance,  $P_n$ , is computed in accordance with Article 6.9.4.1, where the elastic critical buckling resistance,  $P_e$ , is determined as the minimum of Equation 6.9.4.1.2-1 (elastic flexural buckling) and Equation 6.9.4.1.3-2 (elastic flexural-torsional buckling), as noted in Table 6.9.4.1.1-1 of the *AASHTO LRFD BDS*.

For tees and double angles loaded in the plane of symmetry, the nominal flexural resistance is computed in accordance with *AASHTO LRFD BDS* Article 6.12.2.2.4. The nominal flexural resistance is taken as the smallest value based on yielding, lateral torsional buckling, flange local buckling, or local buckling of tee stems and double angle web legs, as applicable. The equations for computing the nominal resistance for each of these criteria are presented in Articles 6.12.2.2.4b through 6.12.2.2.4e. Moment magnification should be considered as specified in Article 4.5.3.2.2b.

For tees and double angles subject to combined axial compression and flexure in which the axial and flexural stresses in the flange of the tee or the flange legs of the angles are additive in compression, e.g., when a tee is used as a bracing member and the connection of this member is made to the flange, a bulge in the interaction curve occurs. As a result, *AASHTO LRFD BDS* Equations 6.9.2.2.1-1 and 6.9.2.2.1-2 may significantly underestimate the resistance in such cases. Alternative approaches attempting to capture this bulge have proven to be generally inconclusive or incomplete [1]. Therefore, it is recommended that Equations 6.9.2.2.1-1 and 6.9.2.2.1-2 be conservatively applied to these cases.

## 4.2 Fatigue Design of Cross-frame Members

Fatigue design should be considered in the design of cross-frame members, especially in horizontally curved and/or skewed I-girder bridges, where cross-frames can transmit significant live load forces through the structure and the force effects in these members are determined from a refined analysis. In these cases, the fatigue live load forces in the cross-frame members should be considered in the design of the members and their connections. Refer to NCHRP Report 962 [16] for information on research that has been completed relative to the checking of fatigue in cross-frame members. As of this writing, recommendations from this research are being considered for possible adoption into the next edition of the *AASHTO LRFD BDS*.

## 4.3 Welded and Bolted Connection Details

The AASHTO/NSBA Collaboration publication, *Guidelines for Design Details* [59], shows preferred details for connecting cross-frame and lateral bracing members to girders. Additionally,

the NSBA publication, *Practical Steel Tub Girder Design* [60], provides bracing connection details in tub girders that are based on preferred detailing practices for cost-effective fabrication. In both publications, the details provided do not reflect any specific actual design conditions but are only preferred types of details. All details require careful analysis and consideration, and the preferred details may not always be applicable.

This section contains a number of pictures of details that are not recommended as standard practice details. Generally, if details such as these are used, special consideration must be given by the designer with regard to load paths and load transfer through the various structural components. Although the pictures focus on tub girders, many of the basic principles also apply to a variety of different bracing systems. A brief description of the picture is given for each detail.

In Figure 55, the WT for the top flange lateral truss on the box girder had an improper orientation, and an incorrect size. The stem of the WT was oriented upwards, which increases likely interference with the metal deck forms. The stem of the WT should point downward so that the flat surface of the flange is available for the construction personnel to walk on and also so that the WT can be placed very near the top flange. Also, orientating the WT so that the flange is nearer to the top flange decreases the eccentricity between the flange and the WT member, and thus decreasing subsequent bending moments in the WT caused by eccentric loading. A larger eccentricity results in a very inefficient load path for the lateral bracing system as the load from the flange is applied to the WT member in a very eccentric manner. This eccentricity must be considered in the design of the lateral bracing member. Furthermore, in the case shown in Figure 55, the diagonals were also improperly sized. Torsional loads on the box produced compression in alternating diagonals that was unaccounted for, and members around the supports near the regions of maximum torsion buckled with only the steel dead load acting on the girders.



A) WT – Stem up

B) Buckled Diagonal

**Figure 55 Improper orientation and sizing of WT section used for top flange lateral bracing member**

In Figure 56, the WT section is properly oriented; however, the top strut of the cross-frame is located well below the flange to avoid interference between the two members. Refer to Section 3.1.4 for a further discussion on the recommended maximum eccentricity for these types of details. The top strut of the internal cross-frame also participates in the lateral bracing system. This detail

results in a very inefficient load path between the two members since force components must be transferred through the web between the two members. The designer must consider how this force is transferred in the design of this connection. As an alternative, the top strut should be located as close as possible to the same plane as the lateral bracing system, and ideally, as close as possible to the top flange.



**Figure 56 Strut offset below diagonal**

Many poor bracing details are the result when working lines of the bracing members are forced to intersect. An example of this is the top flange truss that is being fabricated in Figure 57. The picture shows that very large gusset plates were used in an attempt to have the working lines of the diagonals and the top struts intersect. In the case shown here, the diagonals can cause a significant eccentric moment on the gusset plate connection to the top flange, which must be considered in the design of this connection. Better behavior would result if the diagonals were offset slightly and bolted directly to the underside of the flange, thereby eliminating the gusset connection plates. Although the working lines may not intersect with this detail, many stability bracing systems can be offset from the working points by as much as 10% of the unbraced length with very little impact on the structural performance. For tub girders, the designer can usually offset the working line by approximately a flange width with little effect on the performance. Connection eccentricities in the plane of the truss have very little impact on the performance of the bracing system.



**Figure 57 Large gusset plates used so working lines of bracing members intersect**

As shown in Figure 58, eccentric connections can lead to poor behavior of the lateral bracing members, unless properly accounted for in the design. In this case, a 1-inch thick shim plate was utilized to lower the top flange lateral truss to avoid interference with the permanent metal deck forms. Even though the bolted connections were fully tightened, the shim plate increased the eccentricity of the WT section and significantly increased the bending of the member. Under steel dead load, the compression diagonals experienced large bending deformations.

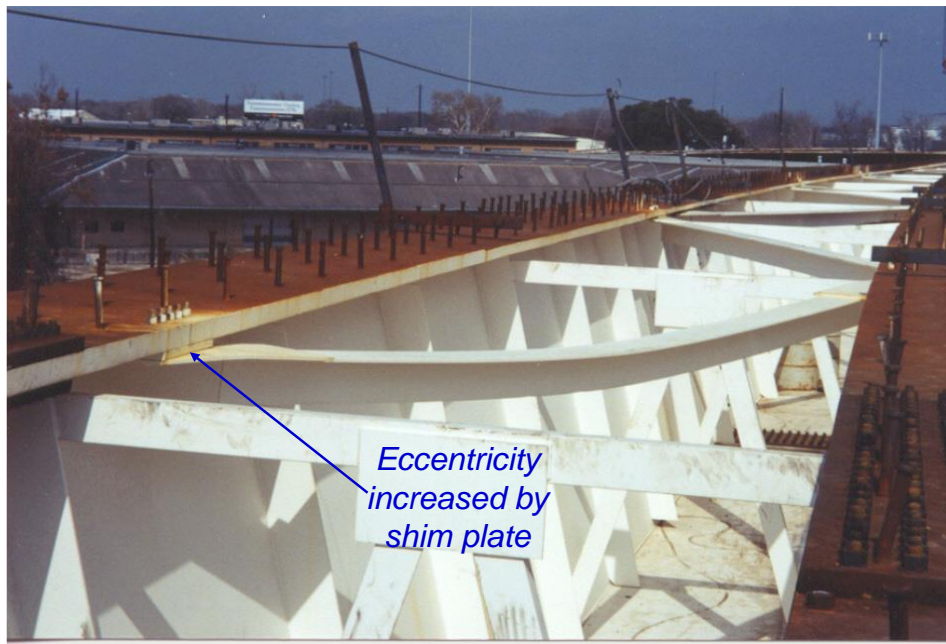


**Figure 58 Shim plates can significantly increase the eccentricity of WT sections**

The use of shim plates to lower top flange lateral bracing members in an effort to clear permanent metal deck forms is not recommended herein. Instead, consider using a deeper concrete haunch if

possible, and reserve the use of shims as a last resort. If it is determined that shims will be used, consider the effects of connection eccentricity on the top flange lateral bracing member design moments, and address the potential for bolt bending in the bolted connection design.

Figure 59 shows a partial depth end diaphragm that results in a poor load path that cannot anchor the top flange lateral truss. The top flange lateral truss must be sufficiently anchored to the end of the tub girder. The partial depth end diaphragm was used to accommodate a thickened armor joint at the end of the bridge. However, the thin web of the box girders may not be stiff enough to anchor the very large diagonal forces in the top flange lateral truss. The torsional stiffness of the box is therefore reduced, which can lead to large deformations. In this case, the load path must be considered in the design of this lateral bracing system, or a full depth end diaphragm should be used.

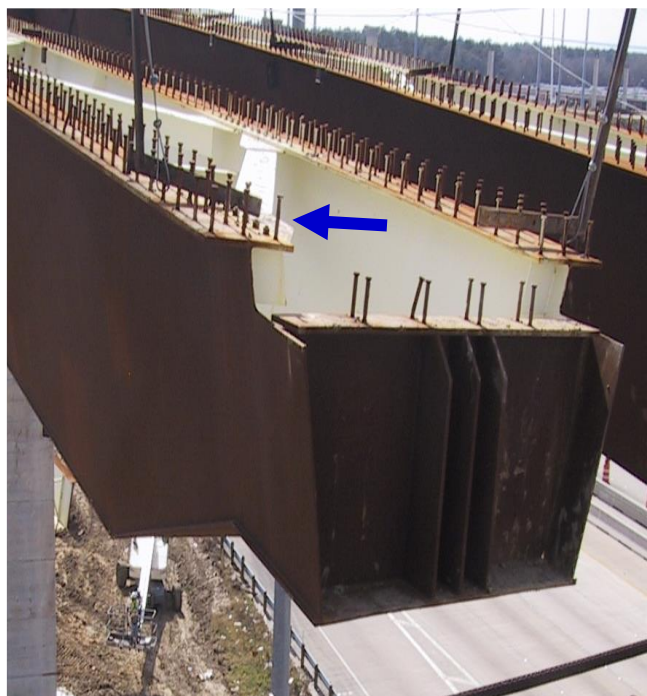


**Figure 59 Partial depth end diaphragm.**

## 5.0 SIMPLIFIED GEOMETRIC PROPERTIES FOR TUB GIRDERS

Symbols are defined in Figure 60.

### 5.1 Shear Center, $e_y$ , for Open and Quasi-Closed Sections [61]

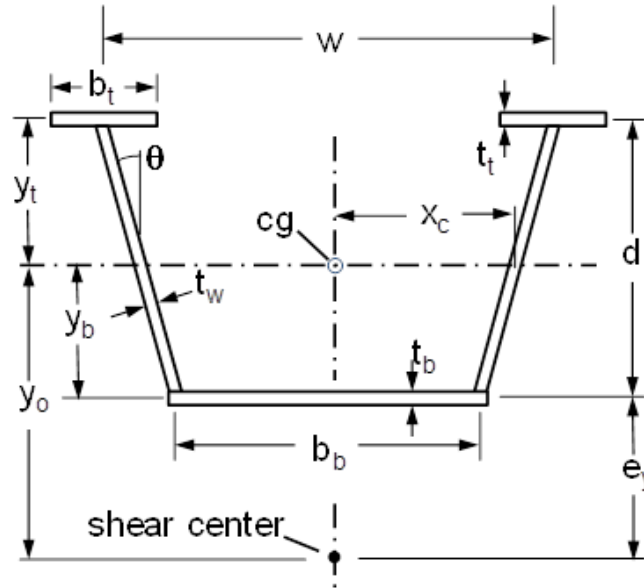


Figure 60 Calculation of Shear Center for Open and Quasi-Closed Sections

$$I_y = \frac{t_b b_b^3}{12} + \frac{d t_w}{6} (w^2 + w b_b + b_b^2) + \left( \frac{t_b b_b^3}{6} + \frac{t_t b_t w^2}{2} \right)$$

$$q_a = \frac{\frac{-t_t b_t w}{t_{eq}} + 0.875 d^2}{\frac{2}{w} \left( \frac{w}{t_{eq}} + 2 \frac{d}{t_w} + \frac{b_b}{t_b} \right)}$$

$$e_y = \frac{d}{I_y} \left[ \left( \frac{t_t b_t}{2} + \frac{w t_{eq}}{12} \right) w^2 - \frac{(2w + b_b) d t_w b_b}{12} + q_a (w + b_b) \right]$$

The shear center location  $e_y$  is measured from the centroid of the bottom flange. A negative value indicates that the shear center is below the bottom flange. For open-section tub girders,  $t_{eq} = 0$  and  $q_a = -b_t t_w$ .

## 5.2 Monosymmetry Coefficient, $\beta_x$ – Open section only [62]

$$\beta_x = \frac{1}{I_x} \left[ y_b A_b \left( \frac{1}{12} b_b^2 + y_b^2 \right) - 2A_t y_t \left( \frac{1}{12} b_t^2 + \frac{w^2}{4} + y_t^2 \right) + \frac{2t_w}{\tan \theta \sin \theta} \left( \frac{x_c}{24} (w^3 - b_b^3) - \frac{1}{64} (w^4 - b_b^4) \right) + \frac{t_w}{2 \cos \theta} (y_b^4 - y_t^4) \right] - 2y_o$$

where  $A_t = b_t t$  and  $A_b = b_b t_b$ . All geometric functions have positive values but  $\beta_x$  will be negative.

## 5.3 Warping Moment of Inertia, $C_w$ – Open section only [62]

$$C_w = \frac{c_a^2 A_b}{12} + \frac{(c_a^2 + c_a c_b + c_b^2) A_w}{6} + \left( \frac{c_c^2}{6} + \frac{c_b^2}{2} \right) A_t$$

where  $c_a = e_y b_b$ ,  $c_b = e_y w + d b_b$ ,  $c_c = b_t (e_y - d)$  and  $A_w = d t_w$

## 6.0 REFERENCES

1. AASHTO. *LRFD Bridge Design Specifications, 9<sup>th</sup> Edition*. American Association of State Highway and Transportation Officials, Washington, DC, 2020.
2. Vlasov, V. *Thin-Walled Elastic Beams, 2nd Edition*. National Science Foundation, Washington DC, 1961.
3. Timoshenko, S. and Gere, J. *Theory of Elastic Stability*. McGraw-Hill, New York, 1961.
4. Corr, D, McCann, D. and McDonald, B. “Lessons Learned from Marcy Bridge Collapse”. Proc., ASCE Forensic Engineering Congress, 2009.
5. Davidson, J., Keller, M. and Yoo, C. “Cross-Frame Spacing and Parametric Effects in Horizontally Curved I-Girder Bridges”, *Journal of Structural Engineering*, ASCE, Vol. 122, No. 9, pp 1089-1096, 1996.
6. NSBA. *Steel Bridge Design Handbook: Structural Behavior of Steel*. National Steel Bridge Alliance, 2021.
7. Fan, Z. and Helwig, T. “Behavior of Steel Box Girders with Top Flange Bracing”, *Journal of Structural Engineering*, ASCE, Vol. 125, No. 8, pp. 829-837, 1999.
8. NSBA. *Steel Bridge Design Handbook: Structural Analysis*. National Steel Bridge Alliance, 2021.
9. AASHTO/NSBA Steel Bridge Collaboration. *G13.1 – Guidelines for Steel Girder Bridge Analysis, 3<sup>rd</sup> Edition*. American Association of State Highway and Transportation Officials, Washington, DC, 2019 .
10. Poellot, W. “Computer-Aided Design of Horizontally Curved Girders by the V-Load Method”. *Engineering Journal*, AISC, Vol. 24, No. 1, pp. 42-50, 1987.
11. Liu, D. and Magliola, R. “End Forces on Cross-Frames in Horizontally Curved Steel I-Girder Bridges”, *Practice Periodical on Structural Design and Construction*, Vol. 15, No. 1, pp. 21-26, 2010.
12. Gaylord, E. and Gaylord, C. *Structural Engineering Handbook, 3<sup>rd</sup> Edition*, McGraw –Hill, New York, 1990.
13. Grubb, M. A. “Horizontally Curved I-Girder Bridge Analysis: V-Load Method”, *Transportation Research Record*, Record N982, Transportation Research Board, Washington, DC, pp. 26-36, 1984.
14. Stith, J., Schue, A., Farris, J., Petruzzi, B., Helwig, T., Williamson, E., Frank, K., Engelhardt, M. and Kim, J. “Guidance for Erection and Construction of Curved I-Girder Bridges”, TxDOT

- Report 0-5574-1, Center for Transportation Research, The University of Texas at Austin, pp. 240, 2010.
15. PennDOT. *Cross-Frame and Solid Plate Diaphragms for Steel Beam/Girder Bridges Design with Refined Methods of Analysis*. Bridge Design Standard BD-619M, Pennsylvania Department of Transportation, 2014.
  16. NCHRP. *National Cooperative Highway Research Project Report 962: Proposed Modification to AASHTO Cross-Frame Analysis and Design*, National Cooperative Highway Research Program, Transportation Research Board, Washington, DC, 2021.
  17. Yura, J. and Helwig, T. "Buckling of Beams with Inflection Points", Proc., Structural Stability Research Council, Annual Stability Conference, pp. 761-780, 2010.
  18. Yura, J. "Fundamentals of Beam Bracing", *Engineering Journal*, American Institute of Steel Construction, Vol. 38, No.1, pp. 11-26, 2001.
  19. Helwig, T. and Yura, J. "Shear Diaphragm Bracing of Beams II: Design Requirements", *Journal of Structural Engineering*, ASCE, Vol. 134, No. 3, pp. 357-363, 2008.
  20. Flint, A. "The Stability of Beams Loaded Through Secondary Members", *Civ. Eng. Public Works Review*, Vol. 46, No. 537-8, pp. 175-177, 259-260, 1951.
  21. Yura, J., Phillips, B., Raju, S., and Webb, S. "Bracing of Steel Beams in Bridges," Research Report 1239-4F, Center for Transportation Research, Univ. of Texas at Austin, October, 80 pp., 1992.
  22. AISC. *Specification for Structural Steel Buildings*. American Institute of Steel Construction, Chicago, IL, 2016.
  23. Taylor, A. and Ojalvo, M. "Torsional Restraint of Lateral Buckling", *J. of Structural Engineering*, ASCE, Vol. 92 No. ST2, pp. 115-129, 1966.
  24. Kitipornchai, S. and Finch, D. "Stiffness Requirements for Cross Bracing", *J. of Structural Engineering*, ASCE, Vol. 112, No. 12, pp. 2702-2707, 1986.
  25. Picard, A. and Beaulieu, D. "Design of Diagonal Cross Bracing", *Part1: Theoretical Study*, *Engineering Journal*, AISC, Vol. 24, No. 3, pp.122-126, 1987 and *Part2: Experimental Study*, Vol. 25, No. 4, pp. 156-160, 1988.
  26. Helwig, T., Yura, J. and Frank, K. "Bracing Forces in Diaphragms and Cross-Frames", Proc., Structural Stability Research Council Conference "Is Your Structure Suitably Braced?", pp. 129-140, 1993

27. Chen, B., Yura, J., Williamson, E. and Frank, K. “Top-Lateral Bracing System for Trapezoidal Steel Box-Girder Bridges”, Report 0-1898-4, Center for Transportation Research, U. of Texas at Austin, January, 116 pp., 2003.
28. Ziemian, R., Ed. Stability of Angle Members, Chapter 11, *Guide to Stability Design Criteria for Metal Structures, 6th Edition*. J. Wiley & Sons, New York, pp. 493-530, 2010.
29. Wang, L. and Helwig, T.. “Stability Bracing Requirements for Steel Bridge Girders with Skewed Supports”, *Journal of Bridge Engineering*, ASCE, Vol. 13, No. 2, pp. 149-157, 2008.
30. Quadrato, C., Wang, W., Battistini, A., Wahr, A., Engelhardt, M., Helwig, T. and Frank, K. “Cross-Frame and Diaphragm Layout and Connection Details”, *TxDOT Report 0-5701*, Center for Transportation Research, 393 pp., 2011.
31. Connor, R.J., and Korkmaz, C. *Fatigue Categorization of Obliquely Oriented Welded Attachments*. Purdue University, West Lafayette, IN, 2020.
32. Wahr, A. “The Fatigue Performance of Cross-Frame Connections,” Thesis, University of Texas at Austin, 228 pp., 2010.
33. Yura, J. A. “The Effective Length of Columns in Unbraced Frames”, *Engineering Journal*, AISC, pp. 37-42, 1971.
34. Helwig, T. and Wang, L. “Cross-Frame and Diaphragm Behavior for Steel Bridges with Skewed Supports”, *Report 1772-1*, The University of Houston, 231 pp., 2003.
35. Yura, J., Helwig, T., Herman, R., and Zhou, C. “Global Lateral Buckling of I-Shaped Girder Systems”, *J. of Structural Engineering*, ASCE, Vol. 134, No. 9, pp. 1487-1494, 2008.
36. Winter, G. “Lateral Bracing of Columns and Beams,” *ASCE Transactions*, Vol. 125, pp. 809-825, 1960.
37. Egilmez, Ozgur O.; Helwig, Todd A.; Jetann, Charles A.; and Lowery, Richard. “Stiffness and Strength of Metal Bridge Deck Forms,” *ASCE Journal of Bridge Engineering*, Vol. 12, No. 4, pp. 429-437, July/August 2007.
38. Helwig, Todd A.; Egilmez, Ozgur; and Jetann, Charles, “Lateral Bracing of Bridge Girders by Permanent Metal Deck Forms,” *Research Report 4145-1*, Report for Texas Department of Transportation, January 2005.
39. Klonaris, G. 2003. “Analytical and Computational Studies on the Torsional and Flexural Response of steel Trapezoidal Box-Girder Bridges”, MS Thesis, Dept. of Civil Engineering, U. of Texas at Austin, 204 pp., 2003.
40. Kollbrunner, C. and Basler, K. *Torsion in Structures – An Engineering Approach*, Springer-Verlag, New York, 1969.

41. Heins, C. "Box Girder design – State of the Art", *Engineering Journal*, AISC, Vol. 15, No.4, pp. 126-142, 1978.
42. Topkaya, C., Widiyanto and Williamson, E. "Evaluation of Top Flange Bracing Systems for Curved Box Girders", *J. of Bridge Engineering*, ASCE, Vol. 10, No. 6, pp. 693-703, 2005.
43. Widiyanto. "General Behavior of a Steel Trapezoidal Box-Girder during Construction", MS Thesis, Dept. of Civil Engineering, U. of Texas at Austin, 398 pp., 2003.
44. Helwig, T., and Fan, Z. "Field and Computational Studies of Steel Trapezoidal Box Girder Bridges", *TxDOT Report 0-1395-3*, The University of Houston, 238 pp., August 2000.
45. Williamson, E., Topkaya, C., Popp, D. and Yura, J. *UTrAp 2.0 Analysis of Steel Box Girders during Construction*, Department of Civil Engineering, Univ. of Texas at Austin, 2004.
46. Kim, K. and Yoo, C. "Interaction of Top Lateral and Internal Bracing Systems in Tub Girders", *J. of Structural Engineering*, ASCE, Vol. 132, No. 10, pp. 1611-1620, 2006.
47. Helwig, T., Herman, R., and Li, D. "Behavior of Trapezoidal Box Girders with Skewed Supports", *TxDOT Report 0-4148-1*, The University of Houston, 198 pp., 2004.
48. Kim, K. and Yoo, C. "Bending Behaviors of Quasi-Closed Trapezoidal Box Girders with X-Type Internal Cross-Frames", *J. of Constructional Steel Research*, Elsevier, Vol. 65, pp. 1827-1835, 2009.
49. Yura, J. and Widiyanto. "Lateral Buckling and Bracing Of Beams – A Re-Evaluation after the Marcy Bridge Collapse", Proceedings, Structural Stability Research Council, Annual Stability Conference, pp. 277-294, 2005.
50. Fan, Z. and Helwig, T. "Distortional Loads and Brace Forces in Steel Box Girders", *J. of Structural Engineering*, ASCE, Vol. 128, No. 6, pp. 710-718, 2002.
51. Helwig, T., Yura, J., Herman, R., Williamson, E. and Li, D. "Design Guidelines for Steel Trapezoidal Box Girder Systems", *Report 0-4307-1*, Center for Transportation research, U. of Texas at Austin, April, 72 pp., 2007.
52. AISC. *Steel Construction Manual, 15th Edition*. American Institute of Steel Construction Chicago, IL, 2017.
53. ASCE. *Design of Latticed Steel Transmission Towers, Standard 10-97*. American Society of Civil Engineers, Reston, VA, 88 pp., 1971.
54. AISC. *Load and Resistance Factor Design Specification for Single-Angle Members*. American Institute of Steel Construction, Chicago, IL, 20 pp., 2000.

55. Lutz, L. "Evaluating Single-Angle Compression Struts Using an Effective Slenderness Approach", *Engineering Journal*, AISC, Vol. 43, No. 4, pp. 241-246, 2006.
56. ASCE. *Design of Latticed Steel Transmission Towers, Standard 10-97*. American Society of Civil Engineers, Reston, VA, 88 pp., 2000.
57. Mengelkoch, N. and Yura, J. "Single-Angle Compression Members Loaded Through One Leg", Proc., Structural Stability Research Council Annual Stability Conference, pp. 201-218, 2002.
58. Kennedy, J. and Madugula, M. "Buckling of Angles: State of the Art", *J. of Structural Engineering*, ASCE, Vol. 108, No. 9, pp.1967-1980, 1982.
59. AASHTO/NSBA Steel Bridge Collaboration. *G1.4 – Guidelines for Design Details, 1<sup>st</sup> Edition*, American Association of State Highway and Transportation Officials, Washington, DC, 2006.
60. Coletti, D., Fan, T., Gatti, W., Holt, J., and Vogel, J. "Practical Steel Tub Girder Design," National Steel Bridge Alliance, 2005.
61. Terry, P. "Steel Trapezoidal Box Girder Section Properties", MS Thesis, Dept. of Civil and Environmental Engineering, U. of Houston, Texas, 126 pp., 2004.
62. Popp, D. "UTrAp 2.0: Linearized Buckling Analysis of Steel Trapezoidal Girders", MS Thesis, Dept. of Civil Engineering, U. of Texas at Austin, 121 pp., 2004.



**Smarter. Stronger. Steel.**

National Steel Bridge Alliance  
312.670.2400 | [aisc.org/nsba](http://aisc.org/nsba)